Marine Ecosystems

SOUTH AUSTRALIAN RESEARCH & DEVELOPMENT INSTITUTE
PIRSA

PIRSA Initiative II: carrying capacity of Spencer Gulf: hydrodynamic and biogeochemical measurement modelling and performance monitoring

John Middleton, Mark Doubell, Charles James, John Luick and Paul van Ruth

SARDI Publication No. F2013/000311-1
SARDI Research Report Series No. 705

ISBN: 978-1-921563-51-5

FRDC Project No. 2009/046

SARDI Aquatic Sciences
PO Box 120 Henley Beach SA 5022

December 2013

Final Report for the Fisheries Research and Development Corporation

PREMIUM FOOD AND WINE FROM OUR CLEAN ENVIRONMENT

FRDC FISHERIES RESEARCH & DEVELOPMENT CORPORATION

SOUTH AUSTRALIA

Government of South Australia
Primary Industries and Regions SA

SARDI
SOUTH AUSTRALIAN RESEARCH AND DEVELOPMENT INSTITUTE

PIRSA Initiative II: carrying capacity of Spencer Gulf: hydrodynamic and biogeochemical measurement modelling and performance monitoring

Final Report for the Fisheries Research and Development Corporation

John Middleton, Mark Doubell, Charles James, John Luick and Paul van Ruth

SARDI Publication No. F2013/000311-1
SARDI Research Report Series No. 705

ISBN: 978-1-921563-51-5

FRDC Project No. 2009/046

December 2013

This publication may be cited as:
Middleton, J., Doubell, M., James, C., Luick, J. and van Ruth, P. (2013). PIRSA Initiative II: carrying capacity of Spencer Gulf: hydrodynamic and biogeochemical measurement modelling and performance monitoring. Final Report for the Fisheries Research and Development Corporation. South Australian Research and Development Institute (Aquatic Sciences), Adelaide. SARDI Publication No. F2013/000311-1. SARDI Research Report Series No. 705. 97pp.

South Australian Research and Development Institute
SARDI Aquatic Sciences
2 Hamra Avenue
West Beach SA 5024

Telephone: (08) 8207 5400
Facsimile: (08) 8207 5406
http://www.sardi.sa.gov.au

DISCLAIMER

Printed in Adelaide: December 2013

SARDI Publication No. F2013/000311-1
SARDI Research Report Series No. 705

Author(s): John Middleton, Mark Doubell, Charles James, John Luick and Paul van Ruth

Reviewer(s): Steven Clarke, Charles James, Xiaoxu Li, Maylene Loo, John Luick, Rick McGarvey, Paul van Ruth, Mark Gibbs

Approved by: A/Prof. Jason Tanner
Science Leader - Marine Ecosystems

Signed:

Date: 17 December 2013

Distribution: FRDC, CSIRO, PIRSA Fisheries and Aquaculture, SA Sardine Industry Association, ASBTIA, SAOGA, SAASC Library, University of Adelaide Library, Parliamentary Library, State Library and National Library

Circulation: Public Domain

TABLE OF CONTENTS

LIST OF FIGURES

LIST OF TABLES

NON-TECHNICAL SUMMARY:

2009/046 PIRSA Initiative II: carrying capacity of Spencer Gulf - hydrodynamic and biogeochemical measurement modelling and performance monitoring

PRINCIPAL INVESTIGATOR: A/Prof John F. Middleton

ADDRESS: Aquatic Sciences, S.A. Research and Development Institute,
PO Box 120 Henley Beach, S.A. 5481
Telephone: 08 8207 5449 Fax: 08 8207 5481

OBJECTIVES

1 To provide Primary Industries and Regions South Australia (PIRSA) with estimates of sustainable carrying capacity by region, season and species for Spencer Gulf, and to investigate the impact of non-supplementary fed species (*e.g.,* oysters) on these estimates.

2 To achieve this overall objective, we will collect data from five areas so as to build, calibrate and validate hydrodynamic, biogeochemical and wave models that describe the biophysical properties of the Gulf. These models and data will then be used to determine the following:

3 Provide measures of connectivity of nutrients for the Gulf, including aquaculture (supplementary fed species) and non-aquaculture (natural and industry) derived nutrient inputs.

4 Provide management with solutions to questions of carrying capacity, sustainability and impact for existing and proposed sites of aquaculture (supplementary fed species).

5 Use the carrying capacity estimates to validate or otherwise, earlier estimates that were obtained from simplified flushing models.

6 Develop and incorporate models for non-supplementary fed species (oysters and mussels) with parameters identified that are critical to model sensitivity.

7 Develop strategies for long-term performance monitoring, management and mitigation strategies.

8 Determine limitations in the ability to deliver the above for other areas (e.g. shelf waters off Ceduna) or species (e.g., scallops).

OUTCOMES ACHIEVED TO DATE: PIRSA Fisheries and Aquaculture will use the results of this study to further refine and develop policy for the future regulation of the carrying capacity of finfish aquaculture production within Spencer Gulf. The area specific differences within Spencer Gulf have been defined at the scales of the cage, lease and zone and will allow for the development of long-term performance monitoring, management and mitigation strategies for aquaculture zones within Spencer Gulf that take into account the variability among the areas and need for area specific requirements. These outcomes will further justify the South Australian Government's approach to sustainable aquaculture development as directed by the *Aquaculture Act 2001*.

The ability to deliver the above for other areas has been determined (e.g., shelf waters off Ceduna) and will help PIRSA determine future resource requirements for other areas of South Australia. The "whole of gulf" approach taken allows PIRSA Fisheries and Aquaculture and other Government agencies (e.g., the Environmental Protection Agency) to evaluate the relative importance of both natural and anthropogenic nutrient sources (i.e., aquaculture, waste water and industrial ocean outfalls).

The methods and approach for this study can form the basis for future studies elsewhere both nationally and internationally. Although Spencer Gulf specific data collected in this project cannot be transferred to other areas, the methods and approach to better define environmental carrying capacity of a given body of water with various sources of nutrient inputs are applicable to other geographical areas, as well as to aquaculture, fisheries and marine-based commercial activities.

In South Australia and elsewhere, the regulation and management of finfish aquaculture lease sites invokes a concept of carrying capacity that is related to the monthly feed rates of farmed fish and the resultant flux (F) of nutrients into the ocean. The optimal flux is related to the maximum nutrient concentration $c_{max,}$ that in turn is limited to be less than a prescribed maximum concentration (c_P) obtained from guidelines elsewhere (*e.g.* Australian and New Zealand Environment and Conservation Council and Agriculture and Resources Management Council of Australia and New Zealand (ARMCANZ): ANZECC/ARMCANZ 2000). The prescribed maximum value c_P, provides an upper limit for the nutrient concentration prescribed to preserve ecosystem health.

In this study, a rapid assessment management tool ("CarCap 1.0") has been developed that will enable PIRSA to make informed decisions on existing and proposed lease sites, as well as compare the distribution and impacts of nutrient inputs from both aquaculture and other anthropogenic sources, including waste water and industrial outfalls. To achieve this, high-resolution hydrodynamic computer models for ocean currents and nutrient dispersal were developed and validated for Spencer Gulf.

The model outputs for the 2010-2011 year of simulation are used to develop this assessment tool in two ways. The first involves providing estimates at each point in the model of a new time scale (T*) of nutrient flushing. This time scale is shown to be related to the maximum nutrient concentration, and the optimal nutrient flux (and monthly feed rate) is given by $F= c_P / T^*$. The results for T* have been incorporated into the interactive software package CarCap 1.0 that will, for a given choice of c_P, allow managers to readily estimate the optimal nutrient fluxes and feed rates at any point in the Gulf and at the scale of the cage or lease. Moreover, since T* and F vary strongly with location, CarCap 1.0 will also enable new aquaculture sites to be chosen to ensure maximal flushing and larger nutrient fluxes and monthly feed rates: the latter to ensure a greater biomass of caged fish and financial return to the farm operator.

The second approach is to couple the hydrodynamic model to a biogeochemical model that allows nutrient concentrations from different sources to be cumulative and recycled between phytoplankton, zooplankton, detritus and sediments. A variety of model scenarios were run to determine the relative importance of various sources of nutrients, including natural (adjacent shelf waters) and anthropogenic (aquaculture, the Onesteel facility at Whyalla and waste water). Shelf waters were found to be the largest source of nitrogen to the gulf, and loss to the atmosphere the largest sink. The additional anthropogenic nutrients input into the Boston Bay region lead to the largest concentrations of phytoplankton in the south-west and along the west coast of the Gulf. However, concentrations of nutrients and phytoplankton remained below the ANZECC/ARMCANZ (2000) water quality guidelines.

All scenario studies have been incorporated into the CarCap 1.0 software. The software allows managers to assess the relative importance of existing sources of nutrients at the scale of the Gulf, and provides the ability to "zoom in" at the scale of the zone and lease. Nutrient, oxygen and phytoplankton concentrations can be examined, and their evolution in time and space easily explored and compared to user prescribed maximum concentrations (c_P), or those determined elsewhere.

The field surveys undertaken to validate the models have also provided the first "whole of gulf" study of the ecology and seasonal dynamics of the lower trophic ecosystem in Spencer Gulf.

KEYWORDS: carrying capacity, aquaculture, outfalls, hydrodynamic, biogeochemical modelling, Spencer Gulf.

ACKNOWLEDGEMENTS:

We thank the crews of the *R.V.* Ngerin and *F.V.* Atlas for their assistance in collecting the field data from the Gulf. Louise Renfrey's assistance in editing this document, and support over the last 5 years, is truly appreciated. Finally, we thank eResearch S.A. for allowing us time on the Tizard supercomputer so as to complete this study. The nutrient data used to drive the model at the Gulf mouth were collected through the national Integrated Marine Observing System.

BACKGROUND:

Aquaculture within Spencer Gulf (Figure 1) and South Australia represents a farm gate value of $228M for 2011/12 (Econsearch 2013).This contributed 53% of the State's total value of seafood production and generating about 2,650 jobs (of which 65% were in regional communities).

Key aquaculture species include southern bluefin tuna, yellowtail kingfish, abalone and oysters, with existing and proposed aquaculture zones around much of the perimeter of Spencer Gulf. The sustainable development of aquaculture depends on an ability to determine the carrying capacity for new and existing zones for supplementary fed species (e.g. finfish, abalone), whereby nutrients are excreted into the environment, as well as for non-supplementary fed species (e.g. mussels, oysters), that can have a mitigating influence through the uptake of nutrients and phytoplankton. In addition, it is important to determine the impact of aquaculture on the marine environment.

The sustainability and impact of aquaculture is directly determined by the physical environment of ocean currents and waves that can act to disperse, transport and dilute nutrients introduced either naturally or by supplementary fed species. Research into the circulation of Spencer Gulf has revealed a complex, seasonally dependent circulation which is described hereafter.

Tides: The resonant nature of the Gulf (Easton 1978) leads to strong tidal currents (~ 1 m/s) in the northern half of the Gulf that can be important for vertical mixing and the shear enhanced diffusion of nutrients.

Thermohaline Currents: A feature of the Gulf is that evaporation exceeds precipitation year round, leading to the formation of dense salty water in the shallow perimeters and upper half of the gulf (Lennon et al. 1987; Nunes and Lennon 1987). The resulting horizontal variations in density have been shown to lead to a clockwise thermohaline density circulation within the Gulf that is modulated by tidal mixing.

Winds: Wind-forced currents are known to be important to transport, vertical mixing and current shear within the gulf. It has previously been shown that oscillatory and seasonally varying mean winds can lead to currents that can largely modify and/or eliminate those due to the thermohaline effects (Bullock 1975; Nixon and Noye 1999; de Silva Samarasinghe et al. 2003). In addition, while mean wind-forced currents in the southern half of the gulf may be small (~ 2 cm/s), they can be important on a monthly basis, with transport distances of 50 km (Herzfeld et al. 2008).

While we have some idea of the physical mechanisms that are important to nutrient dispersal and transport, much less can be said about the naturally occurring phyto/zooplankton ecosystems and the nutrients that support them. Data collected from south-western Spencer Gulf (east of Boston Bay) has identified a peak in phytoplankton abundance that occurs around late autumn/early winter, which is driven by a diatom bloom. Analysis of long term data suggests that predominately diatom blooms have been consistent annual phenomena in the south-western Gulf during late autumn or early winter. The peak in diatoms appears to be made possible, in part, by a summer peak in silica concentrations (>3.5 µmol L-1) (van Ruth et al. 2009a). The annual cycle of productivity in the region appears to begin with a bloom of high primary and secondary productivity through late summer/early autumn. Decreasing secondary productivity in late autumn promotes high phytoplankton biomass at a time when primary production remains high. However, lower phytoplankton growth rates signify the decline of the phytoplankton bloom and the onset of a winter period of low productivity. During late spring/early summer phytoplankton growth rates increase, while primary and secondary productivity remain low. These findings suggest the "bottoming out" of productivity and the beginning of the new cycle (van Ruth et al. 2009b, c).

These speculations will be examined in this project.

This project uses a wide range of methodologies that include the implementation of complex wave software, mathematical Green's function analysis, the measurement of primary productivity and complex biogeochemical models. The results are varied and the chapters below capture the overall outputs, outcomes and results in a simple and concise manner, so as to show how and what the research achieved. Greater detail is presented for the chapters that focus on carrying capacity rather than the oceanographic models described in Chapters 1 and 2. The summary Figure 1 below is referenced in many chapters.

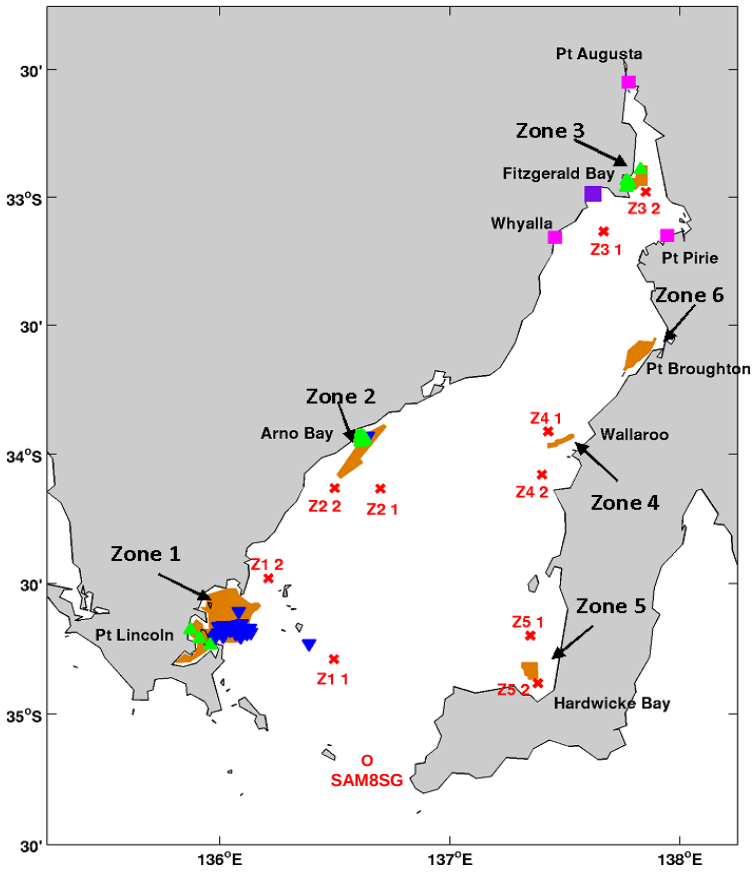

Figure 1 Map of Spencer Gulf showing the location of; the 6 aquaculture zones (brown shaded regions), field survey sites (red crosses), tuna (blue triangles) and finfish (green triangles) aquaculture leases, waste water treatment plants (pink squares) and the Onesteel steel works (purple square). The location of the permanent SAIMOS mooring SAM8SG (Gulf mouth) is indicated by the red circle. The location of aquaculture leases is plotted for the 2010/11 period.

NEED:

PIRSA Fisheries and Aquaculture has indicated that it intends to develop a number of new aquaculture zones around the State over the next 5 years, as well as revisit earlier assumptions of carrying capacity estimates developed by Tanner et al. (2007), in order to meet the anticipated expansion of the aquaculture industry within South Australia. It is also essential that PIRSA is prepared for the increased propagation of southern bluefin tuna, which could see the farmed biomass of this species increase significantly in a few years, particularly in Spencer Gulf where existing aquaculture infrastructure and support services are in place.

The ability to obtain accurate estimates of spatial and temporal variability in the cycling of nutrients through the ecosystems in Spencer Gulf will provide important information about potential risks and impacts of increased aquaculture activities in the Gulf. This need will be met through the development of calibrated hydrodynamic and bio-geochemical models for Spencer Gulf that will also determine the carrying capacity of aquaculture areas, including the concurrent use of both supplementary and non-supplementary fed organisms within each area. Further, the development of strategies for long-term performance monitoring, management and mitigation are needed for the aquaculture areas in Spencer Gulf. These outcomes will further support the South Australian Government's approach to sustainable aquaculture development as directed by the *Aquaculture Act 2001*.

OBJECTIVES:

1 To provide PIRSA Fisheries and Aquaculture with estimates of sustainable carrying capacity by region, season and species for Spencer Gulf, and to investigate the impact of non-supplementary fed species (*e.g.,* oysters) on these estimates.

2 To achieve this overall objective, we will collect data from five areas so as to build, calibrate and validate hydrodynamic, biogeochemical and wave models that describe the biophysical properties of the Gulf. These models and data will then be used to determine the following:

3 Provide measures of connectivity of nutrients for the Gulf, including aquaculture (supplementary fed species) and non-aquaculture (natural and industry) derived nutrient inputs.

4 Provide management with solutions to questions of carrying capacity, sustainability and impact for existing and proposed sites of aquaculture (supplementary fed species).

5 Use the carrying capacity estimates to validate or otherwise, earlier estimates that were obtained from simplified flushing models.

6 Develop and incorporate models for non-supplementary fed species (oysters and mussels) with parameters identified that are critical to model sensitivity.

7 Develop strategies for long-term performance monitoring, management and mitigation strategies.

8 Determine limitations in the ability to deliver the above for other areas (e.g. shelf waters off Ceduna) or species (e.g., scallops).

The achievement of these objectives is detailed in the Conclusions Section below.

CHAPTER 1. A VALIDATED HYDRODYNAMIC MODEL FOR SPENCER GULF AND CONNECTIVITY STUDIES

John Luick, Mark Doubell and John Middleton

1.1 Introduction and Summary

Hydrodynamic models have become standard tools for achieving best practice in aquaculture development in many parts of the world, especially Europe and North America. In part, this has come about due to their ability to provide reliable estimates at a low cost relative to expensive field programs. Typical uses for models include assessment of the impact from nutrient release, deposition of organic matter, and dispersion of chemicals (including medicines used in aquaculture). This chapter describes how the Spencer Gulf models (Objective 2) were validated, and used to determine connectivity through "particle tracking" (Objective 3). The validation is a matter of obtaining a good comparison of model output with observed data, and the process of refining the model through improved topography, reduced diffusion or use of different mixing schemes. Without robust validation, little confidence can be attached to the results.

The essential physical processes at the core of this project are shown to be accurately simulated. It was not felt necessary to include wetting and drying around the edges and northern reaches, or small-scale processes for which we have no data for validation. In the future, new data and faster computers will enable modellers to include more processes. The model velocity fields were also used to track particles and determine the connectivity between aquaculture zones. In summary, the simulation results showed the connectivity between aquaculture zones was greatest between northern and eastern zones during spring and summer. Connectivity between the western zones was greatest during autumn and winter.

1.2a Methods – the Models

For this study, ROMS (Regional Ocean Modelling System; Schepetkin and McWilliams 2005) was used. ROMS (myroms.org) is the *de facto* standard in coastal modelling. It is a multi-purpose, multi-disciplinary oceanic modelling package. It has been successfully coupled with nutrient, wave, atmospheric, ice, and sediment transport models. Many tools have been developed by third parties for analysing ROMS output – for example, LTRANS (described below) is a Lagrangian particle tracking model based on ROMS velocities.

ROMS was run over a series of nested spatial domains. All model domains contain Spencer Gulf, and the adjoining shelf, from which oceanographic data for validation was obtained. The domains, from largest to smallest, were as follows:

- A two-dimensional coastal trapped wave model.

- A "Large Scale Model" (LSM), originally with 5500 m horizontal resolution and 30 vertical levels, later changed to 2500 m resolution and 15 vertical levels. The LSM spanned the shelf from mid-Bight to Victoria.

- A Spencer Gulf Model (SGM) with a 600 m grid, and 15 levels in the vertical (model SG0600). For validation purposes the boundaries were placed far enough to the south and west to include moorings off Kangaroo Island and Coffin Bay (Figure 1.1). This also placed the boundary well away from the mouth of Spencer Gulf, as the entrance is known to be one

of rapid ocean changes which could contaminate solutions in the domain interior. This model is used in Chapter 3 and Chapter 5.

• A second Spencer Gulf Model with the same outer boundaries, but which had a 1200 m grid resolution and 15 levels in the vertical (SG1200). SG1200 was created following coupled model runs of SG0600 with nutrients and waves, which led to run times in excess of two weeks. Tests comparing results from SG0600 and SG1200 demonstrated that the 1200 m grid was adequate for the purposes of nutrient modelling.

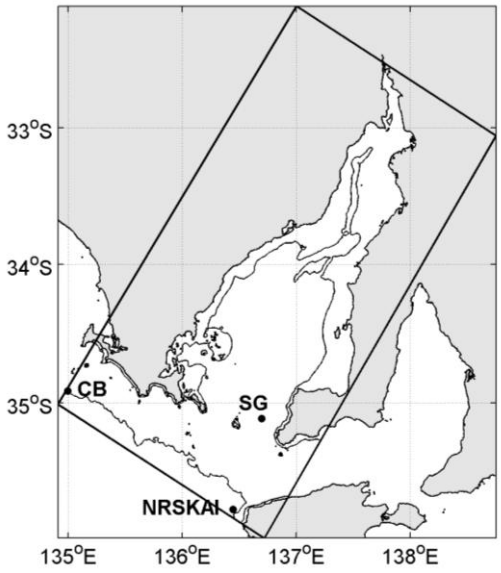

Figure 1.1 Aerial extent of Spencer Gulf model domain. The SAIMOS mooring locations are indicated for Coffin Bay (CB), Spencer Gulf (SG) and Kangaroo Is (NRSKAI). The 20 and 100 m depth contours are plotted.

At the beginning of this project in 2010, the Bureau of Meteorology (BoM) provided their best forcing fields as of that time, known as their “MesoLAPS” suite of models. Early testing, including simulations performed to validate against the Risk and Response project data of 2005/2006 (Tanner and Volkman 2009), was performed using MesoLAPS data. In 2010, BoM switched to a new atmospheric model known as “ACCESS”. The ACCESS data were used for all of the simulations for 2010 onwards. We found that ACCESS had inadequate evaporation from upper Spencer Gulf. Comparison with the nearest operative weather station showed that ACCESS was consistently offset. An offset was then added. The validations shown below are of simulations with the offset data. Aside from evaporation, the ACCESS data were consistent with MesoLAPS.

Harmonic constants were extracted from the latest version of the TPXO tide model (Egbert et al, 1994). These were applied at the open boundary of the LSM. A different strategy was used for most simulations of SG0600: at the end of the simulation, ROMS automatically runs a tidal analysis at each grid point, and stores the results. The stored results were interpolated to the SG0600 open boundary point rather than TPXO data, which are less accurate in gulfs and shallow areas.

Open boundary nudging keeps the boundary reasonably close to long-term or “climatological” values of the open ocean while allowing the Gulf interior to evolve independently. For the LSM simulations, the cells near the open boundary were “nudged” to temperature and salinity from the Climatological Atlas of Regional Seas (Ridgway et al. 2002; 2006), whereas the SG0600 simulations were nudged to the LSM at the open boundary of SG0600. Nudging coefficients decreased linearly from a 3 day time scale at the

boundary to 30 days ten grid points from the boundary (and were zero beyond that). The temperature and salinity initial conditions (starting point values) for the LSM were set to CARS. For SG0600, the initial conditions were determined from the LSM.

Initially, all model runs were on a computer with a single 24-CPU node (we use "node" to mean a set of CPUs that share memory). Through its parallelisation feature, the ROMS software splits the domain into horizontal tiles which can be assigned to different processors to reduce computing time. A typical subdivision in early runs was 6 X 3 (six tiles up by three across), meaning that 18 of the 24 CPUs were used. During the final year, an eResearch SA computer with 28 48-CPU nodes became available and a number of the later experiments were performed on that computer. This enabled tile counts up to 76. Increasing the number of tiles beyond 76 did not lead to improved performance because of 1) increased communication time between tiles, 2) increased communication time between nodes, and 3) increased wait time on a queue before the job started (wait times depend on the amount of computer resources requested).

As both the LSM and SG0600 domains were designed with the same maximum criterion of 200,000 gridpoints, both had runtimes of several days per simulated year.

A full simulation consists of three steps: 1) run the coastal trapped wave model, 2) run the Large Scale Model and finally, 3) run the Spencer Gulf Model. More than one run of the Spencer Gulf model may be performed using the results of a single LSM simulation.

Aquaculture is currently undertaken within six broad zones within Spencer Gulf (Fig. 1). To establish the extent of connectivity between each of the six aquaculture zones, numerical studies were undertaken using the open-source LTRANS particle tracking model (North et al. 2008). The LTRANS model uses predicted current velocities from the SG0600 model. Each grid point within a zone was initialised with 12 particles at 5 m depth. Four seasonal studies tracked a total of 22,584 particles over 90 days using an external (ROMS) time step of 36 hours and an internal LTRANS time step of 10 minutes.

1.2b Methods – Data

Data (temperature, salinity, currents) used for validation was from the following sources:
• The "Risk and Response" project (Tanner and Volkman 2009) installed oceanographic moorings near Port Lincoln.

• The Southern Australian Integrated Marine Observing System (SAIMOS) installed oceanographic moorings on the shelf adjacent to Spencer Gulf from July 2008 onwards (Fig.1.1).

• Historical CTD data from Flinders University surveys in the 1980s (Nunes 1985; Nunes and Lennon 1987; Nunes Vaz et al. 1990).

• Satellite sea surface temperature (SST) data (Schneider et al. 2013).

• Tide data from the global TPXO model (Egbert et al. 1994).

• Sea level data from Thevenard, Port Lincoln, Wallaroo, Whyalla and Port Stanvac (Australian National Tidal Centre website).

• Field data collected during the project between July 2010 and September 2011. Data streams included those from four bottom mooring deployments which measured Acoustic Doppler Current Profiler (ADCP) currents, and time series of conductivity, temperature and depth (CTD).

1.3a Results and Discussion - Model Validation

The model was compared against data from the Risk and Response project (Tanner and Volkman, 2009). The observed freshening of the waters in Boston Bay in April was well-simulated by the model. The model temperatures and salinities tracked the observations quite well through the entire model run.

The model and observed currents were also in good agreement. Both indicated a small northwards net drift over much of the period. The model simulated the observed current amplitude and phases well including the spring-neap cycle (which controls the fortnightly cycle of amplitude).

The model was also compared with the extensive SAIMOS shelf data streams. Up to 90% of the variability of current data in the energy containing weather-band (5-20 days) was explained. The model also reproduced the observed temperature and salinity fields.

The auto-spectra, coherence squared, and phase lags of the principal axis depth integrated transports (model and data) were calculated. The observed transport spectrum was reproduced by the model. The model was able to explain up to 90% of the transport variance for frequencies below 0.3 d^{-1}.

The annual cycle of temperature and salinity was determined for 1984-1986 through monthly sampling by Nunes (1985). The model reproduced the observed seasonal cycle of temperature and salinity with an error of less than 2 ºC and 0.5 psu, respectively. A similar comparison was made for temperature at Port Stanvac in Gulf St Vincent.

The model sea level at tidal and lower frequencies was validated against sea level data both from within the Gulf and on the shelf. Figure 1.2 shows a typical comparison of model and observed sea level in the tidal-frequency band. The model predictions capture both the dodge tide and the interaction between the four main constituents quite well. Tidal amplitudes and phases were in agreement to within 5%.

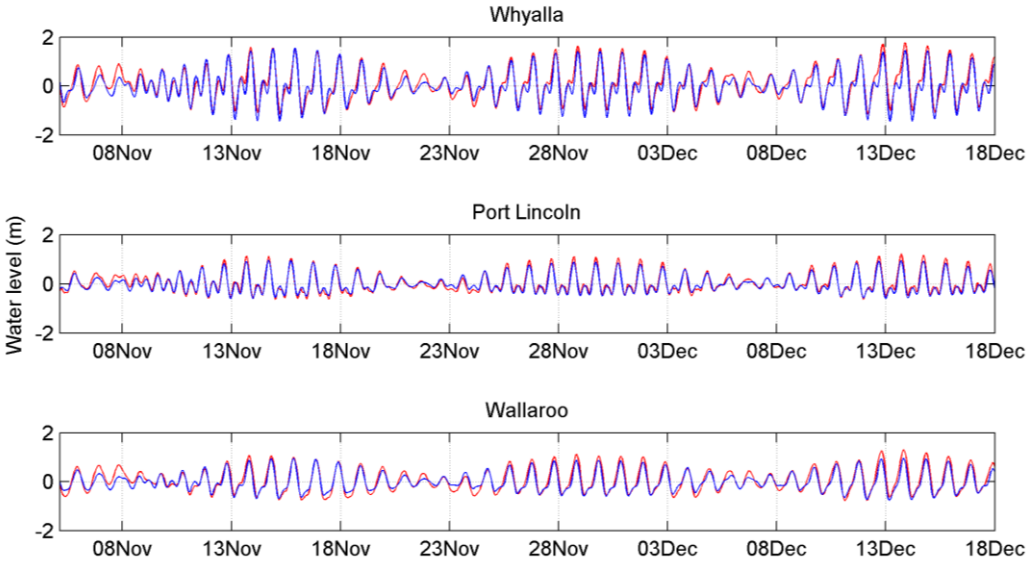

Figure 1.2 Observed (blue) and modelled (red) sea level in the tidal band and at several gulf locations during 2010.

The model was also validated against the data collected in this project (and satellite SST) at several sites in Spencer Gulf. The model temperature was slightly high (<0.1 ^{o}C) in mid-summer, but within acceptable bounds. The model salinity was also slightly high (< 0.3 psu), but again within the bounds of acceptability at the sites, despite slightly over-estimating salinity.

A transect of temperature and salinity was observed during May 2011 as part of field sampling (Fig. 1.3). Visual comparison of the model and observed transects showed reasonable agreement given the dynamic nature of the environment at this location in late May, when the salinity outfall at the mouth of Spencer Gulf is active (and hence water is being drawn down along eastern Spencer Gulf from the north).

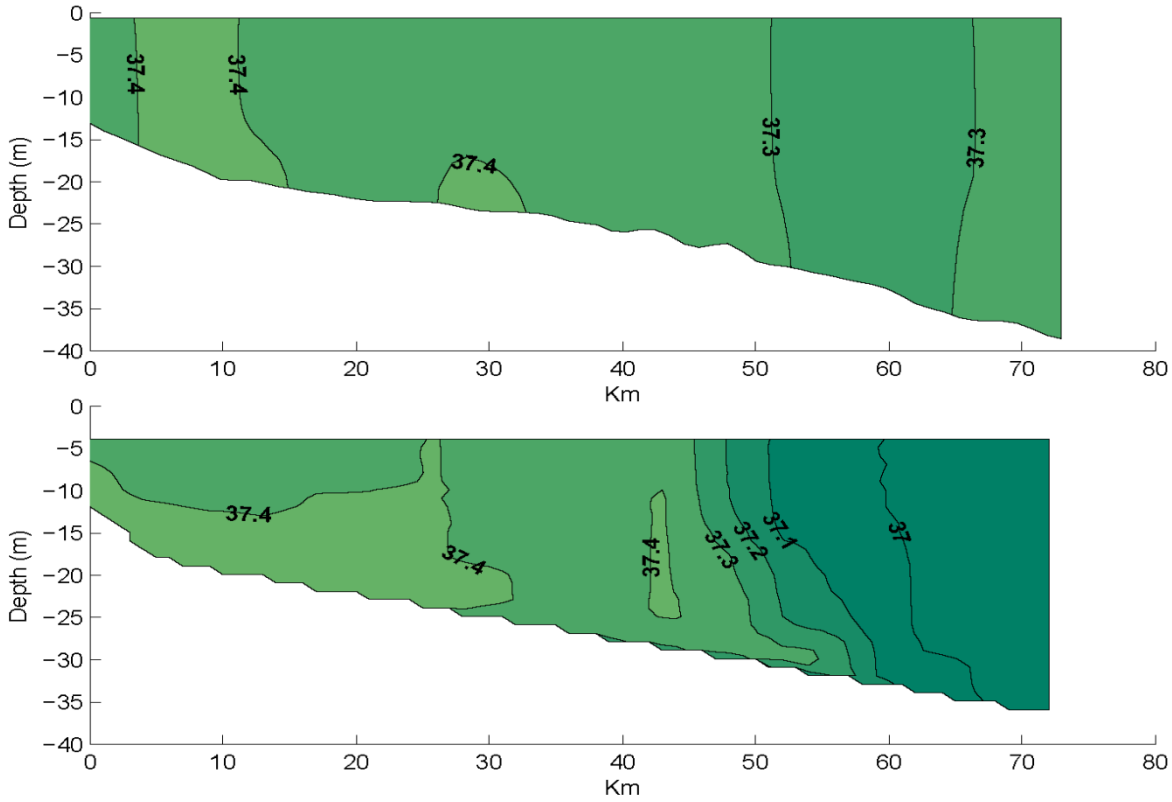

Figure 1.3. Transects of model (upper) and observed (lower) salinities in central Spencer Gulf during late May 2011. Contour interval 0.1 psu.

Maps were drawn of model and observed salinity (Fig. 1.4 a,b). The only available observations were from historical surveys. Given the 26-year gap between the two, the correspondence was acceptable. For example, the 40 psu salinity contour crossed the Gulf at nearly the same point. A similar comparison between model surface temperatures and those from night-time values of satellite SST, found that the difference was within 1 ºC in both winter and summer.

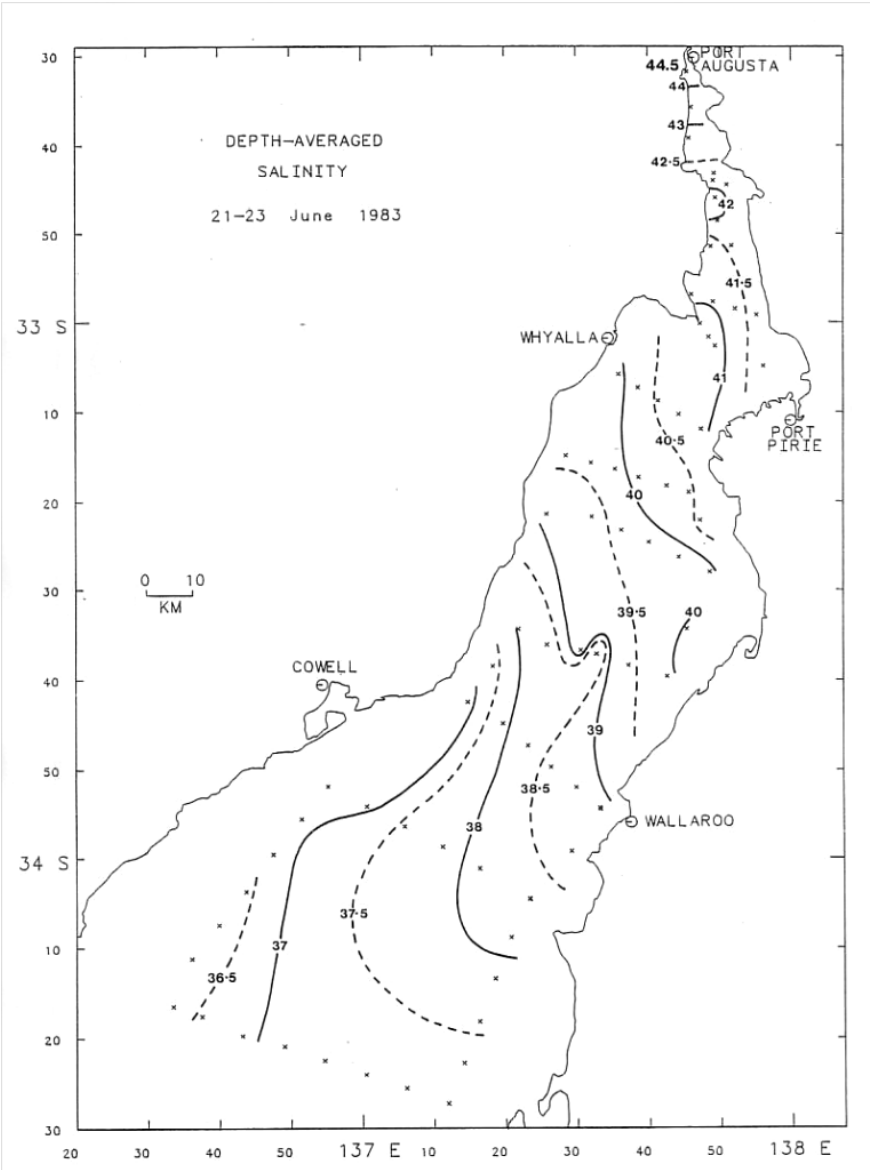

Figure 1.4a. Depth-averaged salinity for June 1983 (Nunes 1985).

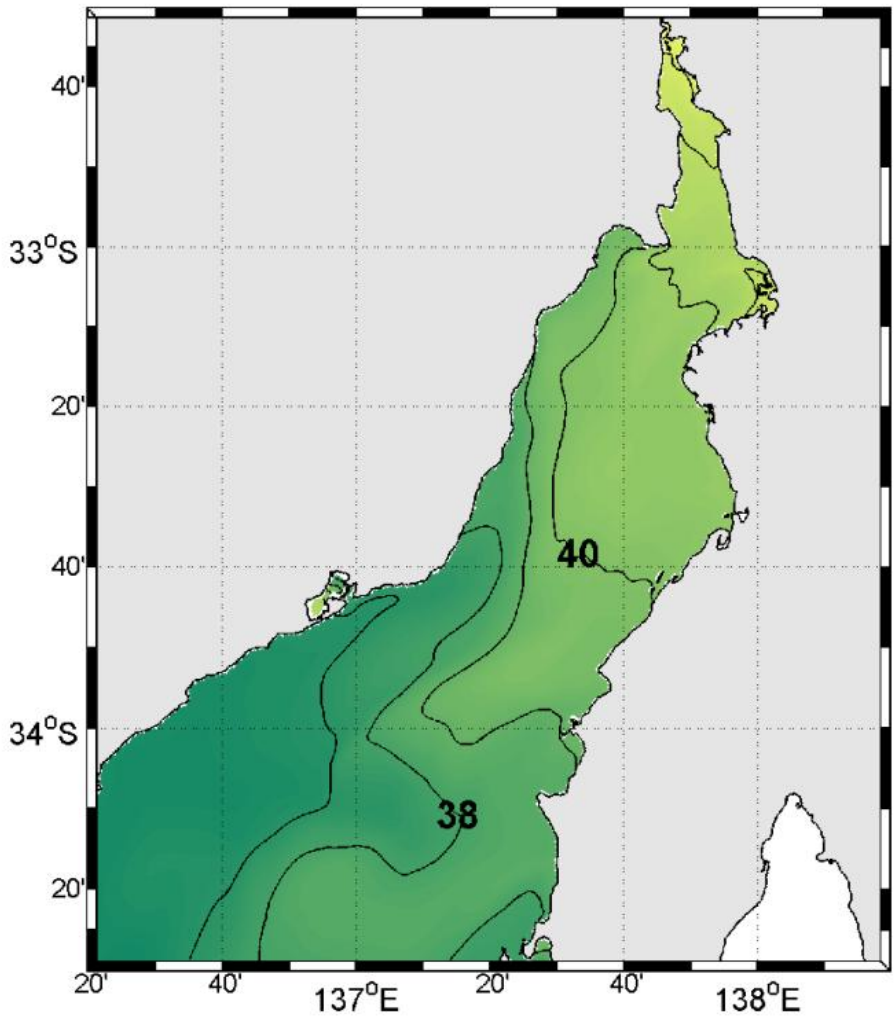

Figure 1.4b. Depth-averaged salinity in ROMS on the 18th June 2011.

1.3b Results and Discussion - Connectivity Studies

Seasonal differences in the residual circulation of Spencer Gulf are most distinct between summer and winter (Fig. 1.5). In summer, residual current speeds are reduced, with mean values of around 0.05 cm s^{-1}. Along the coasts the net flow is typically northward and stronger (~ 3 cm s^{-1}), and there is a weak southward return flow along the central axis of the Gulf. The stronger coastal flows are not shown in Figure 1.5 since only every 10th value is plotted. The model simulation indicates exchange between the shelf and Gulf is limited during summer due to the development of a strong thermohaline front at the entrance to the Gulf. In contrast, during winter the residual circulation is increased as a consequence of local wind forcing and annual flushing due to the outflow saline water.

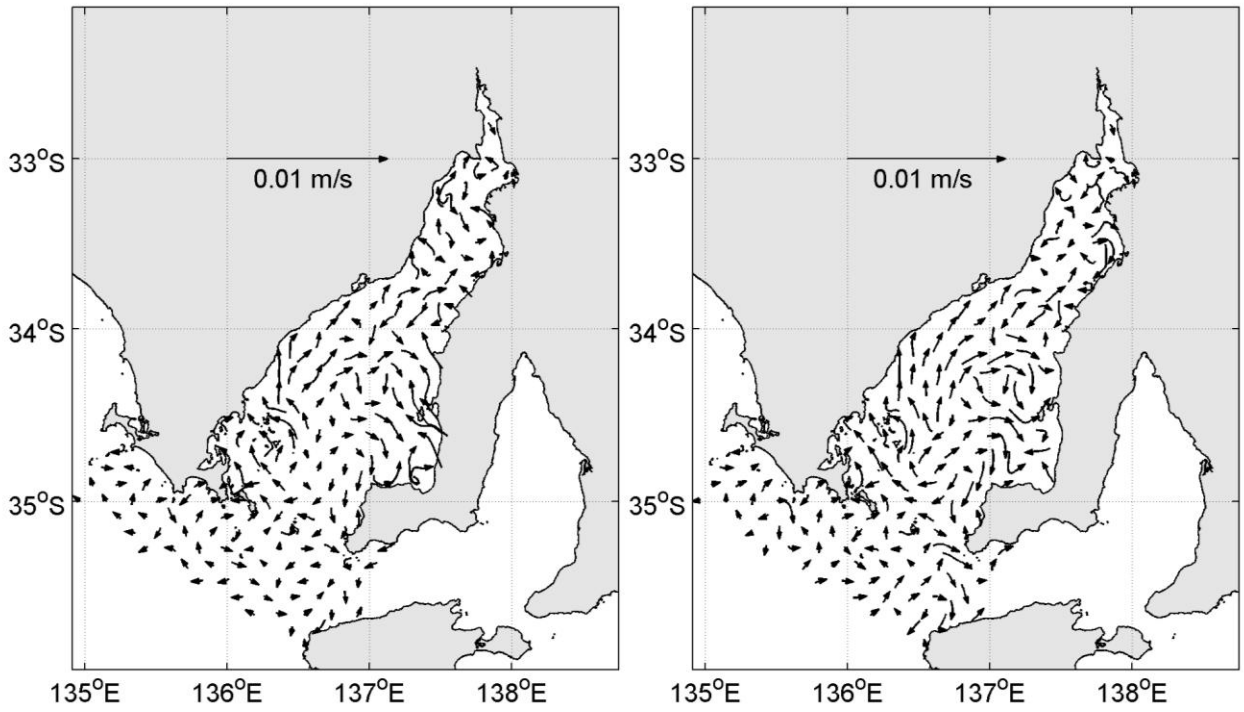

Figure 1.5 Depth and time averaged circulation in the Gulf. Left: summer. Right: winter.

Exchange between the shelf and gulf increases in winter, with inflow on the west associated with stronger currents and a corresponding increase of the outflow in the east. A clockwise circulation pattern develops in the Gulf and mean residual current speeds are around 0.1 cm s^{-1}. Again coastal speeds are stronger and of order 3 cm s^{-1}. Circulation in spring and autumn shows a transitional phase between the summer and winter patterns, respectively.

The effect of the Gulf's seasonal circulation on connectivity between aquaculture zones (Fig. 1) is next determined. Histograms showing the percentage of particles that have arrived from other zones and for each season are shown in Figure 1.6 and 1.7. In summary, the simulation results showed the connectivity between aquaculture zones was greatest between northern and eastern zones during spring and summer. Connectivity between the western zones was greatest during autumn and winter. The time taken to move particles from one zone to the other is consistent with the mean coastal speeds of 3 cm s^{-1} noted above.

More specifically:

- Zone 1 showed generally weak levels of connectivity with other regions. Small levels of connectivity with the eastern zones (Zones 4, 5 and 6) were evident during autumn and winter due to the clockwise circulation pattern present within the southern region of the Gulf.
- Zone 2 showed high levels of connectivity with Zone 1 across all seasons except for summer.
- Zone 3 showed very high levels of connectivity with Zone 6 in spring, summer and autumn. Additional connectivity with Zone 4 was observed in late summer and Zone 2 in autumn and winter.
- Zone 6 showed low to moderate levels of connectivity with each of the zones across the seasons except for winter.
- For Zone 4, moderate levels of connectivity were found with Zone 5 in spring and autumn. Zone 4 also showed low levels of connectivity with Zones 2 and 3.

Connectivity of Zone 4 with other regions was significantly reduced in winter and autumn.

- For Zone 5, connectivity with Zones 1, 2, 4 and 5 was highest during winter and spring.

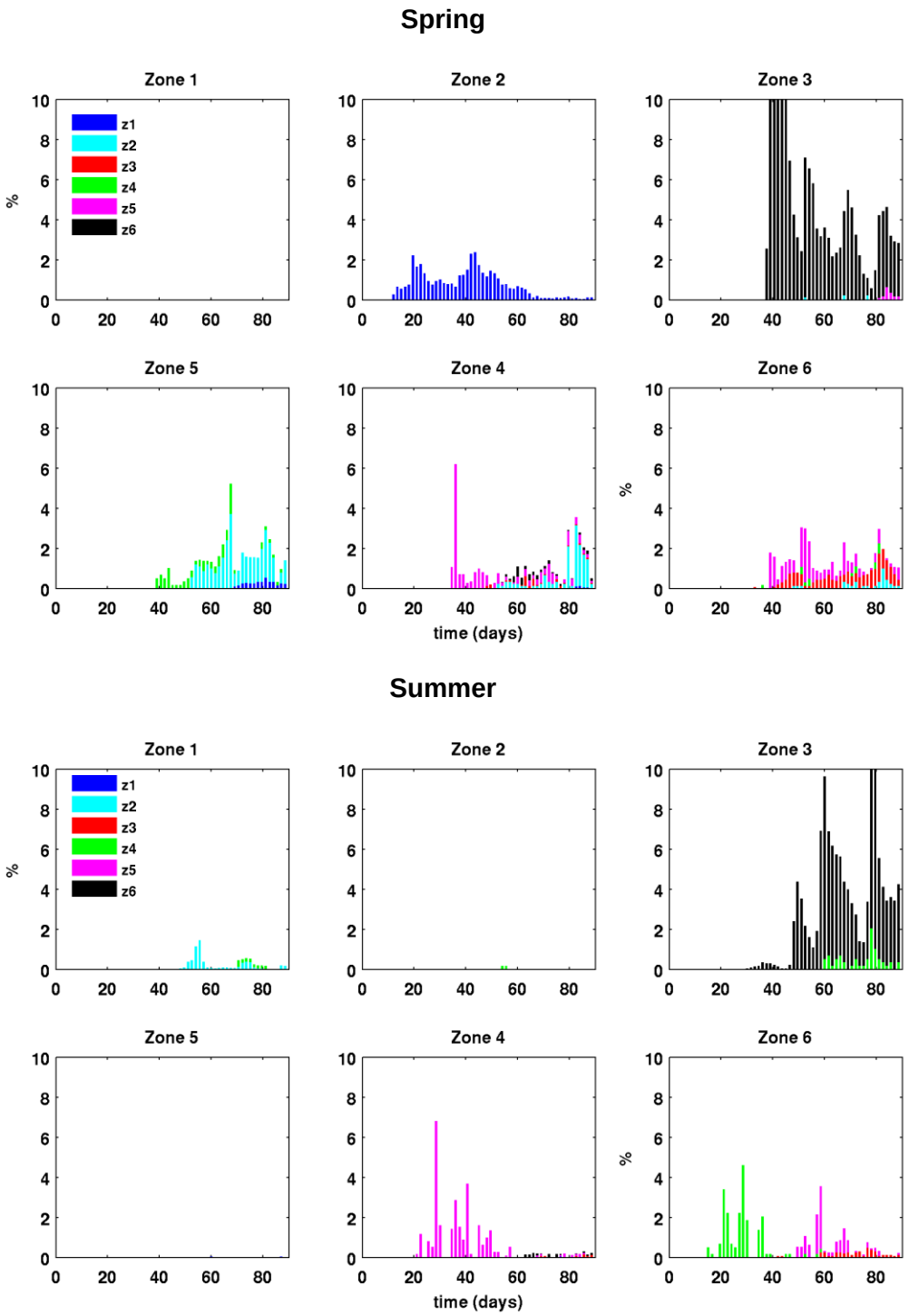

Figure 1.6 Connectivity between aquaculture zones in spring (top panels) and summer (bottom panels). For each day, the percentage of particles within each zone from other zones is shown. Source zones are identified by colour (see legend). See Figure 1 for the location of each zone in Spencer Gulf.

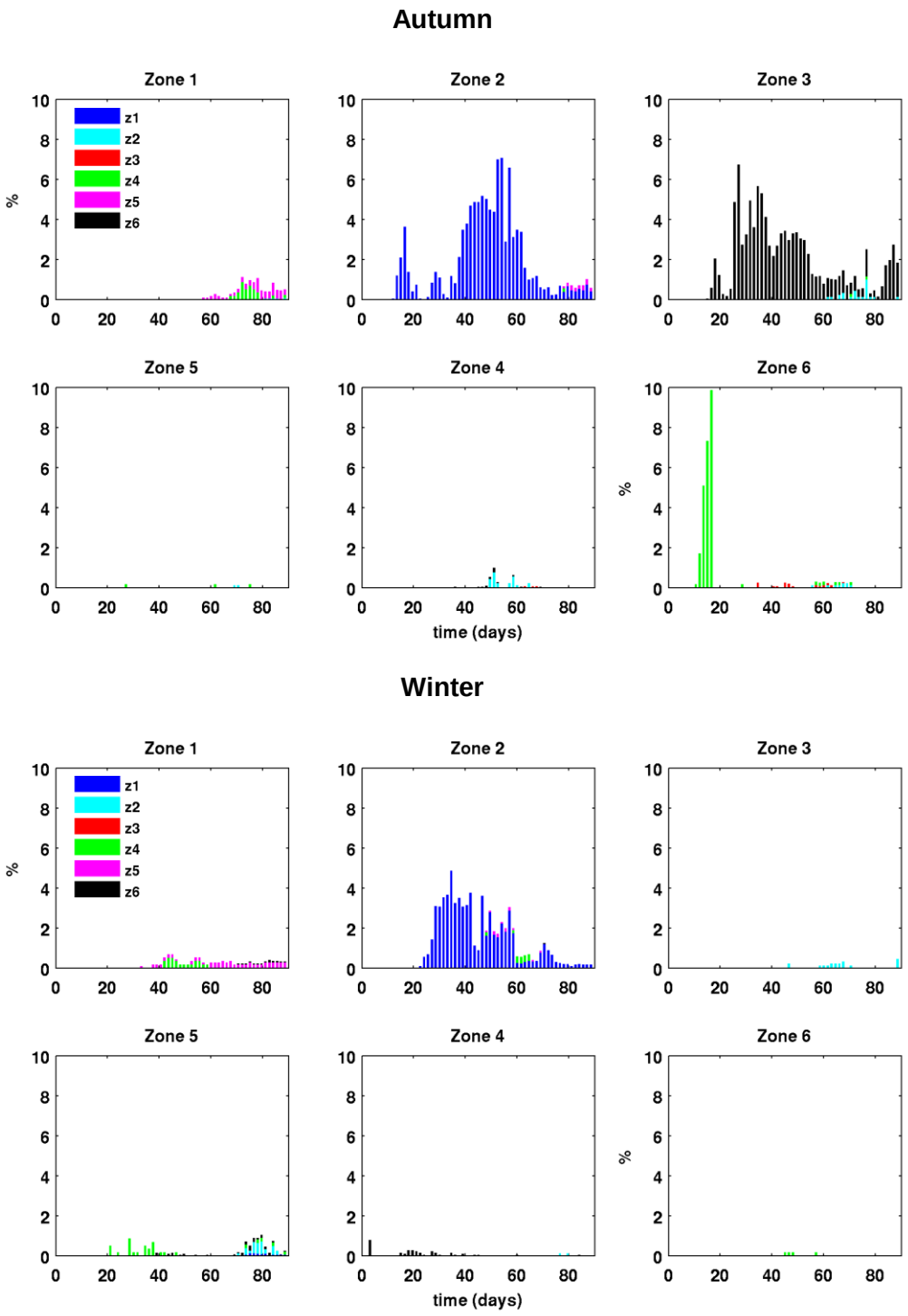

Figure 1.7 Connectivity between aquaculture zones in autumn (top panels) and winter (bottom panels). For each day, the percentage of particles within each zone from other zones is shown. Source zones are identified by colour (see legend). See Figure 1 for the location of each zone in Spencer Gulf.

CHAPTER 2. THE WAVE MODEL

Charles James

2.1 Introduction and Summary

Waves increase bottom orbital currents that may lead to enhanced bottom friction, vertical mixing and a reduction in the amplitude of longer term ocean currents. Such changes may be important to the transport and dispersal of nutrients and phytoplankton. To examine this, a wave model (Objective 2) is coupled to both the Spencer Gulf (hydrodynamic) Model (SGM) discussed in Chapter 1, and the biogeochemical model discussed in Chapter 5. In summary, the waves have only a minor impact on the modelled ocean currents, and distribution of nutrients and phytoplankton, so only a brief summary of the analysis is presented.

2.2 Methods

The Simulating Waves Near-shore (SWAN) model (Booij et al. 1999) adopted here has been used in previous wave studies in and around Spencer Gulf (Jones et al 2012; Hemer and Bye 1999), although coupling with hydrodynamic models was not considered. Software for the SWAN model is included with the Regional Ocean Model System (ROMS) (Haidvogel et al. 2000) and is "pre-coupled" to the hydrodynamic SGM model (Chapter 1), as well as the biogeochemical model (Chapter 5).

SWAN computes the significant wave height and peak wave characteristics (direction, period and wavelength), wave dissipation and bottom orbital velocities, which in turn modify the hydrodynamic results. Surface winds from the Bureau of Meteorology (BoM) and time series of oceanic swell are used to drive the model. The swell data are obtained from the global NOAA/NCEP Wavewatch III model (Alves et al. 2005) and used to force SWAN at the open shelf boundary shown in Figure 2.1, (the two starred circles).

Results were obtained for July 2010 to June 2011 and the 1200 m SGM grid was adopted.

Wave data were obtained from two deployments of an RDI Workhorse (with wave package) at sites Z1 1 (lower Gulf) and Z3 1 (upper Gulf) shown in Figure 1. The data were derived from 5 minute burst samples each hour, of water velocity, sea-surface height, and pressure, collected at 2 Hz. This sampling rate implies that the minimum wave period measured is 2 seconds.

2.3 Results and Discussion

A snapshot of results for the 9th August 2010 is shown in Figure 2.1.The wave height diminishes from about 3 m at the gulf mouth to values of less than 0.5 m at the head of the Gulf. The waves propagate into the gulf and then towards the coasts due to the shallower depths and associated reduction in the phase speeds of the waves.

A time series comparison is presented in Figure 2.2 of model and observed wave height and period for site Z1 1 in the lower Gulf. The data indicate considerable variability over scales of hours that is not predicted by the model.

The results show that the coupled model does a good job of predicting the variations in wave-height and wave-period during the mooring deployment. There is a slight tendency to over-estimate significant wave height, especially the peak between the 20th and 30th of

August 2010, but overall the agreement is remarkable given the complex analysis required to extract observational data from the ADCP.

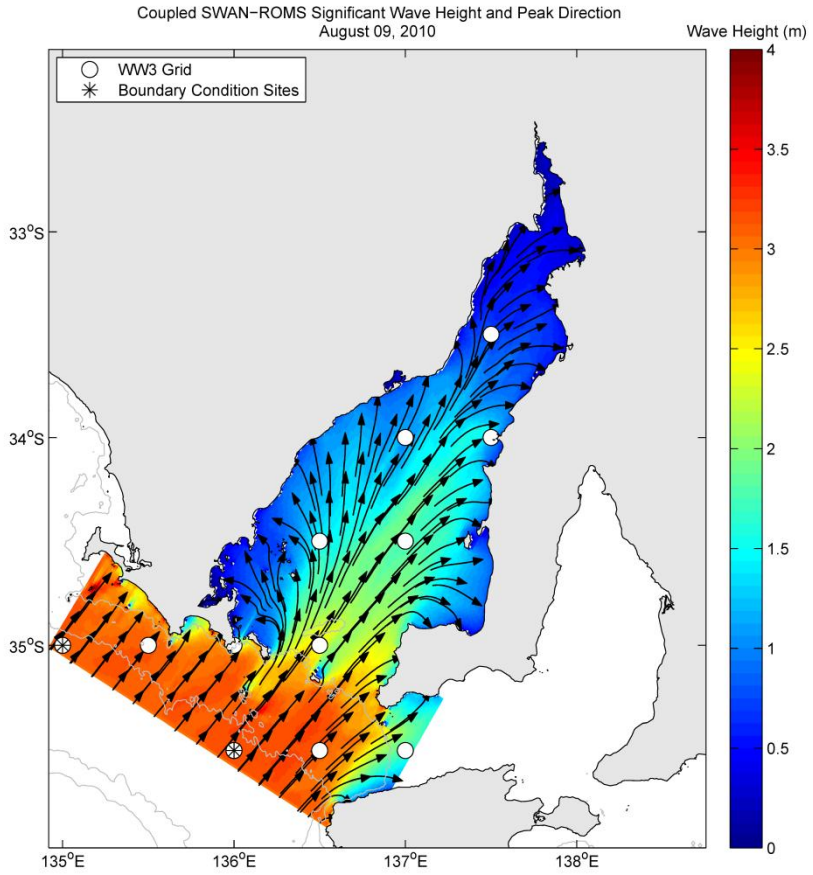

Figure 2.1 Location of Wavewatch III grid points around Spencer Gulf (the circles). The two points used to generate the SWAN boundary conditions are indicated by the white starred circles. Results for the coupled SWAN output are shown for 9th August 2010: the vectors shown indicate wave direction and the colour bar indicates wave height in meters.

In contrast to site Z1 1, the mooring at site Z3 1 was located in upper Spencer Gulf at 33.058 ^{O}S 137.664 ^{O}E (see Figure 1) and in less than 20 m water depth. This location is shallow and quite sheltered from the open ocean, and the wave field should be dominated by local wind forcing, and have a correspondingly lower significant wave height and shorter period.

The results in Figure 2.3 show that the model again does a good job of reproducing the overall variations in significant wave height and period. The significant wave-height is slightly underestimated, but the overall response is satisfactory. For the 2 Hz sampling rate adopted in the observations, periods shorter than 2 seconds cannot be resolved, although the model suggests very little significant wave activity occurs at shorter periods.

Finally, a comparison is presented in Figure 2.4 of temperature, NO_3, NH_4, and phytoplankton at day 320 of model evolution (16th May 2011) with and without the coupled wave model. There are some minor qualitative differences but overall, the results are similar. Inspections of time series also show minor differences where the inclusion of waves acts to smooth the nutrient levels, etc. These results suggest that the model parameterisation of bottom friction (without waves) is adequate for most purposes.

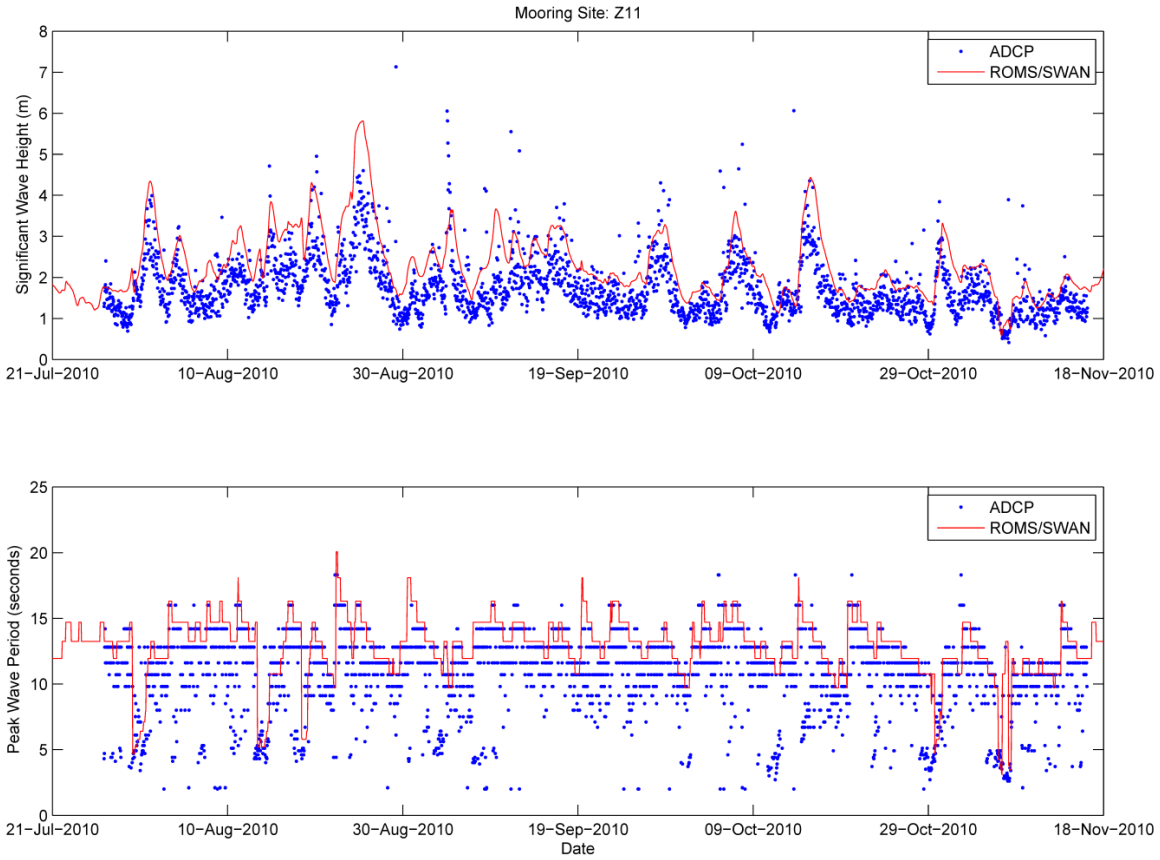

Figure 2.2 Comparison between ADCP data and coupled SWAN model output for the period of the Z1 1 mooring deployment in 2010. The blue dots represent the hourly ADCP observations and the red line represents the hourly model output for the same period.

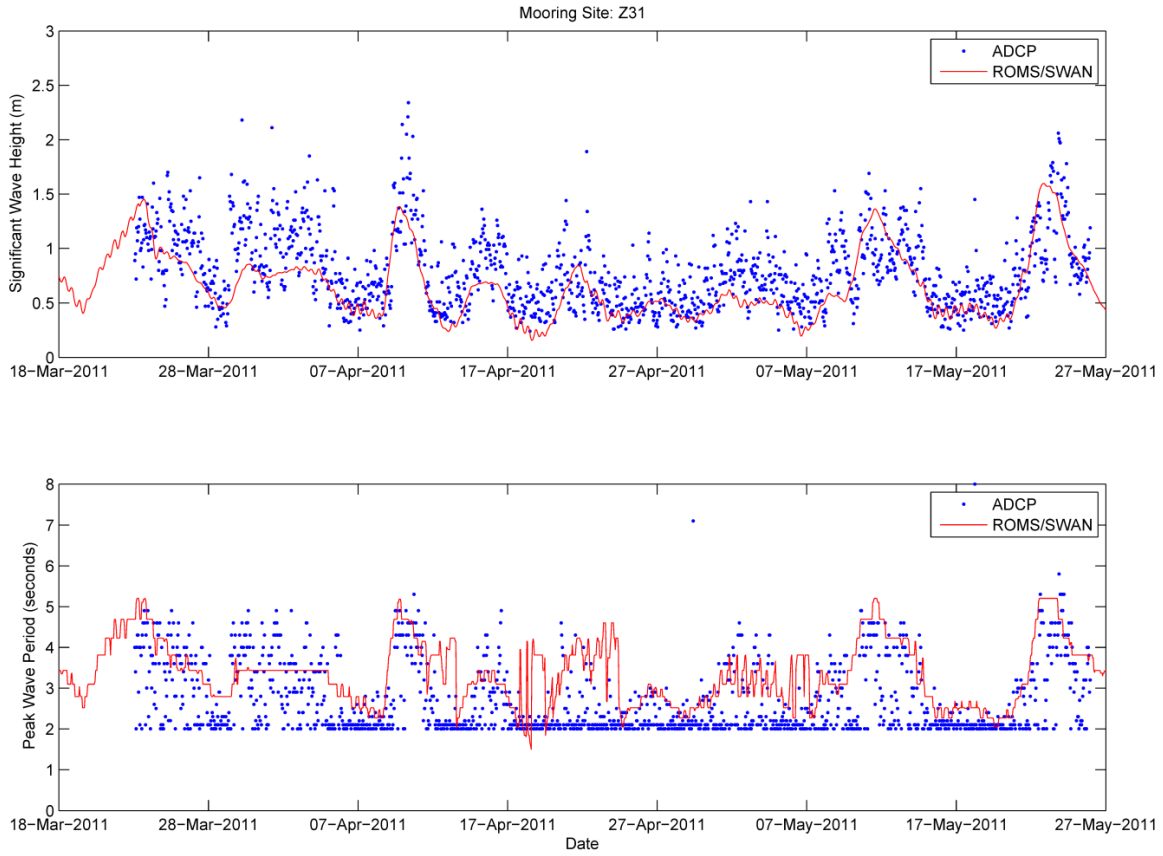

Figure 2.3 Comparison between ADCP data and coupled SWAN model output for the period of the Z3 1 mooring deployment in 2011. The blue dots represent the hourly ADCP observations and the red line represents the hourly model output for the same period.

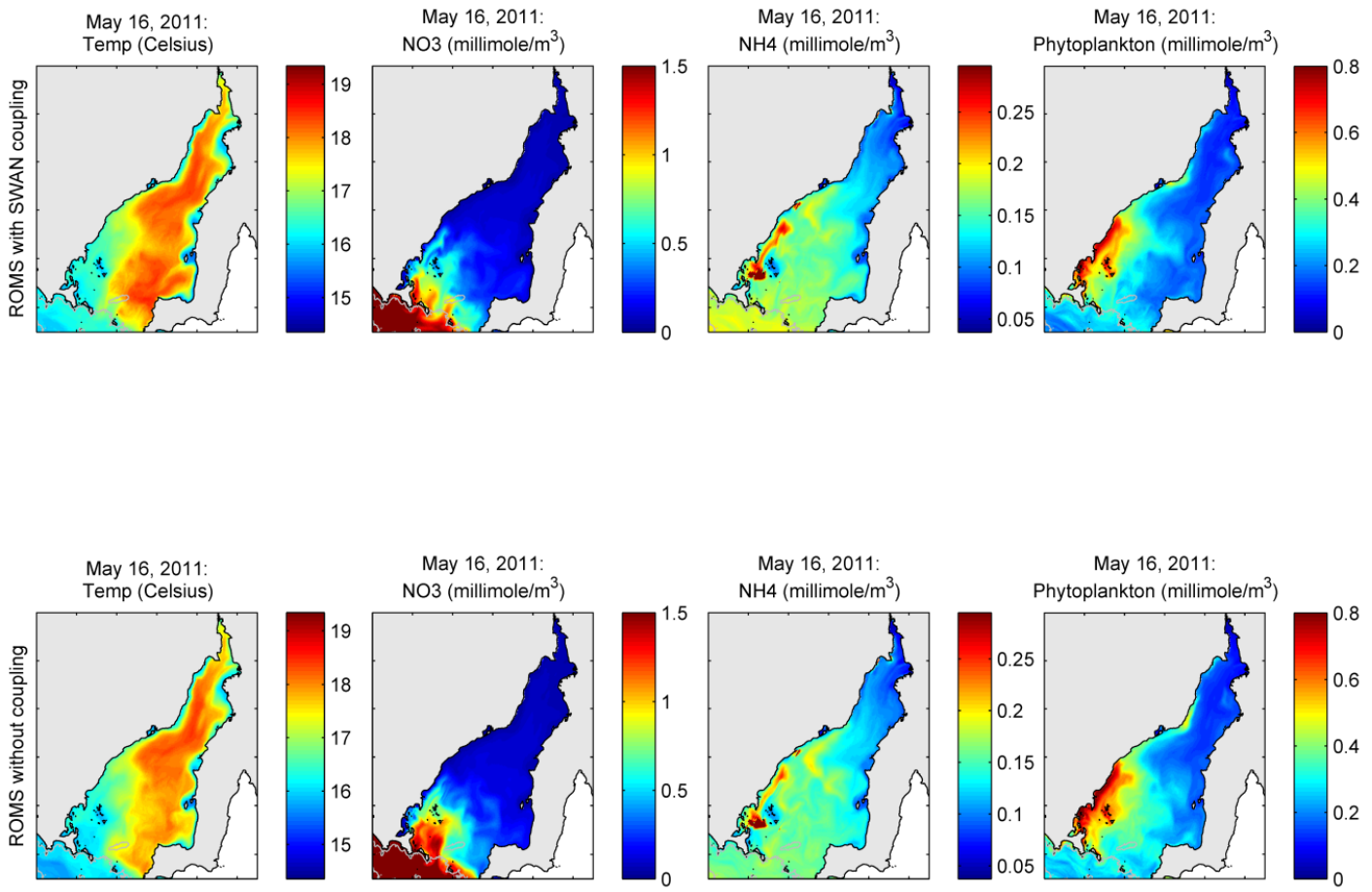

Figure 2.4 Comparison of coupled SWAN model (top) and uncoupled model (bottom) for the variables temperature, NO_3, NH_4, and phytoplankton.

CHAPTER 3. CARRYING CAPACITY FOR AQUACULTURE: RAPID ASSESSMENT USING HYDRODYNAMIC AND NEAR-FIELD, SEMI- ANALYTIC SOLUTIONS

John F. Middleton, John Luick, Mark Doubell

3.1 Introduction and Summary

The carrying capacity for aquaculture cage farming in Spencer Gulf is, in part, based on guidelines that the feed rates and nutrient flux into the lease region are determined such that the maximum nutrient concentration c does not exceed a prescribed value (say c_P) for ecosystem health. The feed rates are in turn used to help determine license conditions of fish biomass for a given lease. This definition of ecological carrying capacity may be contrasted with that of production carrying capacity where the feed rates and fish biomass are determined based on the health of the farmed fish themselves (Gecek and Legovic 2010). In this study the former definition will adopted and uncertainties are summarised at the end of this chapter.

Mathematically exact solutions have been obtained (Middleton and Doubell 2013) that describe the dispersal of an arbitrary nutrient that might arise from a steady flux of nutrients into a source region (cage or lease). These show that to a good approximation, and for a wide variety of flow regimes, the maximum concentration of a nutrient in the cage or lease region can be estimated by c_{max} = F T*. Here, T* is a new time scale of "flushing" that involves both mean currents (advection) and diffusion. The maximum allowed nutrient flux F can then be estimated from: F= c_P /T*. The Spencer Gulf hydrodynamic model, developed and validated in Chapter 1, is used to determine the parameters needed to estimate T* everywhere in Spencer Gulf and as winter time averages. In particular, the hydrodynamic model is used to estimate shear dispersion coefficients that are large and lead to strong diffusive mixing. The estimates of T* have been adopted into CarCap 1.0, a graphical user interface (Chapter 6), that allows managers to rapidly estimate maximum nutrient fluxes (feed rates) and concentrations at new lease sites (Objectives 4, 5 and 7). The optimal siting of new leases is discussed. The results should find application in other finite source flux problems in the coastal oceans including desalination plants and ocean outfalls. The results presented here are a summary of those obtained in the companion studies by Middleton and Doubell (2013) and Middleton et al. (2013).

3.2a Methods: Scale Estimates for Carrying Capacity

First consider a square source region of nutrients defined by the rectangle centred upon the origin:

$$\{-W/2 < x < W/2, -W/2 < y < W/2\} \qquad (3.1)$$

Since the aquaculture industry in South Australia is licensed at the scale of the lease (W ~ 600 m), the focus will be on results at this scale. Results will also be presented at the scale of the cage D=50 m. It is assumed that a constant flux F [kg/(m^3 s)] is applied continuously over this region and at the surface. The depth of the ocean h is assumed constant and the velocity field **u**(t) is assumed to be independent of space but not time. The nutrients need not be well mixed in the vertical, but this will reduce the shear dispersion coefficient (see below).

As part of this study, Middleton and Doubell (2013) obtained time and space dependent exact solutions for the depth averaged concentration c(**x**,t) for a constant nutrient flux F and constant diffusivities. Solutions were obtained for a variety of flow regimes (including weak and strong advection, diffusion and tides). The maximum concentration c_{max} in each case

was found to occur near the downstream edge of the lease or cage region and well approximated by the expression

$$c_{max} = F\,T^* \qquad (3.2)$$

with

$$T^* = T_a/(1+p) = T_d\,p/(1+p) \qquad (3.3)$$

$$p = T_a/T_d \qquad (3.4)$$

and

$$T_a = W/U \text{ and } T_d = W^2/(2K) \qquad (3.5)$$

The time scale $T_a = W/U$ represents the time it takes for a lease to be flushed by the mean current speed U. The diffusive time scale $T_d = W^2/(2K)$ represents the time taken for a spot to diffuse over a distance W and is well known in the literature (*e.g.*, Fisher et al. 1979).

As shown below, very small values of p are not found for the Gulf at the scale of the lease or cage, since the mean velocities U are generally very small. Such values may pertain to regions of the continental shelf where U is larger and K smaller. In this case, advection may dominate the flushing and $c_{max} = F\,T_a$ may be much smaller than that given by diffusion alone.

At the very large scales of the zone (W > 10 km), p can be small and the advective limit holds, so the correct scaling is $c_{max} = F\,T_a$. This is essentially the model used by Collings et al. (2007) and PIRSA to estimate feed rates at the scale of the zone. As will be shown below, this model can underestimate concentrations that might otherwise be found at the scales of the lease and cage.

Indeed, at these scales and for large values of p, $T_a >> T_d$, and diffusive processes dominate. In this case (3.2) becomes $c_{max} = F\,T_d$, and since it is assumed that $T_d << T_a$, the maximum concentrations obtained are much smaller than where advection dominates. Where p=1, $T_a = T_d$ so that $c_{max} = F\,T_d/2$. In this case advection and diffusion are of equal importance in flushing a lease, and the time scale T* is half of T_a or T_d. As will be shown below, large values of p are found for the mid to upper Gulf, indicating that diffusion dominates the flushing, while values of p near unity are found for the coastal regions where the water depth is less than 10 m or so.

The implications of these results are important to carrying capacity within the Gulf. Prescribed maximum concentrations c_P have been developed elsewhere (*e.g.* ANZECC/ARMCANZ 2000). These prescribed maximum levels provide a theoretical upper limit for the nutrient concentration to preserve ecosystem health. Nutrient concentrations that exceed c_P may result in algal blooms and changes to ecosystem components and processes that are harmful to both the broader environment and the farmed fish themselves. The maximum flux of nutrients F can readily be determined by setting the maximum estimated nutrient concentration $c_{max} = FT^*$ to c_P. The maximum nutrient flux (which can be related to feed rates and fish biomass) is then determined from:

$$F = c_P/T^*$$

As will be seen below, the allowed flux can differ by an order of magnitude depending on the relative importance of advection and diffusion.

Two exact solutions illustrate the concentration fields for a) comparable advection and diffusion and b) strong diffusion.

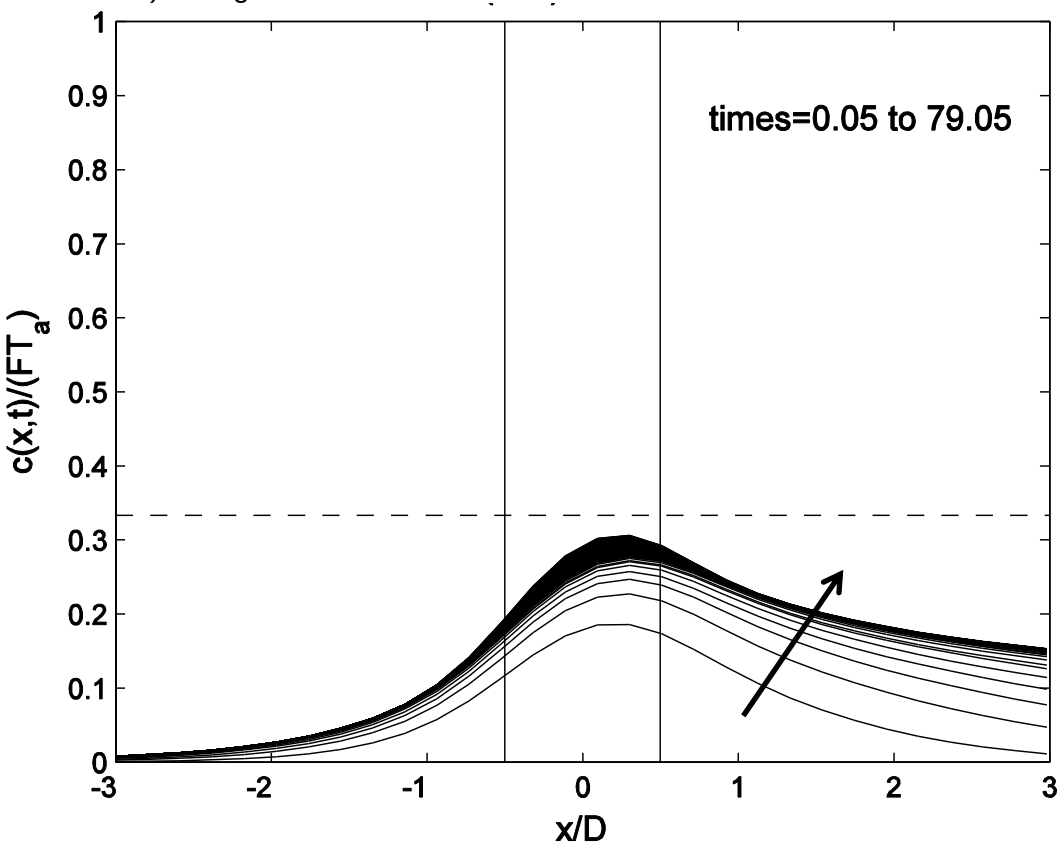

Figure 3.1 Normalised (2-D) nutrient concentration $c(x,0,t)/FT_a$ as a function of distance from the source that lies between x=-D/2 and D/2 - the vertical lines. Solutions are presented at times t equal to (0.05, 1.05, 2.05, 3.05, …., 79.05)T_a and for U= 0.05 m/s and p=2 where advection and diffusive effects are comparable. The horizontal dashed line corresponds to the scale estimate of maximum concentration FT*. The thick black arrow indicates increasing time.

The first case is presented in Figure 3.1 and is for advection in the x - direction (U=0.05 m/s), diffusion in both directions and p=2 so that both effects are comparable. The nutrient source is assumed to lie in the region (3.1) and for a cage where W=D is assumed to be 50 m. The results for the concentration are normalised by the advective time scale T_a. As can be seen, the mean current U leads to larger concentrations in the downstream region x > 0.

A steady concentration field is found after about 20 time scales (T_a) and from (3.2), the predicted maximum concentration, scaled by $F\,T_a$, is given by $c_{max}/F\,T^* = 1/(1+p) = 1/3$ and very close to the exact value of about 0.3. In addition, the maximum occurs near the "downstream" edge of the cage, and is much less than that would be obtained if only advection were present and $c_{max}/F\,T_a = 1$.

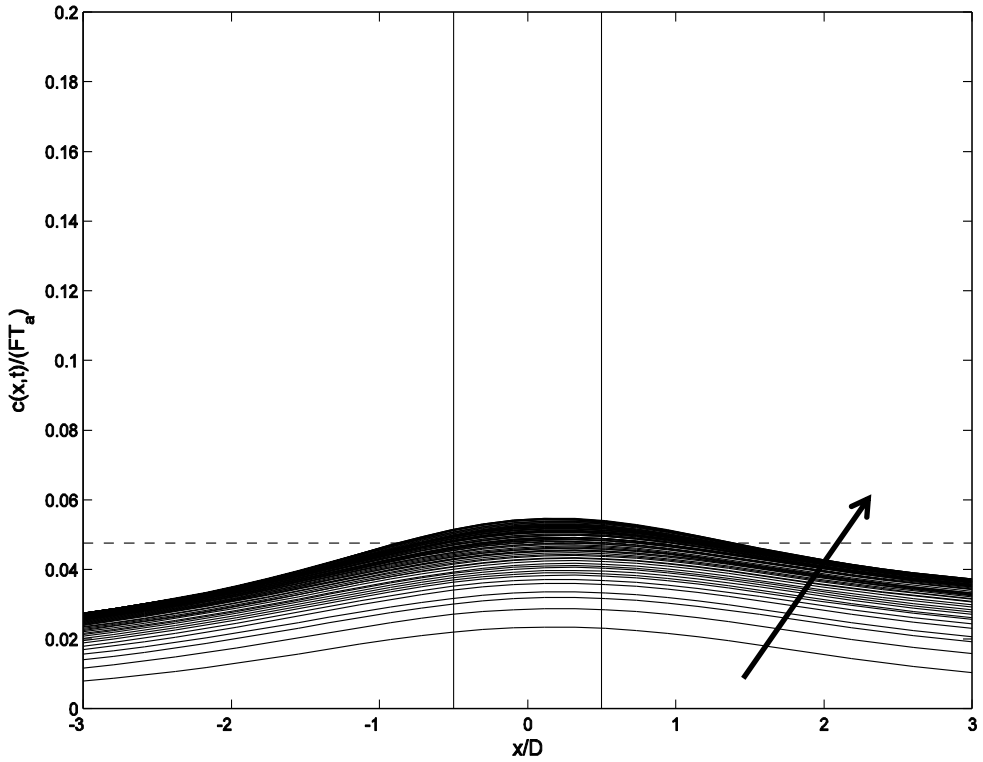

Figure 3.2 Normalised (2-D) nutrient concentration $c(x,0,t)/FT_a$ as a function of distance from the source that lies between x=-D/2 and D/2 - the vertical lines. Solutions are presented at times t equal to (0.05, 1.05, 2.05, 3.05, ….,79.05)T_a and for U=0.05 m/s and p=20 where diffusive effects are dominant. The horizontal dashed line corresponds to the scale estimate of maximum concentration FT*. The thick black arrow indicates increasing time.

Now consider the same case but with diffusion increased by a factor of 10 (p=20). The concentration field (Figure 3.2) is quite smeared and the maximum values again occur in the cage. The predicted maximum value is c_{max} /F T* = 1/(1+p) =1/21 = 0.048 and close to the exact maximum of about 0.054. Moreover, the maximum concentration is about 16% of that shown in Figure 3.1. As expected, increasing the diffusion decreases concentrations.

3.2b Methods: Estimates of the oceanographic parameters

The simple estimates (3.2)-(3.5) needed for the determination of the maximum allowed nutrient flux (and feed-rate) F= c_P/T* involve a number of oceanographic parameters including the mean vector speed (U), the root, mean square (r.m.s.) tidal velocity (U_K) and the horizontal diffusivity. Seasonal (90 day) averages of these parameters have been obtained from the hydrodynamic Spencer Gulf Model (SGM) outlined in Chapter 1. The model grid size is 600 m and the results have been validated against historical data and data collected as part of this project (Figure 1). More detail is presented in Middleton et al. (2013). Results are only presented for winter, although those for the other seasons are qualitatively similar. Estimates of the parameters are presented for all four seasons in CarCap1.0.

For winter, the mean vector speeds are typically very small and of order 2 cm/s.
A notable feature of the Gulf is that it is resonant with respect to the semi-diurnal (12 hr) tides. This leads to r.m.s. (depth averaged) tidal velocities (U_K) that are large (Figure 3.3) and range from 0.3 to 1.0 m/s.

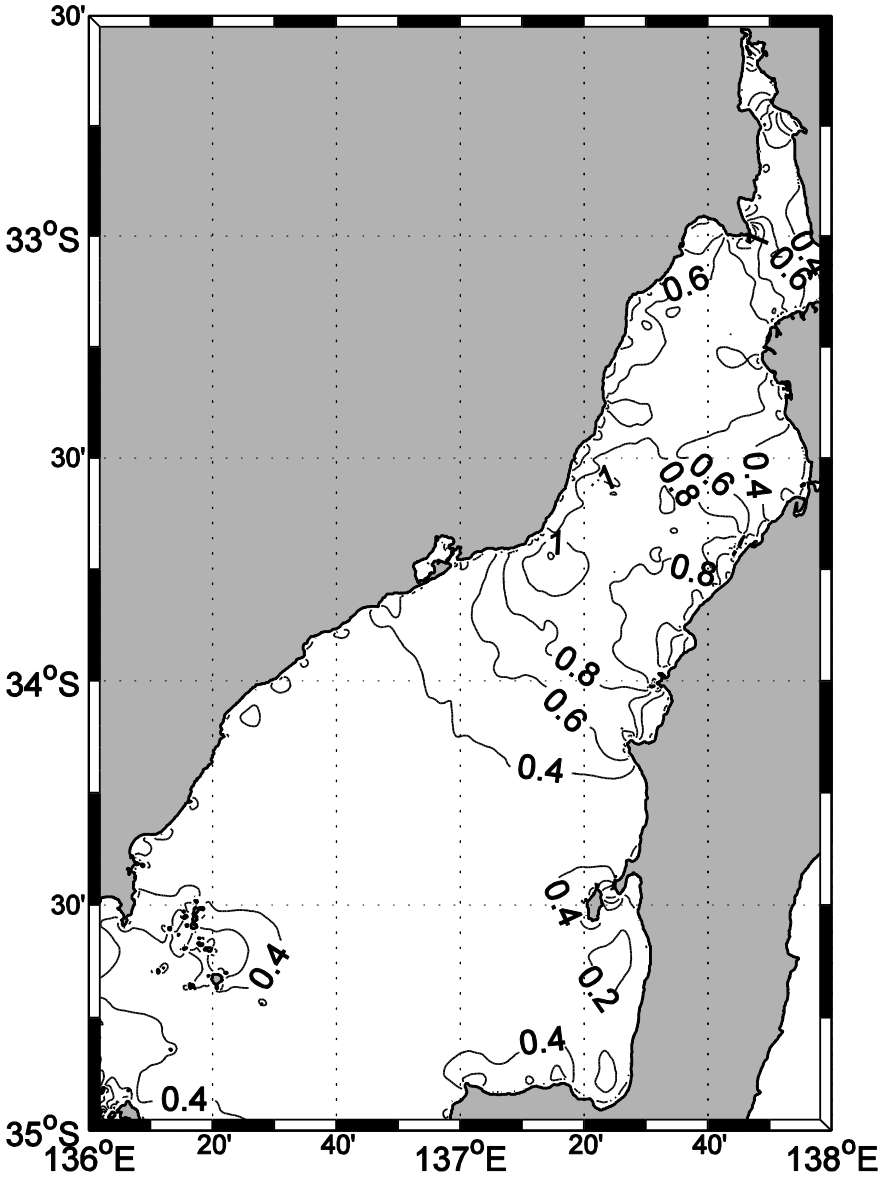

Figure 3.3 The r.m.s. tidal velocity U_K for the gulf and winter. Contours are plotted at 0.2 m/s intervals.

Near the sea floor friction greatly reduces the tidal velocities and the vertical shear gives rise to a process known as shear dispersion and horizontal diffusion is greatly enhanced (Fischer et al. 1979). To understand this mechanism, consider a vertically uniform "line source" of nutrient. After some time, the vertical profile of concentration will become sheared in the vertical due to tidal advection. This gradient is then reduced due to vertical mixing and the effective horizontal diffusion of the nutrient is much larger than that due to turbulence alone. For very strong vertical mixing, the nutrient concentration at each stage of the tide will be constant with depth and the horizontal dispersion largest. In the absence of vertical mixing, the "line source" will be sheared on the flood tide and then returned to its initial state on the ebb tide: the effective horizontal dispersion will be zero.

The efficiency of the dispersion depends on the ratio of the (12 hr) time scale of the tide (T_T) to the time scale T_V for the water column, depth h, to be mixed. The latter scale is given by $T_V=h^2/K_V$ where K_V is the vertical diffusivity. The efficiency function $\gamma = \gamma (T_T / T_V)$ is given by Fischer et al. (1979) and is small for $(T_T / T_V) << 1$ (weak vertical mixing), about 0.7 for

$(T_T / T_V) \sim 1$ and unity for $(T_T / T_V) >> 1$. The effect of vertical mixing appears the model for the shear dispersion coefficient, (Middleton et al 2013) which depends on γ, through:

$$K_s = (1/2)\, \gamma\, (hU_K)^2 / (378 K_v) \qquad (3.6)$$

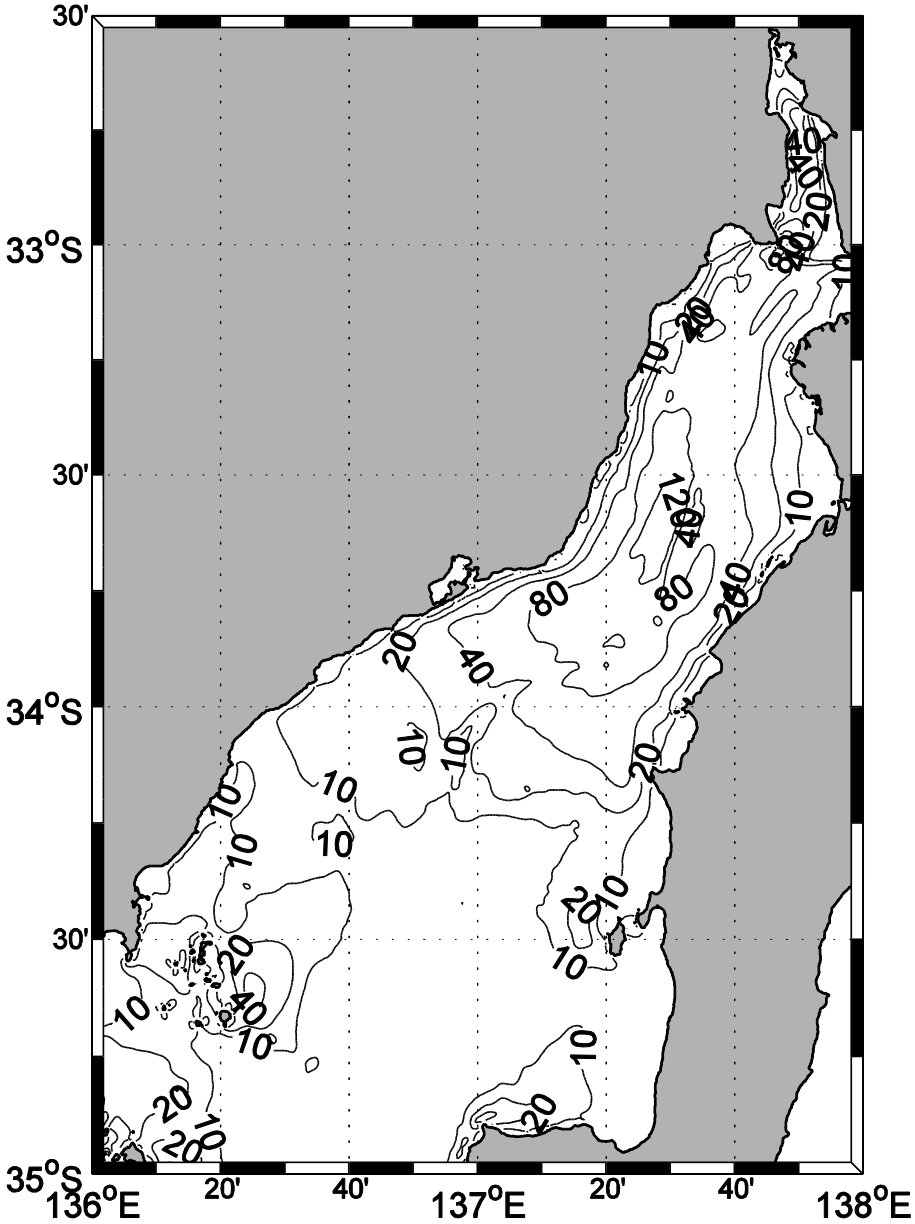

Figure 3.4 The time averaged shear dispersion coefficient K_S calculated from (3.6). Contour levels are [10, 20, 40, 80, 120, 160, 200] m^2/s.

Seasonal and depth averaged values of K_v, T_v and γ were determined from the hydrodynamic model. The vertical mixing scale was found to vary from 5 hrs near the coast to more than 20 hrs in the middle of the Gulf. The corresponding values of the efficiency function γ are 0.9 to 0.3, respectively.

Despite this, the large tidal velocities shown in Figure 3.3 lead to very large values of the shear dispersion coefficient (Figure 3.4). Values of K_S in the mid-Gulf are up to 120 m^2/s. This new and important result implies that the diffusivities greatly exceed those due to turbulence and will lead to very strong diffusion and dilution of nutrients within the Gulf. Moreover, since the r.m.s. tidal velocities U_K are well predicted, the diffusivities given by (3.6) should be reasonably robust.

From the above, the time scales (3.3) to (3.5) of horizontal advection and diffusion, etc. can be determined at the scale of the lease (W = 600 m) and at each (600 m) hydrodynamic model grid cell for all of Spencer Gulf.

3.3a Results and Discussion: Estimated Parameters for Carrying Capacity

Consider first results for the gulf region shown in Figure 3.3. Results are then presented for the much smaller Boston Bay region where cage aquaculture is quite intensive (Figure 1). Results for the time scales of flushing are again based on the scale of the lease (W = 600 m).

The relative importance of diffusion to advection is given in the plot of $p = T_a/T_d$ shown in Figure 3.5. Along the coast and at depths h < 10 m, p is about one so that advection and diffusion are of equal importance. However, as the coastal water depth increases, p also increases to around 3 to 5, as diffusion results in greater flushing. In deeper water and in the mid to upper Gulf, p becomes large (>10), and diffusion greatly enhances and dominates flushing at the 600 m scale of the lease.

The spatial variability of the flushing time scales and p is important to the siting of leases, feed rates and optimising financial return to the industry. Based on the analysis above, a lease sited in deeper coastal water where p is large, can adopt a relatively higher feed rate for a given prescribed concentration maximum $c_{P,}$ since the nutrient flux $F = c_p [1+p] /T_a$ increases with p. Thus, higher feed rates, faster fish growth and/or biomass are “permissible” where diffusion dominates the flushing of the lease. Of course, there will be additional logistical costs in maintaining leases farther offshore. A caveat here is that the predicted concentrations are for one lease only.

Results for the net scale of flushing T* are shown in Figure 3.6. The shear diffusion results in rapid flushing in the mid Gulf (T* ~0.5 hrs). In the region west of Boston Island, the upper gulf and along the coast, the time scale T* is larger (2 - 4 hrs).

Now consider the scale T* for the Boston Bay region, where aquaculture activity is quite intense (Figure 1). For convenience, inner and outer regions are defined in Figure 3.7 by waters to the west and east of the line between Cape Donington and Bollingbroke Point. The typical values of the parameters in the outer region (Table 3.1) are generally similar to those presented above for the lower Gulf.

Table 3.1. The estimated winter oceanographic parameters and time scales for the inner and outer regions of greater Boston Bay.

Parameter	Units	Inner Region (west)	Outer region (east)
U (vector mean speed)	m/s	0.01	0.03
U_K (r.m.s. tidal speed)	m/s	0.1	0.4
K_s (shear dispersion)	m^2/s	1 - 5	7 - 20
$p = T_a / T_d$	-	1	3 - 5
$T^* = T_a /(1+p)$	-	10 – 30	2 - 9

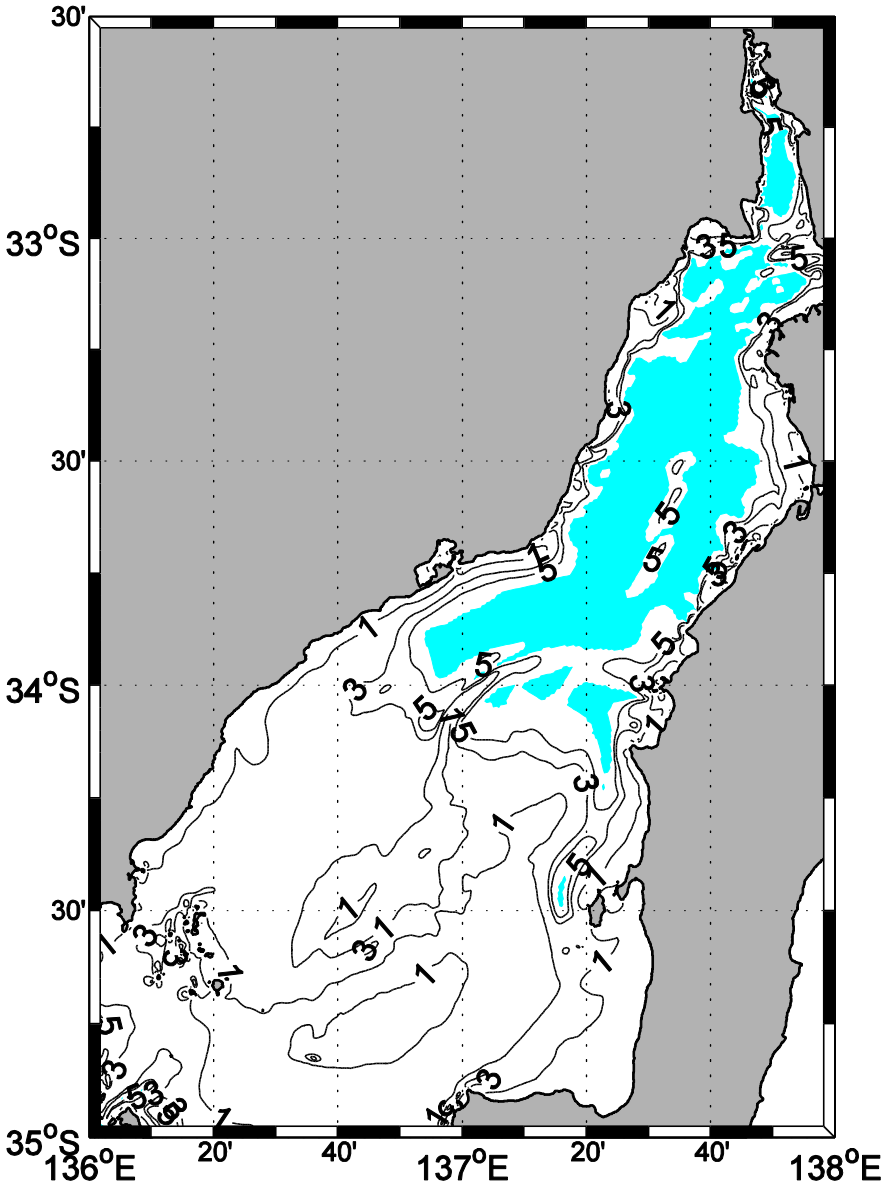

Figure 3.5 The ratio of the advective to diffusive time scales $p=T_a/T_d$ based on time averaged parameters. Contour values plotted are 1, 3 and 5 and the blue shaded area corresponds to values greater than or equal to 10 hrs.

For the inner region, the weaker mean speeds U ~ 0.01 m/s lead to larger flushing scale T_a that is 10 – 30 hrs or 2-3 times those found in the main Gulf. The r.m.s. tidal velocities U_K ~ 0.1 m/s are also smaller than those in the main Gulf where U_K ~ 0.4 - 1.4 m/s, and lead to longer diffusive time scales T_d. In summary, the inner western region is poorly flushed compared to the Gulf generally. In addition, the presence of the islands and bays will lead to greater nutrient concentrations than those predicted by the formulae adopted here. This is because the analysis and formulae have been derived on the assumption that the lease region exists in an infinite ocean with no coastal barriers to nutrient diffusion and dilution.

The approach taken in the above work provides an advanced tool to obtain a reasonable estimate of maximum nutrient fluxes (feed rates) and concentrations. However, it is worth noting, the formulae do not take into account the cumulative effects of multiple leases or the effect of nutrient cycling by ecosystem processes on the predicted nutrient concentration. To account for these processes coupled hydrodynamic-biogeochemical models, such as those presented in Chapters 5 and 6, are necessary.

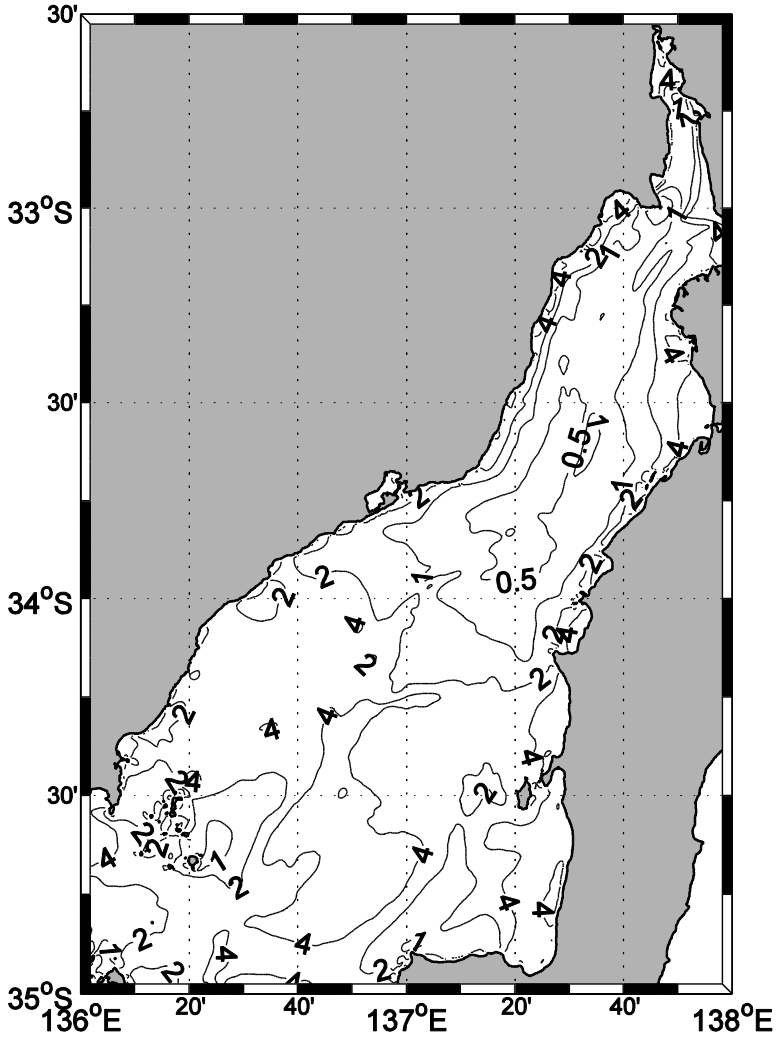

Figure 3.6 The net time scale T*= T_a /(1+p) for flushing of a 600 m square lease. Contour values are [0.5, 1, 2, 4] hours.

The above hydrodynamic model parameters have been incorporated into a graphical user interface (Chapter 6), so as to allow managers to rapidly estimate the maximum nutrient fluxes F and monthly feed rates for new aquaculture lease sites.

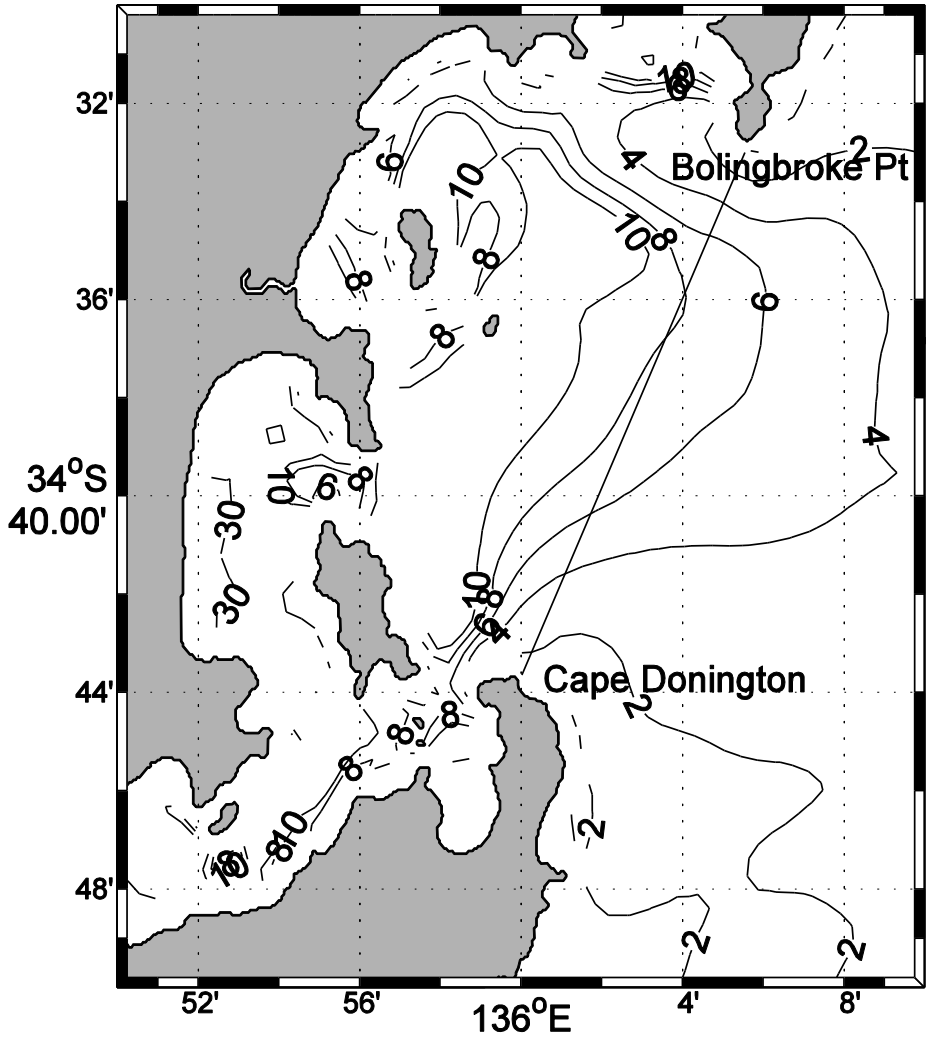

Figure 3.7 The net time scale $T^* = T_a/(1+p)$ for flushing a 600 m square lease and for the larger Boston Bay region. Inner (western) and outer (eastern) sub-regions are defined by the line linking Cape Donington and Bolingbroke Point. Contour values are [2, 4, 6, 8, 10, 30] hours.

3.3b Results and Discussion: carrying capacity at the scale of the lease, cage and zone.

As noted above, information on feed rates (and fluxes) is only available at the scale of the lease and on a monthly basis. The question arises as to how the results above, obtained at the scale of the lease, can be interpreted, as typically, feed is spread over six or so 50 m cages in each lease.

In the companion analysis, Middleton et al. (2013) have considered the case where the feed rate $f=(hD^2)F$ applied to one cage, scale D, is equal to that $f=(hW^2)F$, applied to a lease, scale W. They show that if the diffusive limit pertains at the scale W of the grid, then the maximum concentrations are the same as those at the scale D of the cage. The explanation

for this result is that the very strong diffusion smears the nutrient concentrations to be the same. This is illustrated by Figure 3.2. As noted above, the diffusive limit holds for most of the mid and upper regions of Spencer Gulf.

Now, if the feed rate f is spread over say 6 cages in one lease, then the concentrations of each cage must add to give a maximum value that is equal to that of the lease. That is, the maximum concentrations obtained at the scale of the lease are directly applicable to the realistic scenario of feeding 6 cages in one lease. The result only pertains to the case where the diffusive limit holds and p >> 1.

Middleton et al. (2013) also examined the carrying capacity model that was adopted by Collings et a.l (2007) at the scale of the zone (W*). This model assumes the advective limit where

c_{max}*= F T_a and T_a =W*/U

Middleton et al (2013) show that because the length of the zone W* is much larger than that of the lease (W), the ratio of predicted maximum concentrations c_{max}*/c_{max} = 2W/W* is small and about 1/10th. That is, the Collings flushing model predicts concentration values that may be small compared to those found at the scale of the lease (and cage). Such low concentration values may provide a misleading measure of actual concentrations at the scale of the lease and cage and indicate that feed rates may be higher when they should not.

An additional refinement could also be included in CarCap 1.0. For Spencer Gulf, the semi-diurnal constituents lead to the so called dodge tide, where the 12 hour tidal amplitude is modulated by a 30 day sinusoidal signal. At neap tides, the tidal currents vanish for several days while at spring tides the tidal currents and mixing are at a maximum. In the companion study, Middleton and Doubell (2013) have shown that the feed rates and nutrient fluxes can be modulated so that fluxes are smallest during neaps and largest during spring tides. Using this approach, it can be shown that the nutrient concentrations will not exceed the prescribed maximum value c_P.

The development of the solutions here and CarCap 1.0 will provide managers with a quantitative tool to aid in the sustainable development of finfish aquaculture in the Gulf. However, it should be used with caution and as an aid to management – not a replacement for other tools. Moreover, the guidelines for maximum concentrations (e.g., ANZECC/ARMCANZ 2000) do not specify how long the ecosystem may sustain such values without harm. More research in this area is indicated.

CHAPTER 4. SPATIAL AND TEMPORAL VARIATION IN PRIMARY AND SECONDARY PRODUCTIVITY AND LOWER TROPHIC ECOSYSTEM FUNCTION IN SPENCER GULF

Paul van Ruth, Mark Doubell

4.1 Introduction and Summary

This study represents the first comprehensive examination of lower trophic ecosystem function in Spencer Gulf. The results outlined in the following chapter provide a qualitative and quantitiative description of variability in the structure of the pelagic ecosystem of the Gulf, including planktonic biomass and abundance, physiological rates that lead to the accumulation and decline in this biomass/abundance, and the physical and chemical environmental parameters on which these processes depend. Results from this Chapter have been used in the optimisation, calbration and validation of the Nitrogen, Phytoplankton, Zooplankton and Detritus (NPZD) biological model developed during this project (Objectives 2, 4 and 7).

Spatial and temporal variations in physical and chemical drivers of productivity (*i.e.* irradiance and macro-nutrient concentrations) were closely linked to variations in meteorological and oceanographic conditions. Spencer Gulf was characterised by relatively low concentratons of macro-nutrients (oxides of nitrogen (NO_x), ammonia (NH_3), phosphate (PO_4), silica (SiO_2)), which were often at levels potentially limiting for phytoplankton growth. As a consequence, phytoplankton biomass was typically low by global standards. There was a strong seasonal pattern in primary productivity, with highest productivity in summer/autumn, and low productivity in winter/spring. In response, meso-zooplankton abundances generally decreased through winter into spring and increased in summer, with high grazing impact through summer/autumn, and lower grazing impacts in winter/spring.

Our results suggest that the lower trophic ecosystem of Spencer Gulf is regulated by “bottom up” factors, with potential primary productivity restricted by phosphorus limitation. This is an unusual feature for marine ecosystems, which are more typically nitrogen or silica limited. The result is relatively low rates of primary productivity that prevent the accumulation of high concentrations of phytoplankton biomass. As a consequence, secondary productivity is also relatively low, and grazing plays a minor role in keeping phytoplankton biomass low. In Spencer Gulf, meso-zooplankton appear to be responding to phytoplankton biomass rather than controlling it. While phosphorus limitation likely restricts overall productivity in the region, variations in nitrogen concentrations are driving variations in phytoplankton biomass and abundance, and primary productivity.

The annual cycle of productivity in the Gulf appears to begin with a period of relatively high (for the region) primary and secondary productivity through summer/autumn. Decreasing secondary productivity in late autumn, when primary production remains relatively high, promotes the autumn/early winter peaks in biomass. Increasing phytoplankton growth rates through winter most likely reflect the influx of nutrients from shelf waters and aquaculture, but rates of primary productivity are low due to the short day-lengths and reduced irradiance characteristic of winter months. Decreasing phytoplankton growth rates through spring into summer may signal the bottoming out of productivity as available nutrients disappear, and the beginning of the new cycle.

4.2 Methods

Samples for the analysis of physical, chemical and biological parameters were collected over 10 field surveys between July 2010 and August 2011. Surveys were conducted at approximtely 4-6 weekly intervals at 10 sites covering 5 of the 6 main aquaculture zones in SG (Fig. 1). A Seabird SBE 19-plus conductivity, temperature and depth (CTD) recorder fitted with a Biospherical QSP-2300 underwater Photosynthetically Active Radiation (PAR) sensor with log amplifier (Biospherical Instruments Inc., San Diego, CA, USA) was used at each station during each sampling trip to provide information about sea surface temperature, salinity and irradiance for use in determinations of primary and secondary productivity. At each station, surface (1 m below the water surface) and bottom (1 m above the sea floor) water samples were collected for macro-nutrient, pigment and phytoplankton community analysis. Meso-zooplankton samples were collected via vertical tows with a 150 µm mesh plankton net (30 cm net-mouth diameter), lowered to within 1 m of the sea floor and retrieved vertically at approximately 1 m s^{-1}. Studies investigating primary productivity were undertaken seasonally (in November 2010, and February, April, and August 2011) at stations Z1 1, Z3 1 and Z4 1. Secondary productivity was estimated from zooplankton biomass using temoerature dependent relationships detailed below.

Physical and chemical drivers of productivity

The coefficient of downwelled irradiance (K_d) was derived from the slope of the semilog plot of irradiance versus depth, using data from stations sampled between 7 am and 7 pm. The euphotic depth (Z_{eu}) was calculated by substituting K_d into the Beer-Lambert equation (Kirk 1994):

$$Z = \ln(E_Z / E_O) / K_d$$

Where E_z is the irradiance at depth z, E_o is the surface irradiance, and $Z = Z_{eu}$ when E_z is 1% of E_o (that is, when $\ln(E_z/E_o) = 4.61$).

For each water sample collected, 100 ml was filtered through a 0.45 µm filter for macro-nutrient analysis, which took place at SARDI Aquatic Sciences. Dissolved ammonium (NH_3, APHA-AWWA-WPCF 1998a, detection limit 0.071 µM), oxides of nitrogen (NO_x, APHA-AWWA-WPCF 1998b, detection limit 0.071 µM), phosphate (APHA-AWWA-WPCF 1998c, detection limit 0.032 µM) and silicate (SiO_2, APHA-AWWA-WPCF 1998d, detection limit 0.333 µM) were determined by flow injection analysis with a QuickChem 8500 Automated Ion Analyser.

Phytoplankton biomass, abundance and community composition

The pigment composition of water samples was measured using High Pressure Liquid Chromatography (HPLC). Two litre water samples were filtered through stacked mesh (to retain cells >5 µm) and Whatman GF/F filters (nominal pore size 0.4 µm, to retain cells <5 µm), allowing the examination of size fractionated phytoplankton biomass. Filters were snap-frozen and stored at -80 °C prior to analysis via the gradient elution procedure of Van Heukelem and Thomas (2001) on an Algilent 1200 series HPLC system at SARDI Aquatic Sciences.

A detailed inventory of phytoplankton taxa and their cell abundances was obtained from one litre samples fixed with acidified Lugol's iodine solution. Enumeration and identification of phytoplankton to genus or species level was carried out by Microalgal Services, Victoria, Australia, using traditional taxonomic methods.

Meso-zooplankton biomass, abundance and community composition

For each sample, the contents of the net were washed into a sample jar, topped up to 1 litre, and fixed with formalin (5% final volume). In the laboratory, samples were rinsed through a 35 µm mesh sieve. The contents of the sieve were rinsed into 100 ml measuring cylinders and allowed to settle for 24 hours, after which settling volumes were recorded. Samples were then decanted into 120 ml jars and resuspended in 100 ml of water (i.e. concentrated 10x). Enumeration and identification of meso-zooplankton to genus level was carried out using traditional taxonomic methods. Organism numbers were recorded as individuals m^{-3} in the water column using the volume swept by the net, calculated as the distance travelled by the net (estimated using a general oceanics flow meter suspended in the mouth of the net) multiplied by the area of the net mouth. Settling volumes were recorded as ml m^{-3} using the volume swept, and converted into displacement volumes using a factor for samples without gelatinous zooplankton (0.35, see Wiebe et al. 1975; Wiebe 1988). Displacement volumes were then converted to biomass (mg C) using a factor of 21 for samples with displacement volumes < 1 ml, and a factor of 41 for samples with displacement volumes 1-10 (Bode et al. 1998).

Primary productivity

Primary productivity in the water column was calculated based on methods outlined by Parsons et al. (1984), Lohrenz et al. (1992), and Mackey et al. (1995). Three independent 2 litre surface water samples were collected for each experiment. Samples were collected in opaque bottles and kept cool, with light excluded during experimental set-up. The samples were then exposed to light. Seven irradiance levels were used, by modifying the amount of natural sunlight reaching the experimental bottles via shading. Irradiances included 0% (dark), 0.4%, 1.2%, 1.5%, 6.5%, 50%, and 100% of natural sunlight. From each independent water sample, 1 x 250 ml polycarbonate bottle was prepared for each irradiance level. A ^{14}C stock solution with an activity of 200 µCi ml^{-1} was prepared by adding 2 ml of sodium bicarbonate (GE Life Sciences $NaH^{14}CO_3$, 1 mCi ml^{-1}) to 8 ml of Na_2CO_3 solution (concentration 0.12 g L^{-1}). A known quantity of $NaH^{14}CO_3$ (20 µCi) was mixed into each replicate bottle via the addition of 0.1 ml of ^{14}C stock solution. Bottles were then incubated in a flow-through water bath for 24 hours at *in-situ* water temperatures in sunlight. Irradiance was measured every minute with a Licor Li-1400 data logger and quantum sensor, with the mean irradiance logged every 30 minutes over the 24 hour period, then integrated to provide daily integral irradiances. Post-incubation, samples were filtered at low vacuum pressure through 25 mm Whatman GF/F filters, rinsed with filtered seawater, placed into 5 ml scintillation vials and frozen until further analysis. Filters were thawed at room temperature and exposed to 200 µl of 5N HCl for 12 hours to drive off any remaining $^{14}CO_2$. Four millilitres of scintillation fluid (Ultima Gold high flashpoint LSC cocktail) was then added to each vial and, after 24 hours, radioactivity was determined as disintegrations per minute using a scintillation counter (Packard Tricarb 2100TR). Total CO_2 concentration in the samples was estimated from salinity using the method of Parson et al. (1984). Measured photosynthetic rates were fitted to the hyperbolic tangent equation of Jasby and Platt (1976):

$$P^b = P^b_{MAX} * \tanh(\alpha * I / P^b_{MAX})$$

Where P^b_{max} is the maximum biomass specific photosynthetic rate, α is the photosynthetic efficiency, and I is irradiance. Rates were fitted to the above equation in Microsoft Excel using Solver to provide estimates of α, P^b_{max}, and irradiances corresponding to the onset of light saturation of photosynthesis (I_k). These data were used to examine seasonal variations in daily integral productivities according to Tallings model (Talling 1957):

$$\sum P = P^{b}_{\max} / k_d * Ln(I'_o / 0.5 I_k)$$

Where ΣP is the integral productivity, P^{b}_{max} is the maximum specific photosynthetic rate, I'_o is photosynthetically active radiation (PAR) available just below the sea surface (as measured by CTD), k_d is the attenuation coefficient of downwelled irradiance. Integral productivity was multiplied by daylength (D_{irr} obtained from astronomical information on the Geoscience Australia website (www.ga.gov.au/geodesy/astro) and a correction factor of 0.9 to compensate for the decreasing incoming irradiance either side of solar mid-day to provide daily integral productivity (Talling 1957). Phytoplankton turnover time was calculated as standing stock of Chl *a* over maximum photosynthetic rate ($P_{max} = P^{b}_{max}$ * Chl *a*). The gross phytoplankton growth rate was calculated as the inverse of the turnover time.

Secondary productivity

Meso-zooplankton grazing pressure was estimated from zooplankton biomass. Potential growth of the meso-zooplankton was estimated via the empirical relationship of Huntley and Boyd (1984):

$$G'_{\max} = 0.0542 e^{(0.110T)}$$

Where T is temperature (CTD measured sea surface temperature (SST)) and G'_{max} is the maximum mass-specific food-saturated growth rate, which can be used to estimate the assimilative capacity (AC) of the meso-zooplankton community via:

$$AC = 0.7 G'_{\max}$$

Where 0.7 is the estimate of 70% assimilative efficiency proposed by Conover (1978). The assimilative capacity was multiplied by biomass to give an estimate of the potential grazing rate of the meso-zooplankton community.

4.3 Results and discussion

Physical and chemical drivers of productivity

Vertical attenuation coefficients (K_d) varied greatly in space and time, with ranges for each station outlined in Table 4.1. However, with few exceptions, Z_{eu} was greater than the water depth indicating that throughout this study the water column was well-lit from surface to bottom, and thus primary productivity was unlikely to be limited by available irradiance.

Peak nutrient concentrations (particularly NO_x and SiO_2) were comparable to concentrations measured in the upwelled water mass in the eastern Great Australian Bight (van Ruth 2010a, b). Despite this, macro nutrient concentrations in the Gulf were generally low. Seasonal signals were observed across stations for some macro nutrients (Fig. 4.1). NO_x concentrations were generally < 3 µM, with clear peaks observed in Zones 1 and 2 during winter (June to August) and spring (September to November). Summer (December – February) and autumn (March – May) were characterised by periods of very low concentrations, typically below detection limits. NO_x concentrations in Zones 3, 4 and 5 remained low throughout the year (< 0.5 µM), except for Zone 5 during summer. NH_3 concentrations across all zones were relatively stable throughout the year (< 0.3 µM), with maximum concentrations occuring during the autumn and winter periods, particulary in Zone 3 where concentrations exceeded 1 µM.

Table 4.1 Irradiance parameters calculated using data collected between July 2010 and August 2011 with a Photosynthetically Active Radiation (PAR) sensor coupled to a conductivity, temperature, depth (CTD) recorder. *n* = number of measurements, Z = depth (m), K_d = vertical attenuation coefficient of irradiance (m^{-1}), R^2 is the coefficient of determination for the regression of irradiance with depth, and Z_{eu} is the euphotic depth (m). See Figure 1 for station locations.

Station	*n*	Z	K_d	R^2	Z_{eu}
Z1 1	8	36.0 - 43.5	0.07 - 0.17	0.92 - 0.98	27.1 - 65.9
Z1 2	6	16.0 - 25.1	0.08 - 0.14	0.95 - 0.98	32.9 - 57.6
Z2 1	10	17.6 - 24.0	0.07 - 0.20	0.91 - 0.99	23.1 - 65.9
Z2 2	9	17.0 - 40.1	0.07 - 0.17	0.94 - 0.99	27.1 - 65.9
Z3 1	5	14.1 - 18.5	0.15 - 0.24	0.94 - 0.99	19.2 - 30.7
Z3 2	4	7.7 - 20.1	0.13 - 0.28	0.97 - 0.99	16.5 - 35.5
Z4 1	8	14.8 - 22.8	0.06 - 0.28	0.92 - 0.99	16.5 - 76.8
Z4 2	5	4.6 - 9.2	0.23 - 0.41	0.96 - 0.99	11.2 - 20.0
Z5 1	5	13.0 - 18.6	0.15 - 0.33	0.93 - 0.98	14.0 - 30.7
Z5 2	3	8.1 - 12.6	0.19 - 0.26	0.97 - 0.99	17.7 -24.3

PO_4 concentrations were typically very low both spatially and temporally, with 145 of the 196 samples measuring below the detectable limit (0.01 µM). Intermittent high concentrations of PO_4, as large as 1.07 µM, were observed at different stations, but showed no clear pattern in space or time. Si levels were typically low, with concentrations ranging from ~0.5 - 1 µM for Zones 1, 2, 4 and 5 across the study period. Si concentrations were always greatest in Zone 3, where a clear peak in concentrations (~2 - 5 µM) was observed during the autumn/winter period.

Examination of stoichiometric ratios (Si:N and P:N, where N is equal to NOx + NH_3) indicated periods of potential nutrient limitation for each of the measured macro-nutrients in each zone, with the exception of Si in Zone 3 (Fig. 4.2). However, stoichiometric ratios only become useful as indicators of potential nutrient limitation of primary productivity if nutrient concentrations are below levels considered limiting to phytoplankton growth (see van Ruth et al 2010a). Figure 4.1 indicates periods when each macro-nutrient is at concentrations likely to limit phytoplankton growth. Of most interest, however, is the fact that PO_4 is almost always found at concentrations likely to limit phytoplankton growth. This is very unusual for marine waters. A limited supply of phosphorus has been shown to affect oceanic primary productivity over long time scales (thousands of years), by influencing the supply of nitrogen. However, phosphorus is not generally a factor limiting marine phytoplankton growth on shorter time scales (such as seasonal scales, Tyrrell 1999). Nitrogen inputs into the Gulf appear to be large enough to promote the draw-down of phosphorus levels to limiting concentrations, making Spencer Gulf a somewhat unique, phosphorus limited marine ecosystem. However, while phosphorus limitation likely restricts overall productivity in the region, variations in nitrogen concentrations are driving variations in phytoplankton biomass and abundance, and primary productivity.

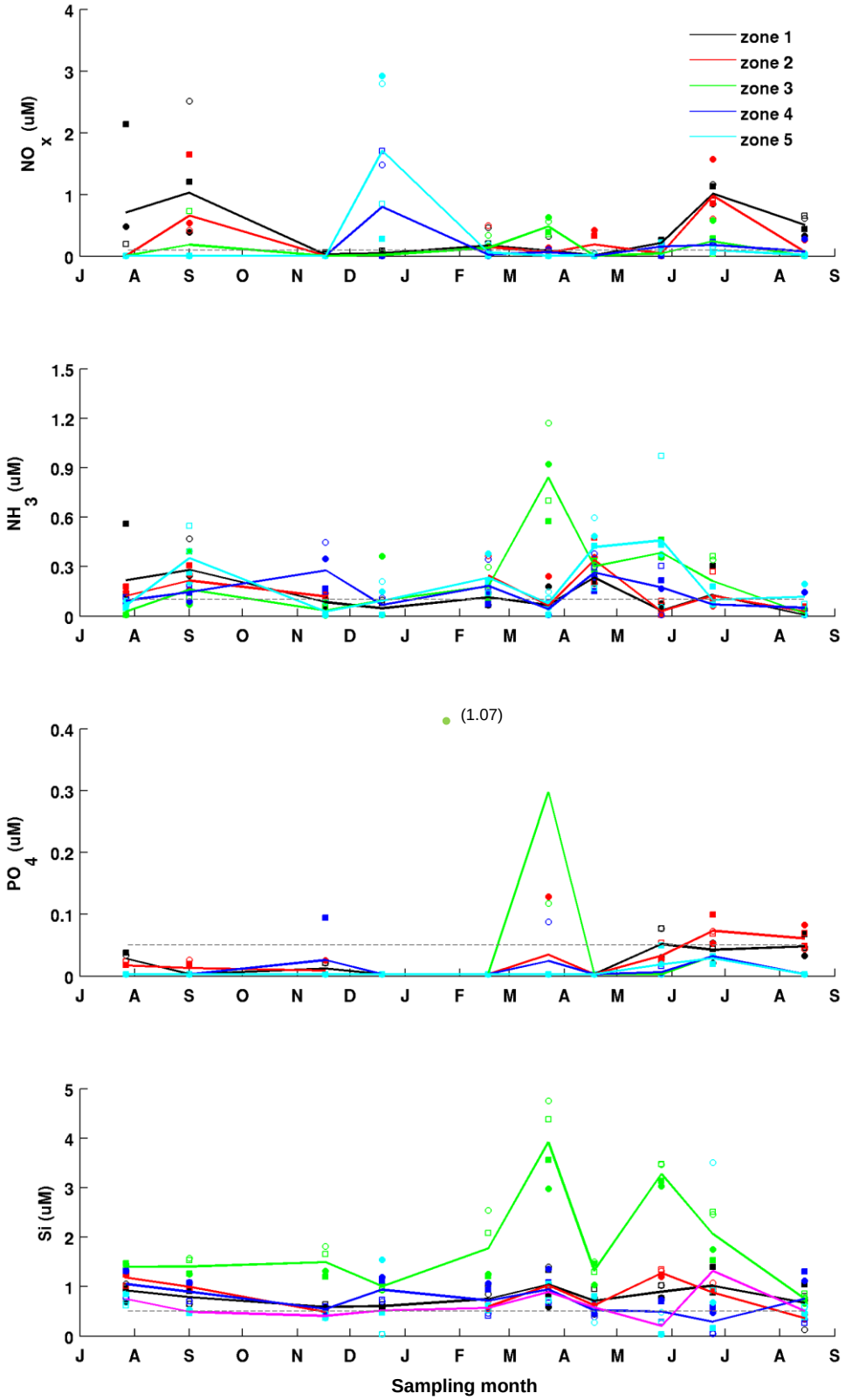

Figure 4.1 Temporal variation in macro-nutrient concentrations (µM) in Spencer Gulf between July 2010 and August 2011. Surface and bottom samples indicated by circles and squares, respectively. Solid symbols represent station 1 in a given zone, open symbols represent station 2 in that zone. Solid lines represent the mean concentration for each zone. Grey dashed lines represent nutrient levels considered limiting for phytoplankton growth (see van Ruth et al. 2010a). See Figure 1 for station locations.

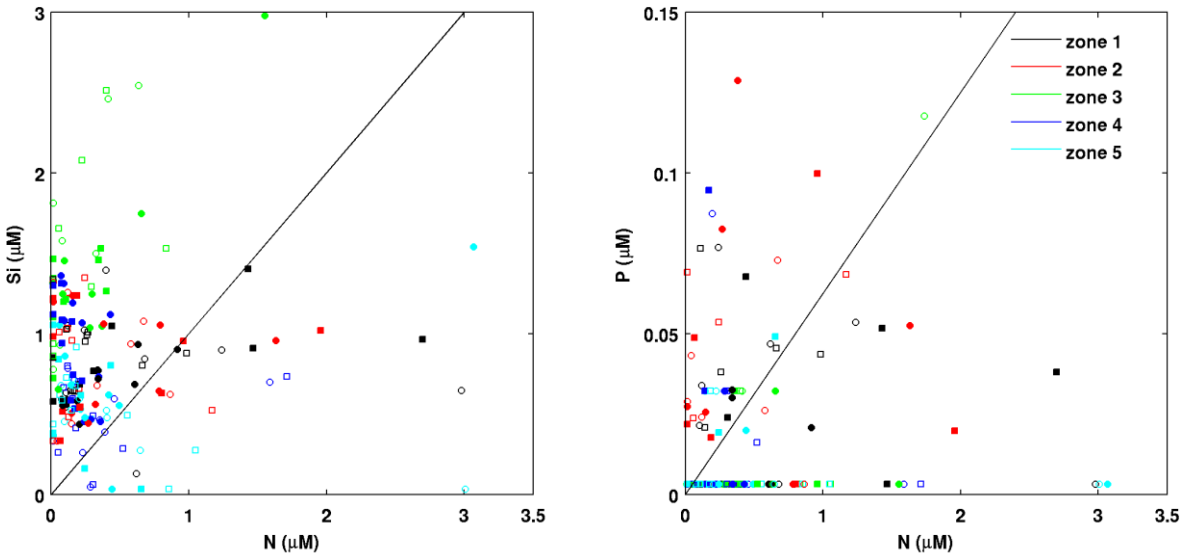

Figure 4.2 Variation in stoichiometric ratios in Spencer Gulf between July 2010 and August 2011. Solid symbols represent station 1 in a given zone, open symbols represent station 2 in that zone. Solid black lines represent the Redfiled ratio for the elemental composition of phytoplankton (1:1 Si:N, 16:1 N:P). Points above the line indicate potential nitrogen limitation. Points below the line indicate potential silica (left) or phosphorus (right) limitiation. See Figure 1 for station locations.

Phytoplankton biomass and abundance

Phytoplankton biomass, measured as the concentration of chlorophyll *a* (chl *a),* was generally low (< 0.5 µg L^{-1}) across the Gulf, comparable to levels reported for oligotrophic waters off western and south eastern Australia (0.1 – 0.7 µg L^{-1}, Gibbs et al. 1986; Hallegraeff and Jeffrey 1993; Hanson et al. 2005), and offshore waters of the eastern and central Great Australian Bight (< 0.1 – 0.4 µg L^{-1}, van Ruth et al 2010a). The highest biomass (~0.8 - 0.9 µg L^{-1}) was observed in Zone 3 during summer and Zone 5 during winter (Fig. 4.3), but peaks in chl a concentrations were ~50% lower than previously measured in south western Spencer Gulf (1.5 – 2.5 µg L^{-1}, Port Lincoln Tuna Farming Zone, van Ruth et al 2009a), but were similar to peak concentrations reported for south eastern Gulf St Vincent (~0.8 µg L^{-1}, van Ruth 2010, 2012), and concentrations measured in mid-shelf and coastal waters in the eastern and central Great Australian Bight (0.6 – 1.0 µg L^{-1}, van Ruth et al 2010a). For Zones 1, 2, 4 and 5a, clear seasonal pattern was observed in the temporal variation of phytoplankton biomass, characterised by low biomass during late winter/spring and higher biomass in autumn/early winter. Size fractionated analysis showed the phytoplankton biomass in Spencer Gulf was dominated by cells smaller than 5 µm at all times (Fig. 4.3).

Analysis of the ratio of different phytoplankton accessory pigments to total chl *a* showed the phytoplankton community in Spencer Gulf was dominated by three main taxa; diatoms, cyanobacteria and haptophytes (Fig. 4.4). Throughout the study period cyanobacteria generally dominated the phytoplankton community in Zones 1, 2, 4 and 5. Diatoms dominated the community in Zone 3 (the only Zone which did not show any evidence of potential silica limitation of phytoplankton growth).

Mean total phytoplankton abundances were generally < 200,000 cells L^{-1} (Fig. 4.5). Mean abundances in Zone 3 and Zone 5 were generally higher than mean abundances in Zones 1, 2, and 4. Peaks in total phytoplankton abundance were driven by peaks in diatom abundance and, to a lesser extent, peaks in flagellate abundance. Dinoflagellate

abundances remained below 100,000 cells L^{-1} throughout the study. Mean abundances in Zone 3 increased through summer to peak in March 2011. Peaks in mean total abundance in Zone 5 occurred in August/September 2010, December 2010 and June 2011. Mean total phytoplankton abundance was lowest in Zone 2, generally < 100,000 cells L^{-1}. Interestingly, the winter 2011 peaks in total abundance in Zones 1 and 4 had different drivers. The increase in Zone 1 was predominately due to flagellates, and the increase in Zone 4 was due to diatoms.

Analysis of the drivers of variation in phytoplankton community composition reveals that temporal variation in the phytoplankton community was most strongly influenced by changes in temperature and PAR, such as would be expected in the transition from summer to winter. Spatial variation in community composition was most strongly influenced by changes in density and the availability of NH_3 and NO_x (van Ruth and Doubell 2013).

The patterns in phytoplankton biomass and abundance reported in this study (autumn/winter peaks, dominance of total biomass by the small size fraction (cells < 5 µm in size), diatom driven variations in total abundance are in agreement with patterns identified in previous studies in south western Spencer Gulf (van Ruth et al 2009a) and south eastern Gulf St Vincent (van Ruth 2010, 2012).

Meso-zooplankton biomass and abundance

There were no clear spatial or temporal patterns in mean meso-zooplankton biomass or abundance (Fig. 4.6), indicative of the typical patchy nature of plankton community dynamics (Mackas et al. 1985). There was a general decrease through winter into spring before an increase through summer, decreasing again through autumn into winter. Biomass was generally < 60 mg C m^{-3}, with peaks in Zone 1 in December 2010 and June 2011. Zones 3 and 4 had peak biomass in summer (~Dec – Feb), and Zone 5 peaked in December 2010. Biomass in Zone 2 was < 30 mg C m^{-3} for the duration of the study. Abundances were generally < 40,000 organisms m^{-3}, in agreement with previous studies in south western Spencer Gulf (van Ruth et al. 2009b, c). Peaks in abundance in Zone 1 occurred in July 2010 and June 2011. Mean abundance in Zone 3 peaked in February 2011 and in Zone 4 in July 2010. In Zone 5 the peak occurred in April 20011. Mean abundances in Zone 2 were < 10,000 organisms m^{-3} throughout the study. Peaks in zooplankton biomass and abundance were not coincident with peaks in phytoplankton biomass and abundance due to the uncoupling of phytoplankton and zooplankton life cycles (Trumble et al. 1981; Mann and Lazier 1996).

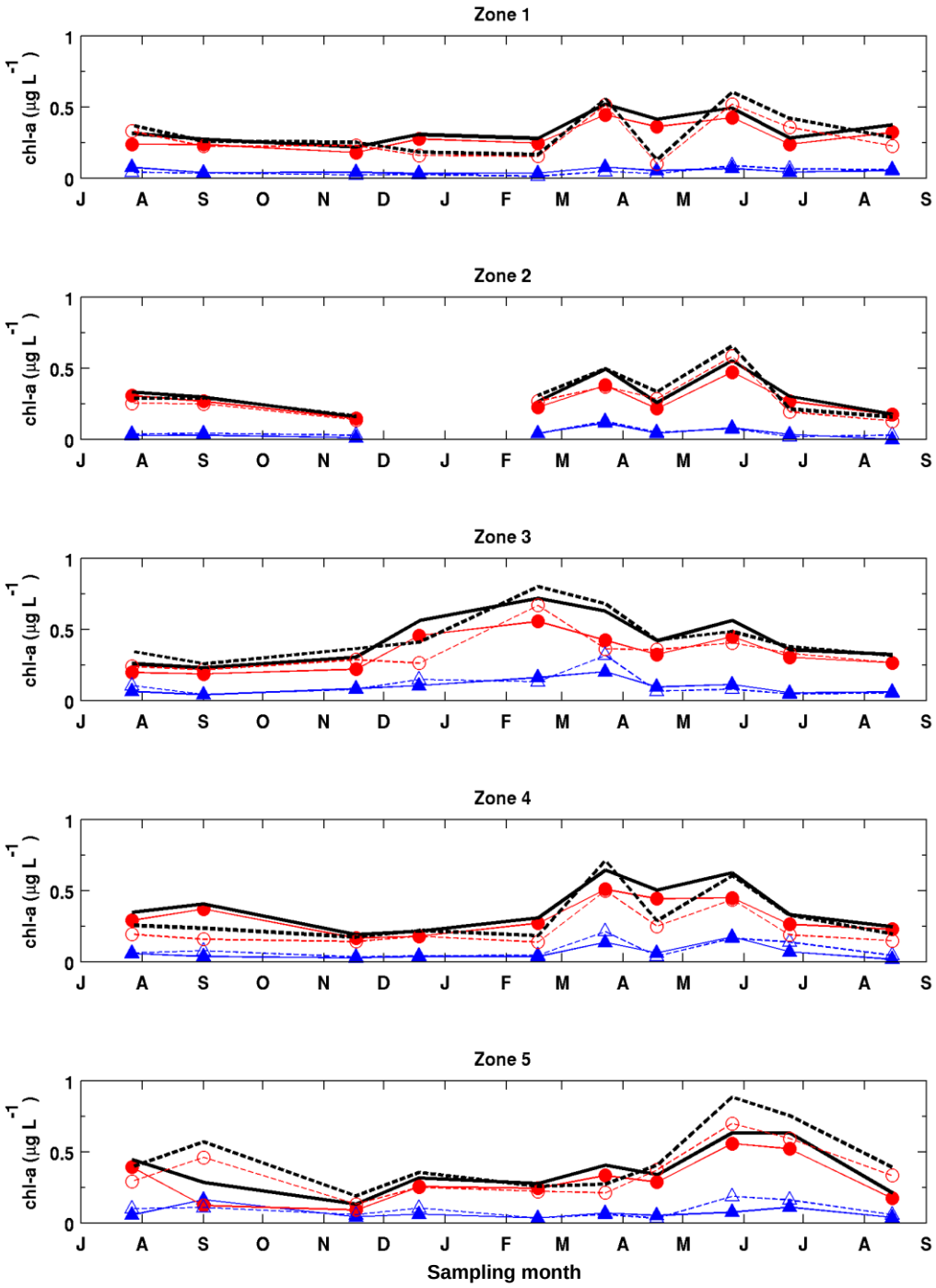

Figure 4.3 Variation in phytoplankton biomass (Chl *a*) in Spencer Gulf between July 2010 and August 2011. Solid symbols and lines represent station 1 in a given zone, open symbols and dashed lines represent station 2 in that zone. Black lines - total depth averaged chl *a* concentration. Blue line and triangle markers – depth averaged chl *a* contribution from cells > 5 µM in size. Red line and circle markers - depth averaged chl *a* contribution from cells < 5 µM in size. See Figure 1 for zone locations.

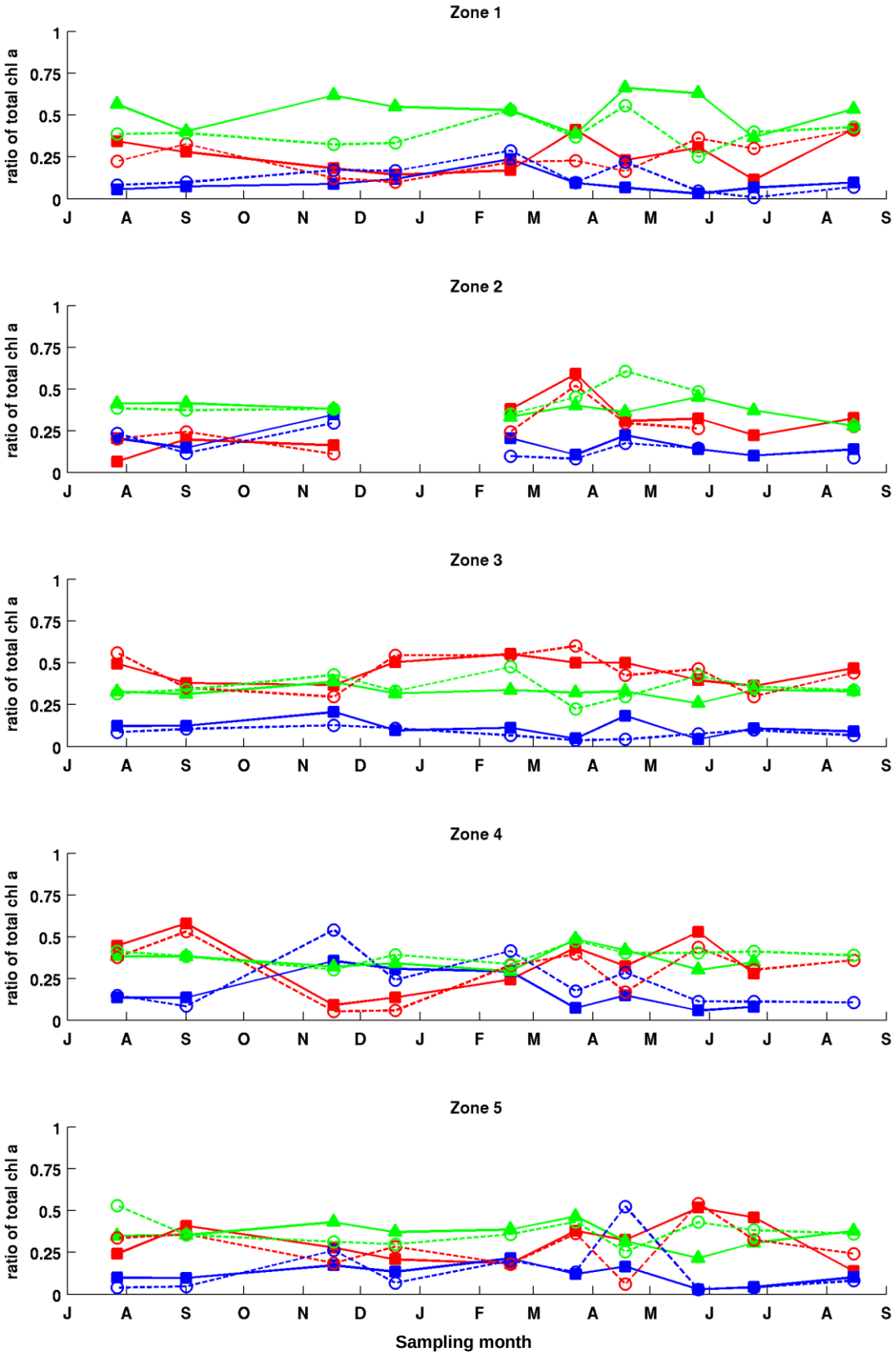

Figure 4.4 Variation in the community composition of phytoplankton in Spencer Gulf between July 2010 and August 2011, determined by the analysis of marker pigments. Blue - cyanobacteria, green - haptophytes, red - diatoms. Solid symbols and lines represent station 1 in a given zone, open symbols and dashed lines represent station 2 in that zone. See Figure 1 for zone locations.

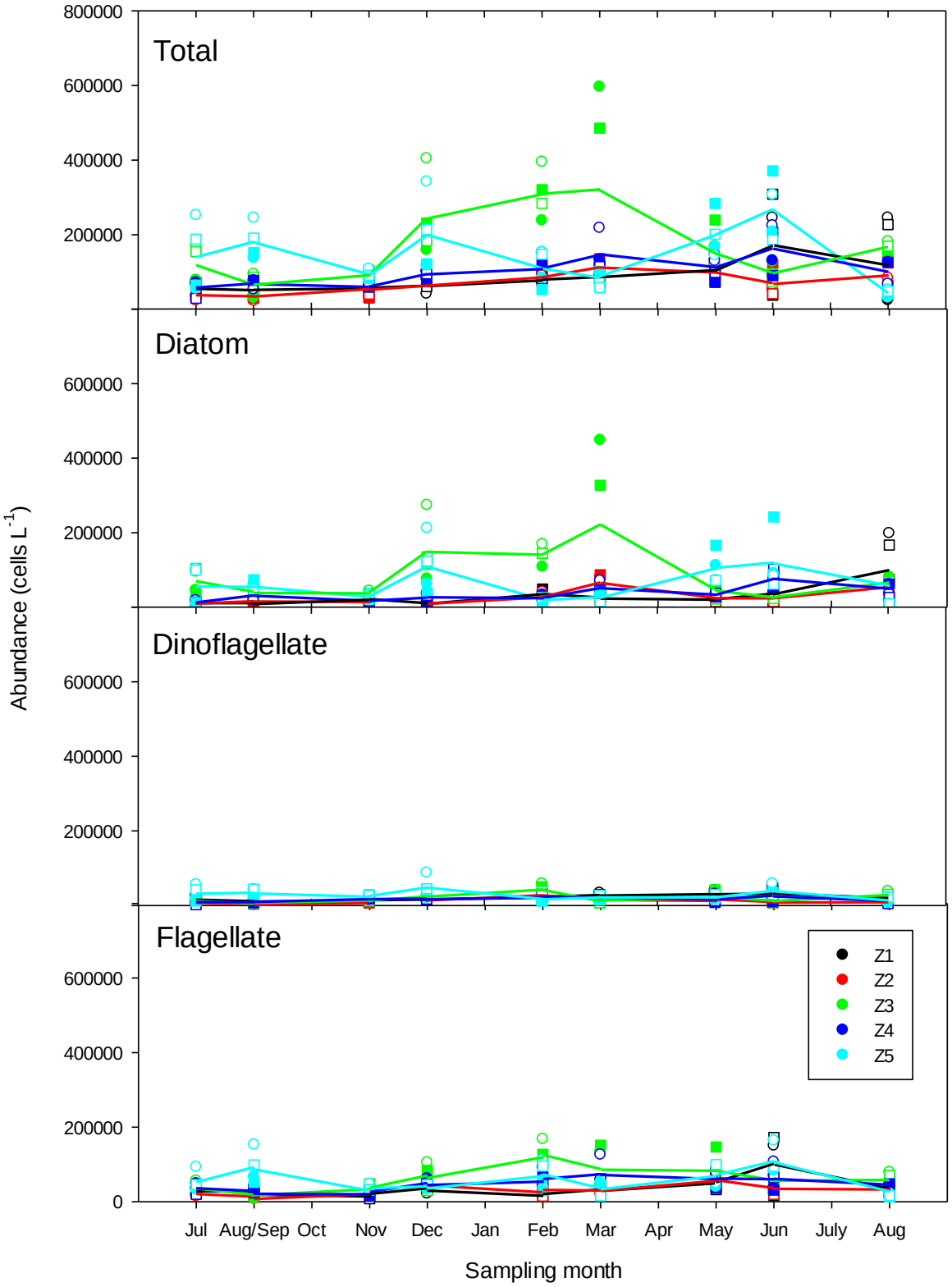

Figure 4.5 Phytoplankton abundances measured in Spencer Gulf between July 2010 and August 2011. See Figure 1 for station locations. Circles represent surface samples, squares represent bottom samples. Solid symbols represent station 1 in a given zone, open symbols represent station 2 in that zone. Lines indicate mean abundance for a given zone.

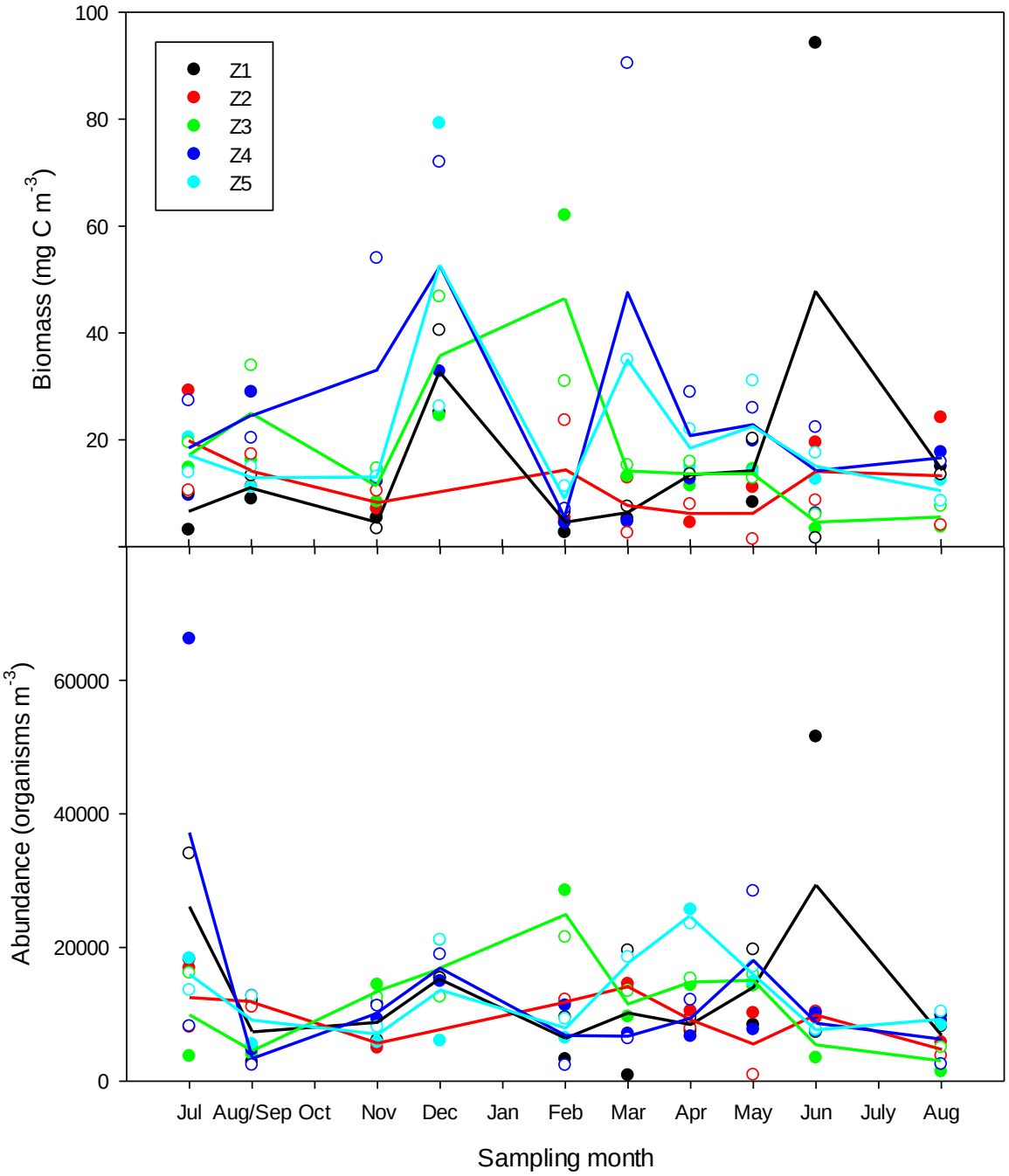

Figure 4.6 Meso-zooplankton biomass and abundance measured in Spencer Gulf between July 2010 and August 2011. See Figure 1 for station locations. Solid symbols represent station 1 in a given zone, open symbols represent station 2 in that zone. Lines indicate means for a given zone.

Primary productivity

Primary productivity was lowest in winter/spring (<200 mg C m^{-2} d^{-1}), and highest in summer/autumn (317 – 859 mg C m^{-2} d^{-1}, Table 4.2, Fig. 4.7). A similar pattern has been reported previously for waters of south western Spencer Gulf (van Ruth et a.l 2009b, c). Highest productivity occurred throughout the Gulf in February 2011, with Zone 4 the most productive (859 mg C m^{-2} d^{-1}). Summer/autumn rates of primary productivity could be classified as low to intermediate on a global scale, and tended toward the lower end of the scale of rates reported for mid-shelf and coastal waters of the eastern and central Great Australian Bight (800 - 1600 mg C m^{-2} day^{-1}, van Ruth et al 2010a), and for localised upwellings off south west Western Australia (849 – 1310 mg C m^{-2} day^{-1}, Hanson et al 2005). Winter productivities were low, comparable to rates measured in oligotrophic waters of a) the Leeuwin current off south west Western Australia (110 - 530 mg C m^{-2} d^{-1}, Hanson et al. 2005), b) the Australian Indonesian Coastal and South Sub-Tropical Convergence provinces defined by Longhurst et al (1995) and c) the north and South Atlantic sub-tropical gyres (18 - 362 mg C m^{-2} d^{-1}, Maranon et al 2003). There were no clear spatial patterns in primary productivity, although productivity was generally highest in Zone 4, except in April 2011. P^b_{max} was generally higher in Zones 3 and 4 (> 4 mg C (mg chl)$^{-1}$ hr^{-1}, Table 4.2). Highest P^b_{max} was measured in Zone 3 in April 2011 (4.92 mg C (mg chl)$^{-1}$ hr^{-1}), but this didn't translate into high daily integral productivity due to the short day length at that time of the year. Low daily integral productivity in November 2010 was due to low irradiances, and low productivity in August 2011 was due to low irradiances, short day lengths, and particularly in Zone 1, low P^b_{max}. Gross phytoplankton growth rates were high in November 2010, decreasing into February 2011, before increasing again through April 2011 to peak in August 2011 (Fig. 4.7).

Table 4.2 Seasonal variation in photosynthesis/irradiance parameters used in the calculation of daily integral primary productivity in Spencer Gulf. D_{irr} is day length in decimal hours, I'_o is the irradiance just below the sea surface (µmol m^{-2} s^{-1}), K_d is the attenuation coefficient of downwelled irradiance (m^{-1}), Chl *a* is surface extracted chlorophyll *a* concentration (µg L^{-1}), I_k is the irradiance corresponding to the onset of light saturation of photosynthesis (µmol m^{-2} s^{-1}), α is the photosynthetic efficiency (mg C (mg chl)$^{-1}$ hr^{-1} (µmol m^{-2} s^{-1})$^{-1}$), P^b_{max} is the biomass specific maximum photosynthetic rate (mg C (mg chl)$^{-1}$ hr^{-1}), and DIP is the daily integral productivity (mg C m^{-2} d^{-1}). See Figure 1 for station locations.

Station	Month	D_{irr}	I'_o	K_d	Chl *a*	I_k	Alpha	P^b_{max}	DIP
Z1_1	Nov-10	14.0	150	0.12	0.2	18.36	0.14	2.58	151
	Feb-11	13.3	1392	0.07	0.2	18.25	0.19	3.39	582
	Apr-11	11.2	1411	0.09	0.4	46.95	0.05	2.26	414
	Aug-11	10.8	1652	0.10	0.2	15.83	0.10	1.66	172
Z3_1	Nov-10	13.9	150	0.17	0.3	45.41	0.06	2.79	116
	Feb-11	13.2	385	0.17	0.6	12.92	0.34	4.35	746
	Apr-11	11.2	884	0.21	0.3	15.44	0.32	4.92	336
	Aug-11	10.9	395	0.15	0.3	18.94	0.11	2.08	152
Z4_1	Nov-10	13.9	150	0.13	0.2	15.84	0.19	3.06	173
	Feb-11	13.3	1392	0.11	0.3	9.17	0.50	4.62	859
	Apr-11	11.2	884	0.28	0.5	11.81	0.30	3.52	317
	Aug-11	10.8	395	0.10	0.2	15.60	0.20	3.10	238

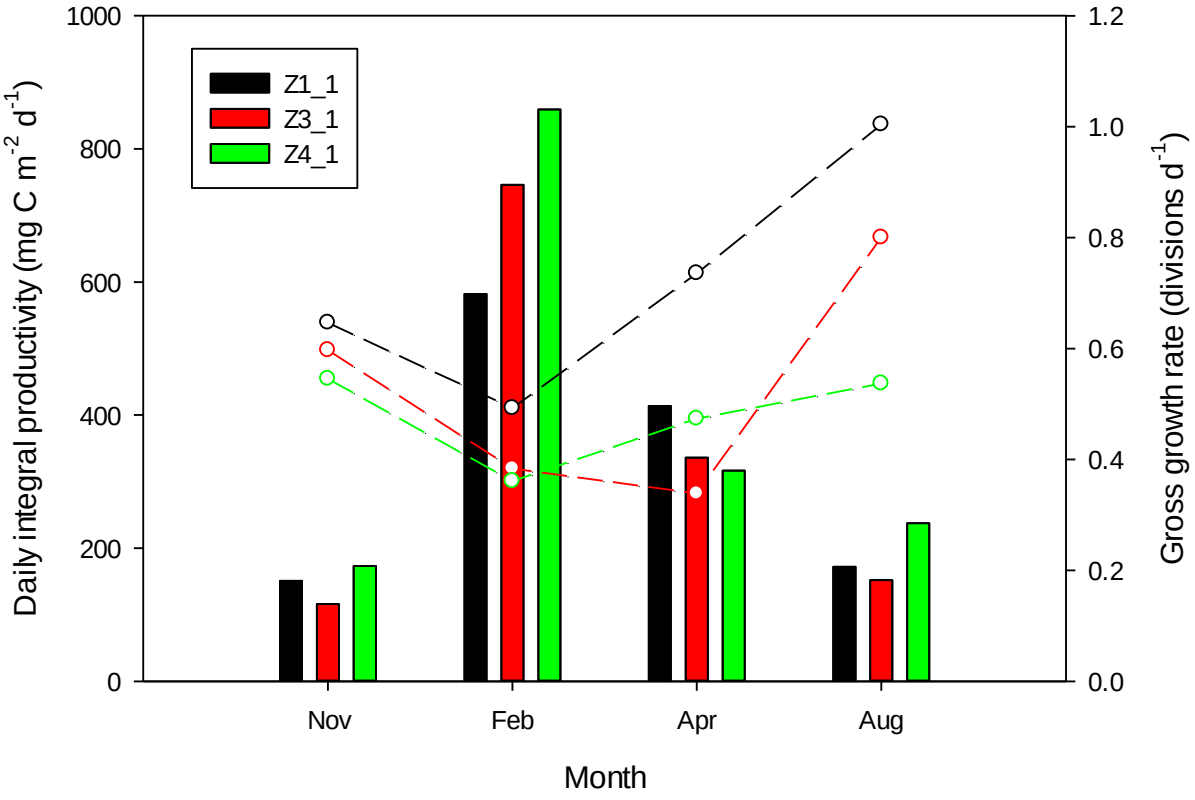

Figure 4.7 Seasonal variation in daily integral primary productivity (bars) and gross phytoplankton growth rate (dashed lines) in Spencer Gulf between November 2010 and August 2011. See Figure 1 for station locations.

Secondary productivity

Grazing impact was also spatially and temporally variable in this study (Fig. 4.8). Peaks in mean grazing impact were generally due to high impact in one of the stations within a zone. For example, in Zone 1, grazing peaked in December 2010 and again in June 2011. The December peak was driven by high biomass at station Z1_2, and the June peak by high biomass at Z1_1 (Table 4.3). Mean grazing impacts were generally higher through summer/autumn (20 -51 mg C m^{-3} d^{-1}), corresponding with periods of high phytoplankton biomass, with lower grazing impacts in winter/spring (5 – 20 mg C m^{-3} d^{-1}). The highest mean grazing impact was measured in Zone 3 in February 2011 (51.0 mg C m^{-3} d^{-1}, Fig. 4.8). This was 30-50% lower than the grazing impact reported previously for south western Spencer Gulf (~75 – 110 mg C m^{-3} d^{-1}, Port Lincoln Tuna Farming Zone, van Ruth et al. 2009b, c).

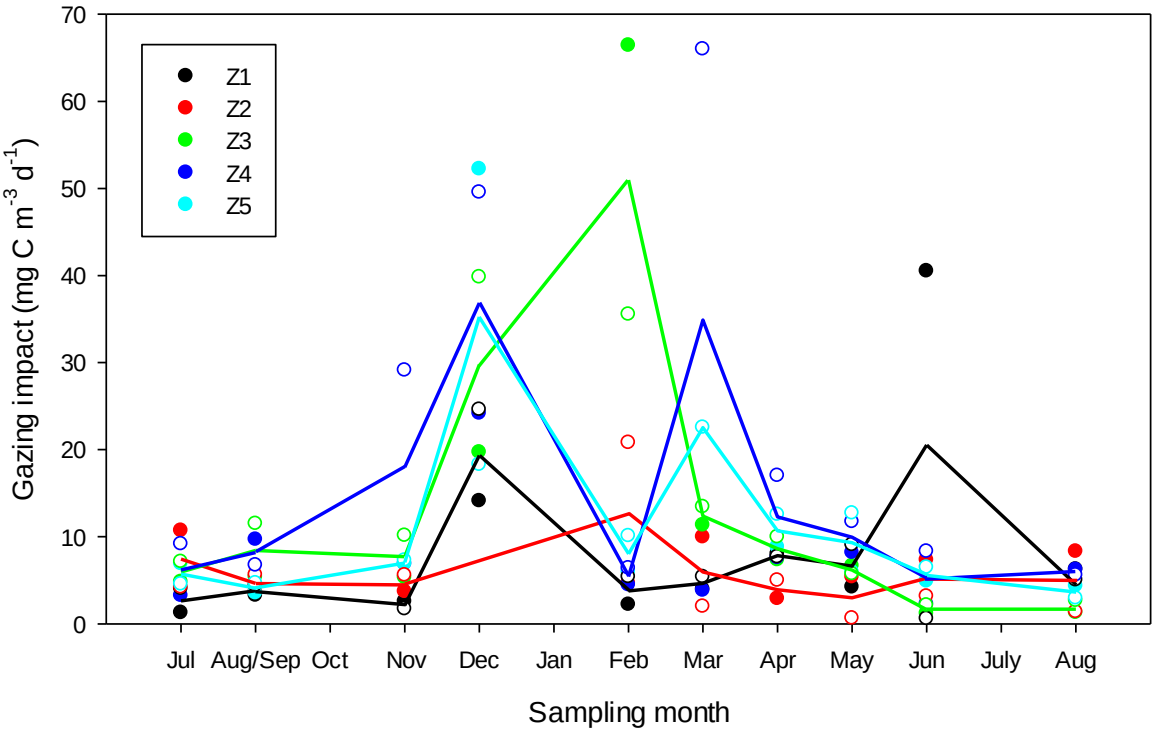

Figure 4.8 Meso-zooplankton grazing impact measured in Spencer Gulf between July 2010 and August 2011. See Figure 1 for station locations. Solid symbols represent station 1 in a given zone, open symbols represent station 2 in that zone. Lines indicate means for a given zone.

CHAPTER 5. MODELLING BIOGEOCHEMICAL CYCLES IN SPENCER GULF: DEVELOPMENT OF A NITROGEN-BASED ECOSYSTEM MODEL AND IMPLICATIONS FOT AQUACULTURE

Mark J. Doubell, Charles James, Paul van Ruth, John Luick, John Middleton

5.1 Introduction and Summary

Nitrogen from finfish aquaculture is the largest source of nutrient discharged into Spencer Gulf's marine environment, and is estimated to account for approximately 95% of the annual anthropogenic nitrogen load (Gaylard, unpublished). Nitrogen is considered the key nutrient which limits plant growth in temperate coastal marine systems (e.g. Nixon 1995; Howarth and Marino 2006), and the cycling of nitrogen by ecosystems can have a major impact on the fate and distribution of the chemicals and biological components of marine ecosystems (Jørgensen 1996). However, the consequences of anthropogenic nutrient discharges on the eutrophication and carrying capacity of Spencer Gulf are poorly understood. The ecosystem model described hereafter provides a three-dimensional physical, chemical and biological simulation that can assist in understanding the carrying capacity of the Gulf's waters for aquaculture.

The biogeochemical model of Fennel et al. (2006) was adapted to the Spencer Gulf marine system (Objective 2). The model includes a sediment component to simulate benthic nitrification-denitrification processes, which play a significant role in the nitrogen cycle of coastal systems (e.g. Nixon and Pilson 1983; Bianucci et al. 2012). Information from field studies (Chapter 4) and the literature is used to parameterise the model. The model includes nutrient imports from the shelf as well as anthropogenic nutrient loads from aquaculture supplementary feeds and other major sources. Validation against data collected during the 2010-2011 field survey (Chapter 4) is used here to show the model is capable of reproducing the general distribution of nutrients, dissolved oxygen and phytoplankton.

Simulation results (Objective 4) indicate the annual import of dissolved nitrogen from the shelf, and nitrogen losses due to benthic (microbial) denitrification, are the largest sources and sinks of nitrogen and strongly influence the yearly cycle of the Gulf's chemical and biological systems. Scenario studies using the model provide a tool for further assessing the cumulative impact of increased anthropogenic loads on the distribution, transport, and accumulation of nutrients and phytoplankton. The scenario studies indicate a small reduction in the buffering capacity of sediment denitrification with increases in aquaculture discharges. Localised increases of up to 50 - 100% for nutrients and phytoplankton are predicted at the scale of aquaculture zones when the total annual nutrient load is increased by a factor of four. However, with the exception of poorly flushed shallow bays in the vicinity of discharges, concentrations of nutrients and phytoplankton typically remain below the ANZECC/ARMCANZ (2000) water quality guidelines.

The model simulations can be rapidly accessed by managers using the newly developed 'CarCap 1.0' graphical user interface (Chapter 6) to make informed decisions on the potential cumulative effects of anthropogenic nutrient loads. By including the influence of ecosystem processes on water quality, the developed model will provide PIRSA with better tools to inform and integrate the process of coastal management for the sustainable development of the aquaculture industry (Objective 7).

5.2 Methods: the Biogeochemical Model

The biogeochemical model adapted and coupled to the Spencer Gulf Model (Chapter 1) was the open-source model developed by Fennel et al. (2006) to understand and quantify biogeochemical cycling in coastal systems (e.g. Bianucci et al. 2012). The model is a representation of the pelagic nitrogen cycle using seven state variables; dissolved inorganic nitrogen (DIN), nitrate (NO_3), ammonium (NH_4), phytoplankton (P), zooplankton (Z), small detritus (D_s) and large detritus (D_L). All state variables have common units (mmol N m^{-3}). The model also tracks phytoplankton, total chlorophyll (CHL) and dissolved oxygen (DO). Figure 5.1 shows a schematic representation of the modelled nitrogen cycle. In coastal and estuarine systems a significant portion of the organic matter deposited to the bottom is mineralised by the benthos over short time scales and only a small fraction is permanently buried (Nixon and Pilson 1983). The model includes a sediment component, which provides a representation of benthic mineralisation processes. Microbially facilitated mineralisation processes in the sediment return a fraction of the deposited organic matter to the water column as an influx of ammonium, and the remainder is lost (as nitrogen) to the atmosphere through nitrate reduction (denitrification).

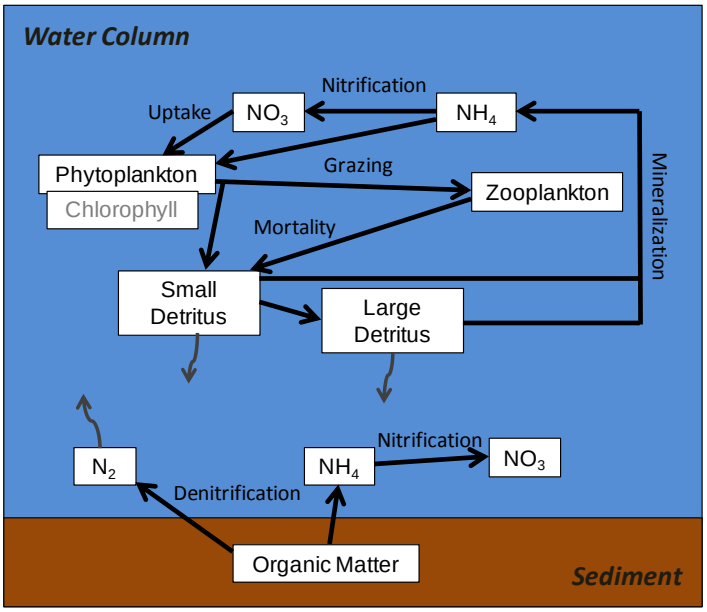

Figure 5.1 Schematic representation of the Fennel et al. (2006) biogeochemical model.

Model parameters, initialisation and boundary conditions

Parameter values for the model were derived from field studies (Chapter 4) and included those for the vertical attenuation of light, initial slope of the photosynthesis-irradiance (P-I) curve, maximum zooplankton grazing rate and phytoplankton mortality rate. Adjustment of the sediment nitrification rate was based on the work of Fernandes et al. (2007). Representative values of the half-saturation of nitrate and ammonium uptake rates and the vertical sinking rate for 'small' phytoplankton which dominate in Spencer Gulf (Chapter 4) were obtained from the literature (e.g., Eppley et al. 1969, Stolte and Reigeman 1995).

The coupled biogeochemical-hydrodynamic model was run for a period of one year commencing on the 1st July 2010. Results were determined using grid sizes of 600 m and 1200 m and found to be quantitatively similar. In view of the very long run times of the former (weeks), results presented here are based on the 1200 m grid size.

Initial values for nutrients and phytoplankton were set to spatially constant values equal to the mean winter concentrations measured during field surveys (Chapter 4). All other state variables were initially set to a constant, small value of 0.1 mmol N m^{-3}. Conditions for nutrients and phytoplankton along the southern and western model boundaries were derived from observations taken through the Southern Australian Integrated Marine Observing System. The model was first run for a period of 1 year. Adjustment time scales for each of the model's state variables were short (on the order of weeks). Daily averaged values for each state variable output on the 31st June 2011 were then used as the initial conditions for all subsequent model simulations beginning on the 1st July 2010.

Table 5.1 Biological model parameter values modified from the default values of Fennel et al. (2006) for the Spencer Gulf model.

Parameter	**Units**	**Value**
half-saturation constant for NO_3 uptake	mmol N m^{-3}	0.50
half-saturation constant for NH_4 uptake	mmol N m^{-3}	0.50
initial slope of P-I curve	mol C $gChl^{-1}$ $(Wm^{-2})^{-1}$ d^{-1}	0.18
maximum grazing rate	(mmol N m^{-3})$^{-1}$ d^{-1}	0.80
phytoplankton mortality	d^{-1}	0.05
remineralisation rate of large detritus	d^{-1}	0.02
maximum nitrification rate	d^{-1}	0.1
sinking velocity of phytoplankton	m d^{-1}	0.05
light attenuation due to seawater	m^{-1}	0.15

The model contains the major sources of anthropogenic nitrogen in Spencer Gulf (Gaylard 2013) including; aquaculture supplementary feeds, three SA Water waste water treatment plants (WWTP) and the Onesteel steelworks. Aquaculture monthly feed data for individual leases were provided by PIRSA. Approximately 37,538 tonnes of baitfish and 6,138 tonnes of manufactured feed were input into the marine environment during the modelled year. Feed data were converted into model units using the relationships given by Fernandes et al. (2007) for baitfish fed to southern bluefin tuna (SBT) and Fernandes and Tanner (2008) for pellets fed to yellowtail kingfish (YTK). Feed nitrogen contents of 3.25% and 7.10% were used for baitfish and pellets, respectively. The amount of soluble nitrogen released from feeds was assumed to be 86% and 72% for SBT and YTK, respectively. As the soluble nitrogen released during farming is primarily the result of excretion, faecal leaching and sediment remineralisation (Fernandes et al. 2007, Tanner et al. 2007), dissolved nitrogen inputs from aquaculture were assumed to be in the form of ammonium (Avnimelech 1999, Schendel et al. 2004).

SBT farming is primarily undertaken in the Port Lincoln aquaculture zone (Zone 1; Fig. 1) and is the largest source of anthropogenic nutrients into the Gulf. Simulated nutrient loads from aquaculture peaked through March to July 2011 (Fig. 5.2). Nutrient loads from WWTP's and Onesteel were significantly smaller compared to those from aquaculture, and contributed less than 10% of the annual anthropogenic load.

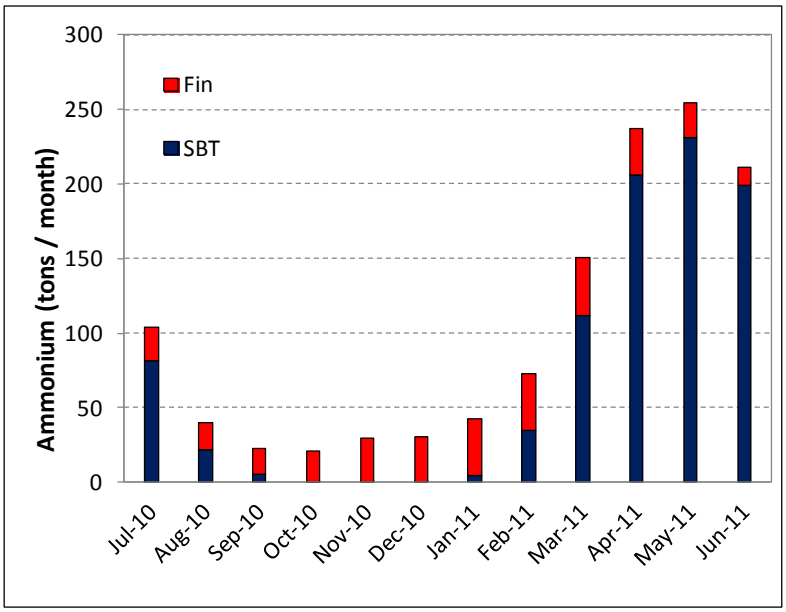

Figure 5.2 Estimated monthly loads (tonnes) of ammonium discharged from southern bluefin tuna (blue) and yellowtail kingfish (red) aquaculture input during the 2010-11 simulation period.

5.3 Methods: Biogeochemical Model Validation

Model simulations for nutrients (NO_3 and NH_4), phytoplankton (chlorophyll *a*) and dissolved oxygen concentrations were compared against *in situ* measurements obtained during the 2010-11 survey period (Chapter 4). Water samples for nutrients and chlorophyll *a* were limited to one surface and bottom sample at each site.

In comparing the simulated and observed concentrations, the general sparseness of observations must be considered relative to the high degree of variability (patchiness) characteristic of marine systems. In marine systems, high levels of biogeochemical variability are driven by the interaction of physical (e.g. tides and mixing) and biological processes (e.g. growth and grazing). This variability occurs across scales from millimetres to kilometres and seconds to days (e.g. Mackas et al. 1988; Martin 2003; Seuront et al. 2001, 2002, Doubell et al. 2009) and may obscure single measurements. A constant conversion factor (Redfield ratio) was used to convert model nitrogen to carbon. A carbon to chlorophyll ratio of 75 was assumed to convert carbon to chlorophyll units (Sathyendranath et al. 2009).

Notwithstanding the paucity of field measurements, the validation presented below shows the model behaviour compares well with the level of predictive capability typical of coastal biogeochemical models (e.g. Xu and Hood 2006; Fennel et al. 2006; Pätsch and Kühn 2008).

Dissolved Inorganic Nitrogen and Chlorophyll from Water Samples

Time series of observed (surface and bottom) nitrate and ammonium concentrations are compared to their model equivalents for each of the 10 survey sites in Figures 5.3 and 5.4 (see Fig. 1 for site locations). The simulated nitrate and ammonium concentrations reproduce the seasonal patterns observed at the stations of Zones 1, 2, 4 and 5, and are typically within the measured range of variability indicated by surface and bottom samples. Nitrate concentrations are highest in winter and lowest in summer and show transitional trends in autumn and spring. Nitrate concentrations decrease northwards away from the Gulf entrance due to utilisation of phytoplankton and are lowest in summer when import from the

adjacent shelf region is limited. Relative to nitrate, ammonium concentrations show less seasonal variability. This is because ammonium concentrations within the Gulf are less influenced by exchange processes with shelf waters. Baseline levels of ammonium are maintained through pelagic and sediment remineralisation processes. Due to the temporal sparseness of observations and the lack of measurement replication it is difficult to further validate the simulated small-scale variability. However, a comparison of the simulated concentrations of nitrate and ammonium at stations in Zone 1 and 2 agrees well with the seasonal pattern and range of concentrations measured since 1997 in the vicinity of the Port Lincoln tuna farming zone (Thompson et al. 2009). The model underestimates nitrate and ammonium in the northern region of the Gulf (Zone 3), and ammonium concentrations at the inshore stations of Zones 4 and 5. This may be because either the input nutrient loads from WWTP's and Onesteel are underestimated or sediment remineralisation rates are not well calibrated for these regions.

Modelled chlorophyll concentrations compare well with the observed mean and seasonal changes (Fig. 5.5). Simulated and observed chlorophyll concentrations throughout the year are generally low and typically less than 1 µg L^{-1}. The simulation shows chlorophyll maxima in spring and late autumn/early winter in the southern region of the Gulf at the stations of Zones 1, 2 and 5. The model successfully predicts the autumn peaks in chlorophyll which have been previously observed in the Port Lincoln tuna farming zone (Bierman et al. 2009; van Ruth et al. 2009a). However, for the south-western region of the Gulf (e.g. stations Zone 1 2, Zone 2 1 and Zone 2 2) the model appears to over predict chlorophyll concentrations in spring. Whilst this may be due to nutrient co-limitation (e.g. phosphorus or silicon, Chapter 4) which is not included in the model, the lack of observational data during the simulated spring peak in chlorophyll obscures the model validation for this period. Consistent with observations, chlorophyll concentrations are lowest at sites of Zones 1, 2, 4 and 5 during summer. Due to its inability to reproduce the higher nutrient levels observed in northern Spencer Gulf (Zone 3) the model fails to reproduce the late summer/early autumn peak in chlorophyll in this region (Fig. 5.3 and 5.4).

Dissolved Oxygen from Profiling

The vertical distribution of oxygen measured by profiling was generally uniform due to mixing. Time series of modelled dissolved oxygen (DO) are therefore compared to observations obtained at the surface and bottom during CTD profiling (Fig. 5.6). Model concentrations show a good agreement with observations at all sites. DO is highest in winter and lowest in summer, and decreases northwards away from the gulf entrance. Factors affecting DO at any specific location in our model include horizontal transport, vertical mixing and local oxygen production and consumption. As expected for Spencer Gulf, horizontal transport due to tidal motions has a dominant role in controlling the observed variability in DO, particularly at sites located in shallower regions of the Gulf.

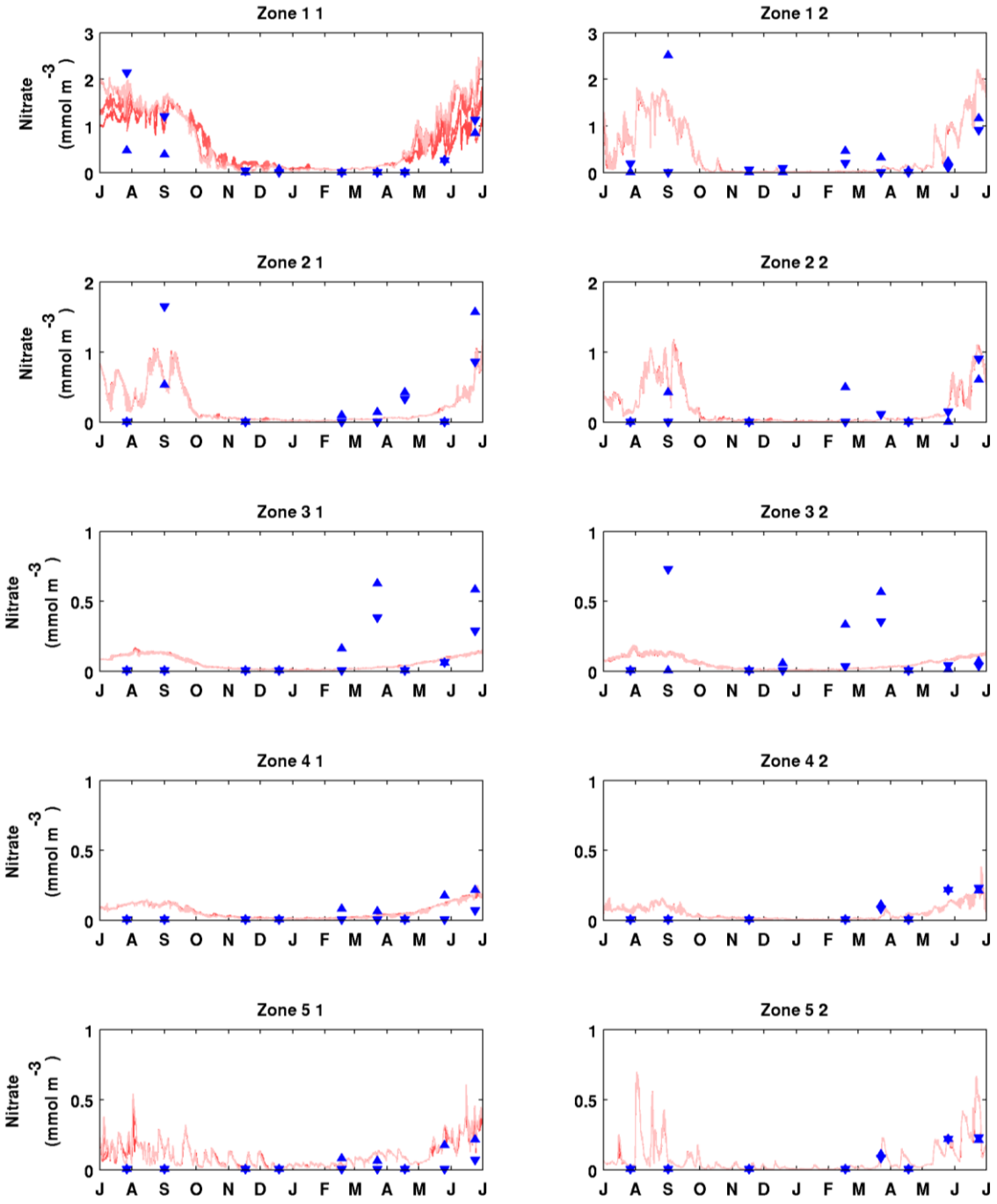

Figure 5.3 The annual cycle of modelled nitrate concentrations (red line; mmol N m^{-3}) compared with observational data from surface (▲) and bottom (▼) water samples conducted at each sampling station in Spencer Gulf (see Fig. 1 for station locations). Lighter red lines correspond to shallower layers and darker lines correspond to deeper layers (where the dark line is not visible, nutrient concentrations were the same for both layers).

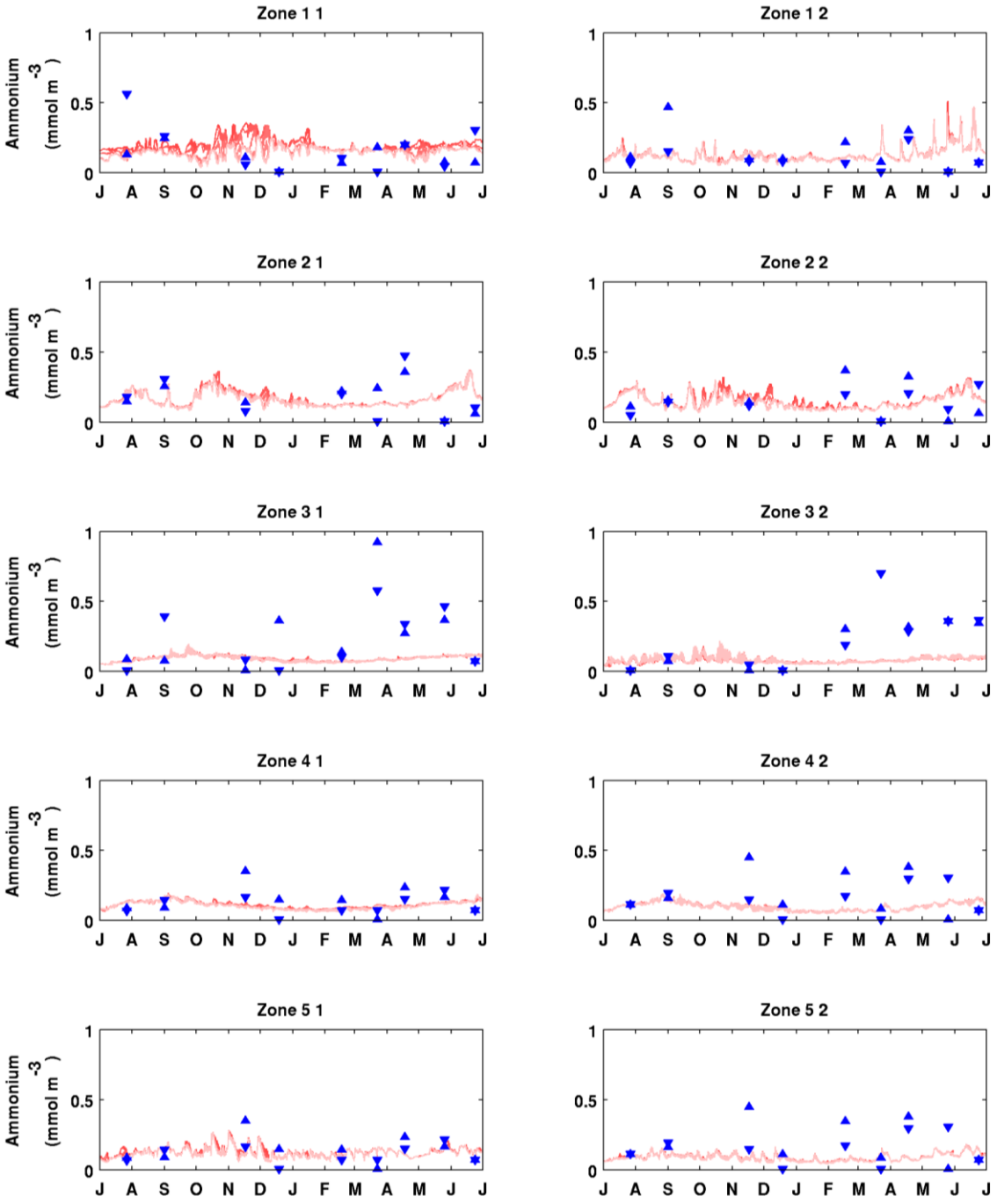

Figure 5.4 The annual cycle of modelled ammonium concentrations (red line; mmol N m^{-3}) compared with observational data from surface (▲) and bottom (▼) water samples conducted at each station in Spencer Gulf (see Fig. 1 for station locations). Lighter red lines correspond to shallower layers and darker lines correspond to deeper layers (where the dark line is not visible, nutrient concentrations were the same for both layers).

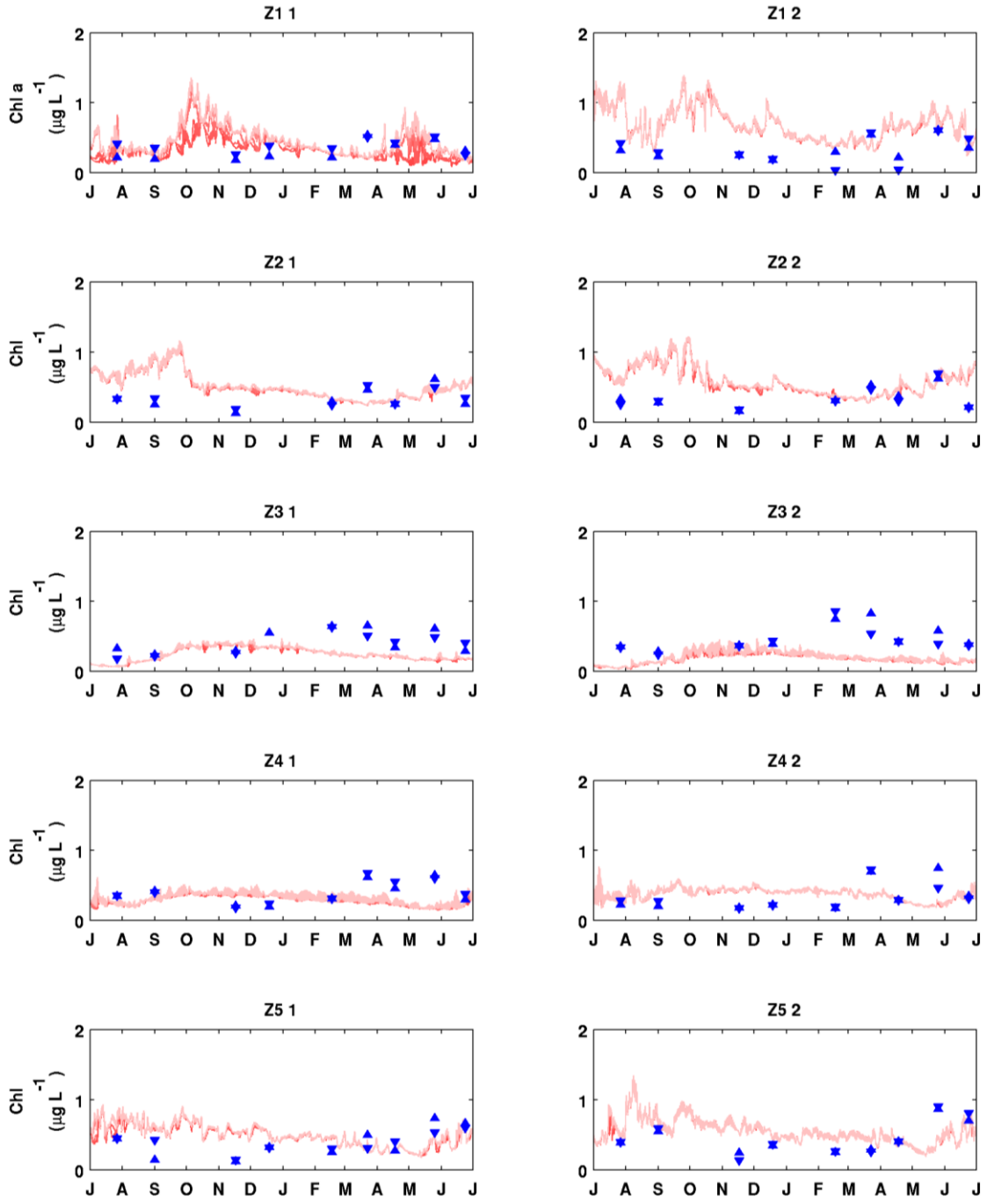

Figure 5.5 The annual cycle of modelled chlorophyll concentrations (red line; µg L^{-1}) compared with observational data from surface (▲) and bottom (▼) water samples conducted at each sampling station in Spencer Gulf (see Fig. 1 for station locations). Lighter red lines correspond to shallower layers and darker lines correspond to deeper layers (where the dark line is not visible, nutrient concentrations were the same for both layers).

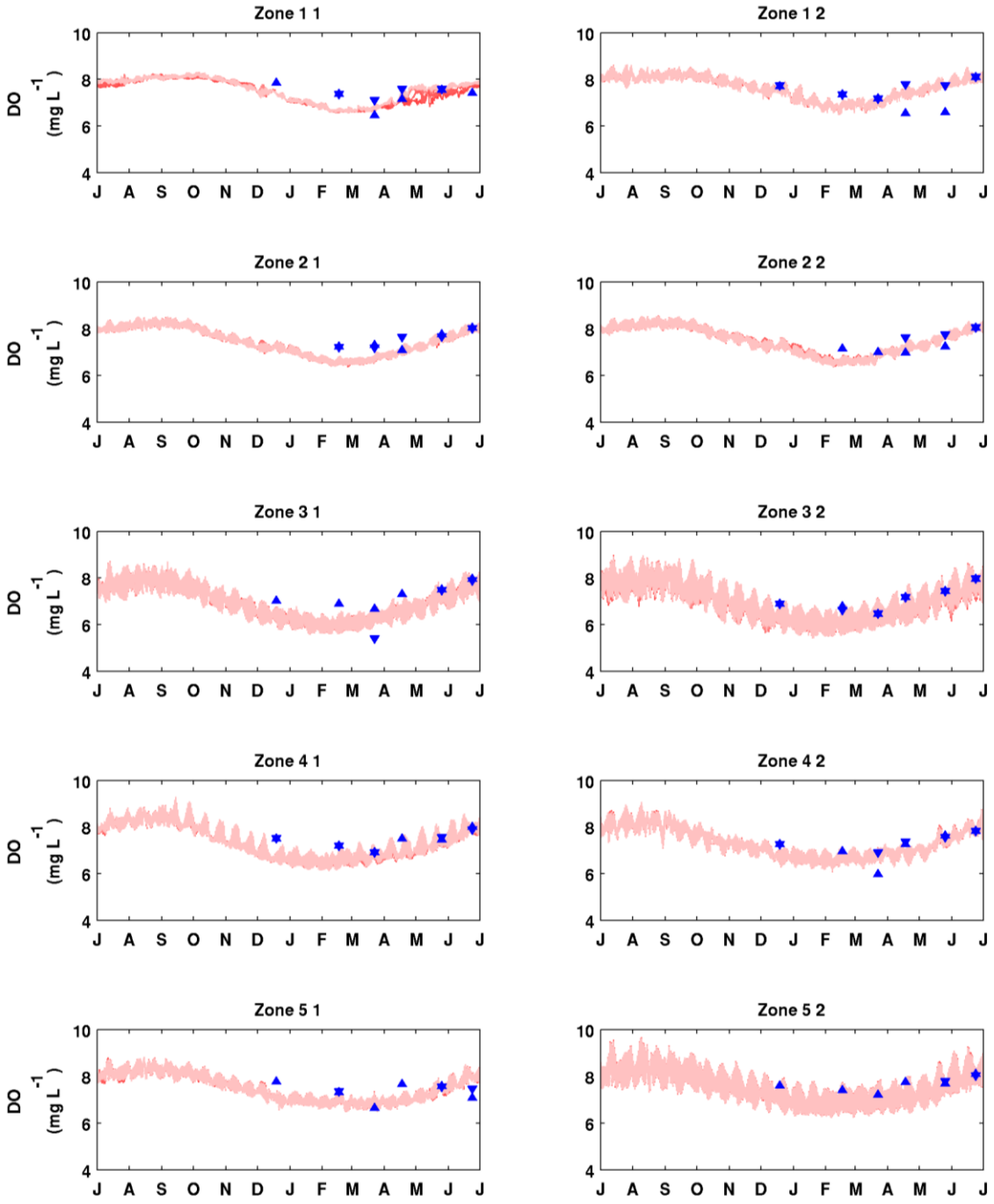

Figure 5.6 The annual cycle of modelled dissolved oxygen concentrations (red line; mg L^{-1}) compared with observational data from profiling. Surface (▲) and bottom (▼) and bottom measures from profiles are plotted for each station in Spencer Gulf (see Fig.1 for station locations). Lighter red lines correspond to shallower layers and darker lines correspond to deeper layers (where the dark line is not visible, nutrient concentrations were the same for both layers).

Sea Surface Chlorophyll and Primary Production

An example of spatial patterns in surface chlorophyll is given in Figures 5.7 and 5.8, where the simulated mean surface chlorophyll concentrations for the months of February and May 2011 are compared to those estimated by satellite (MODIS) remote sensing. Following the evaluation of MODIS chlorophyll data in Spencer Gulf by Bierman et al. (2009), we restrict our comparison to the lower Spencer Gulf region south of 34^{o} 45' S, where water depths are generally greater than 20 m, and chlorophyll is less likely to be overestimated due to bottom reflectance in shallow waters. Both simulated and MODIS chlorophyll concentrations are highest near the coast and in the south-western corner of Spencer Gulf. A general decrease in chlorophyll is observed in the south-central/eastern area of the Gulf. For areas shallower than 20 m, particularly coastal regions on the eastern side of the Gulf, comparison of the remotely sensed chlorophyll concentrations with the model indicate the former overestimates chlorophyll concentrations. The model slightly overestimates surface chlorophyll on the shelf region when compared to the MODIS images.

The simulation of elevated chlorophyll concentrations in the south-west corner of Spencer Gulf was associated with high levels of primary production. Simulated primary production was lowest in the north of the Gulf where the model generally under-predicted nutrient and phytoplankton concentrations. Whilst the spatial patterns of productivity differed slightly to those observed in field studies (Chapter 4), simulated mean daily integral primary productivity for the gulf was 352 mg C m^{-2} d^{-1} and compared well to the mean rate of 355 mg C m^{-2} d^{-1} estimated from direct observations (Chapter 4).

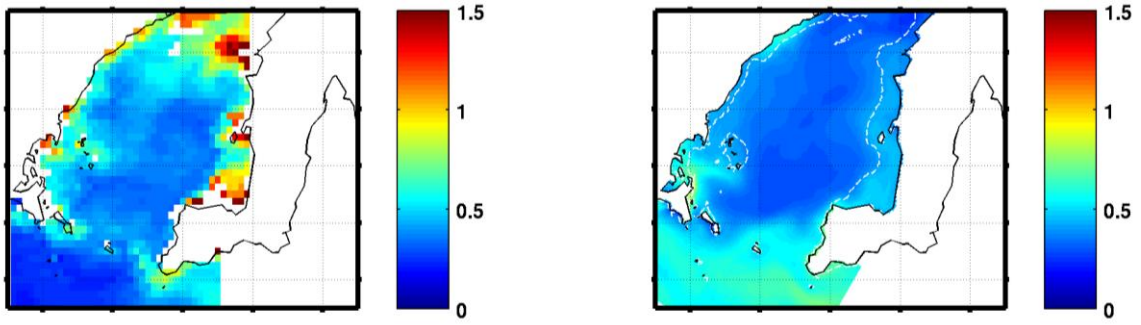

Figure 5.7 Mean sea surface chlorophyll (µg L^{-1}) for February 2011 estimated by (left) MODIS satellite imagery and (right) model simulated with the 20 m isobath plotted for reference. For Spencer Gulf, MODIS data typically overestimates chlorophyll concentrations in waters less than approximately 20 m depth.

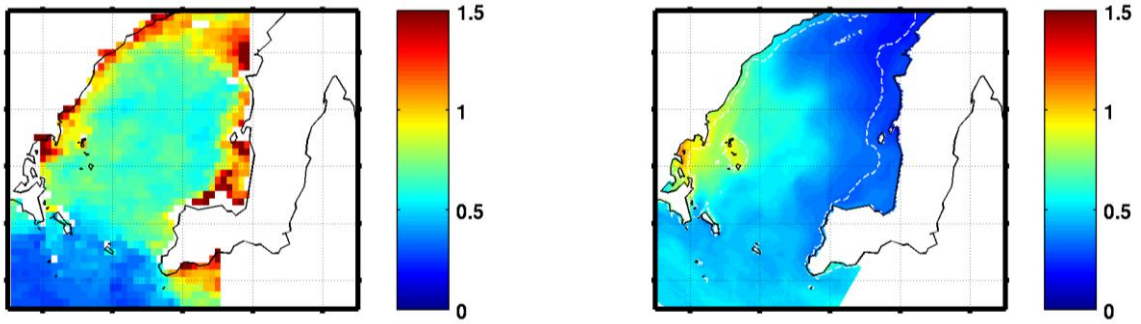

Figure 5.8 Mean sea surface chlorophyll (µg L^{-1}) for May 2011 estimated by (left) MODIS satellite imagery and (right) model simulated with the 20 m isobath plotted for reference. For Spencer Gulf, MODIS data typically overestimates chlorophyll concentrations in waters less than approximately 20 m depth.

5.4 Results and Discussion

Simulation of the annual cycle

Model estimates of seasonal variation, displayed in terms of monthly means for surface concentrations of nutrients and phytoplankton, are shown in Figures 5.9 to 5.11. The simulated annual cycle in Spencer Gulf begins with elevated concentrations of phytoplankton in the south-western corner during winter (July, August 2010). Nutrients generally show an inverse behaviour compared to phytoplankton, and the supply of nitrates from the shelf is largest during the winter months. During winter, nutrients from the shelf (Fig 5.10) and aquaculture (Fig. 5.11) maintain increased levels of nutrients and phytoplankton, which are transported northward along the western coastline and eastward into the southern region of the Gulf as a consequence of the winter circulation (Chapter 1). In early spring (September - October), phytoplankton concentrations increase throughout the Gulf in response to seasonal changes in temperature and light. Whilst the import of nitrate from the shelf is reduced, ammonium supplied from finfish aquaculture, Onesteel and WWTP's helps maintain elevated concentrations of phytoplankton in western and southern Spencer Gulf. Nitrate and phytoplankton concentrations throughout the Gulf are lowest in summer (December to February). During summer, phytoplankton growth is maintained by low levels of ammonium supplied by anthropogenic sources and the remineralisation of organic matter. In early autumn (March, April), phytoplankton concentrations begin to increase again in the south-west corner of the Gulf. The inflow of nitrate from the shelf is still small and limited. However, increases in ammonium discharges from aquaculture provide an additional source of nutrients for phytoplankton. By late autumn (May, June), nutrient concentrations increase from both the import of nitrate from the shelf and ammonium discharges from aquaculture. This increase supports phytoplankton growth. Elevated concentrations of nutrients and phytoplankton are again transported northwards along the western coastline and eastwards across the Gulf by the winter circulation. The seasonal cycle is complete.

The monthly mean values for nutrients and phytoplankton clearly show that the annual variation in meteorological and oceanographic conditions strongly influences the cycle of the chemical and biological system. In particular, seasonal circulation patterns (Chapter 1) are shown to drive the transport of nutrients and phytoplankton in the Gulf (Chapter 4). As a consequence of these circulation features, distinct spatial structures are observed in the distribution of phytoplankton and nutrients. These include the elevated concentrations of nutrients and phytoplankton that are observed around and extending from, regions of anthropogenic discharges (e.g. Port Lincoln, Arno Bay and Fitzgerald Bay aquaculture zones).

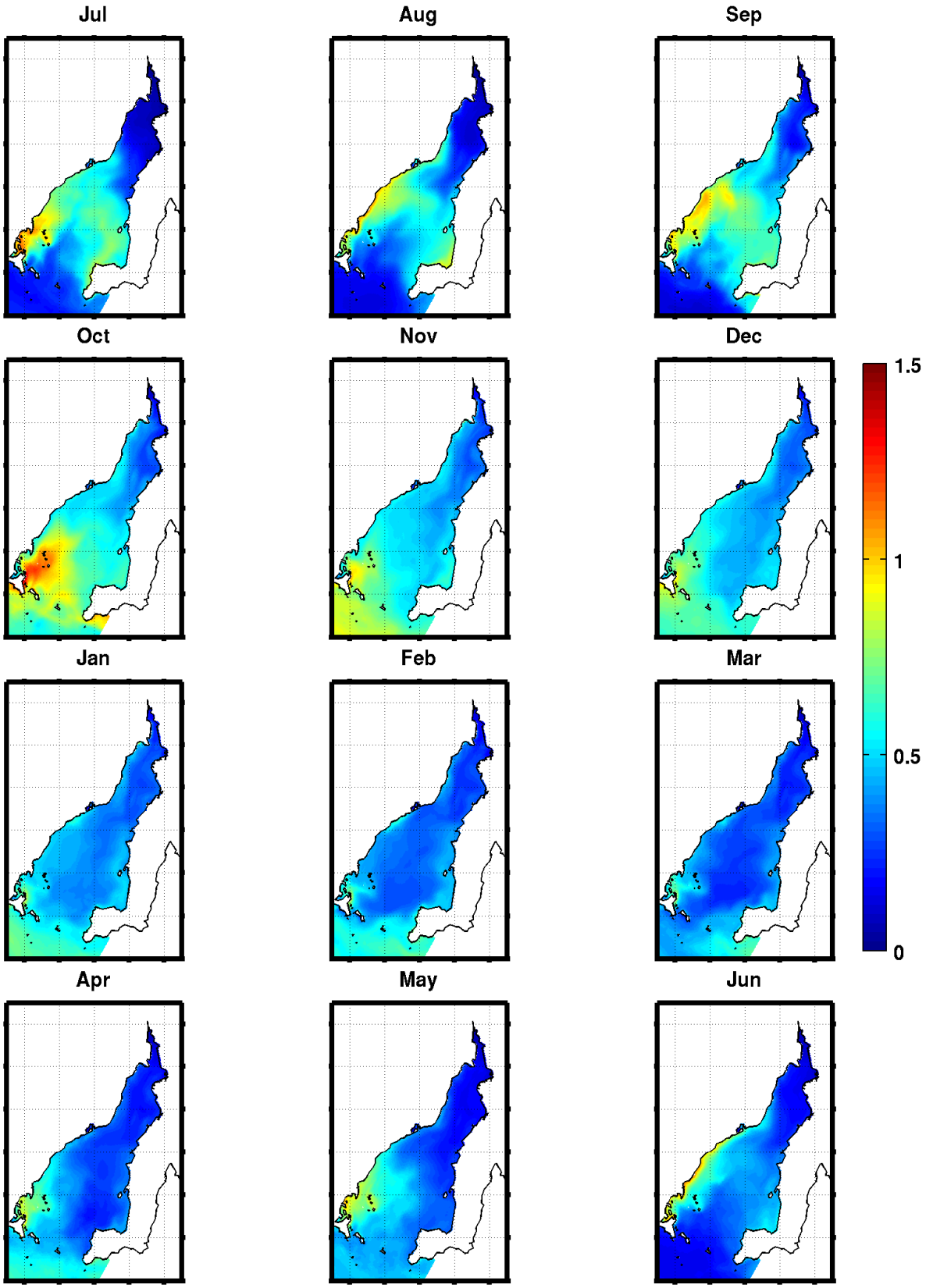

Figure 5.9 Monthly means of simulated surface chlorophyll *a* concentrations in µg L^{-1} for July 2010 to June 2011.

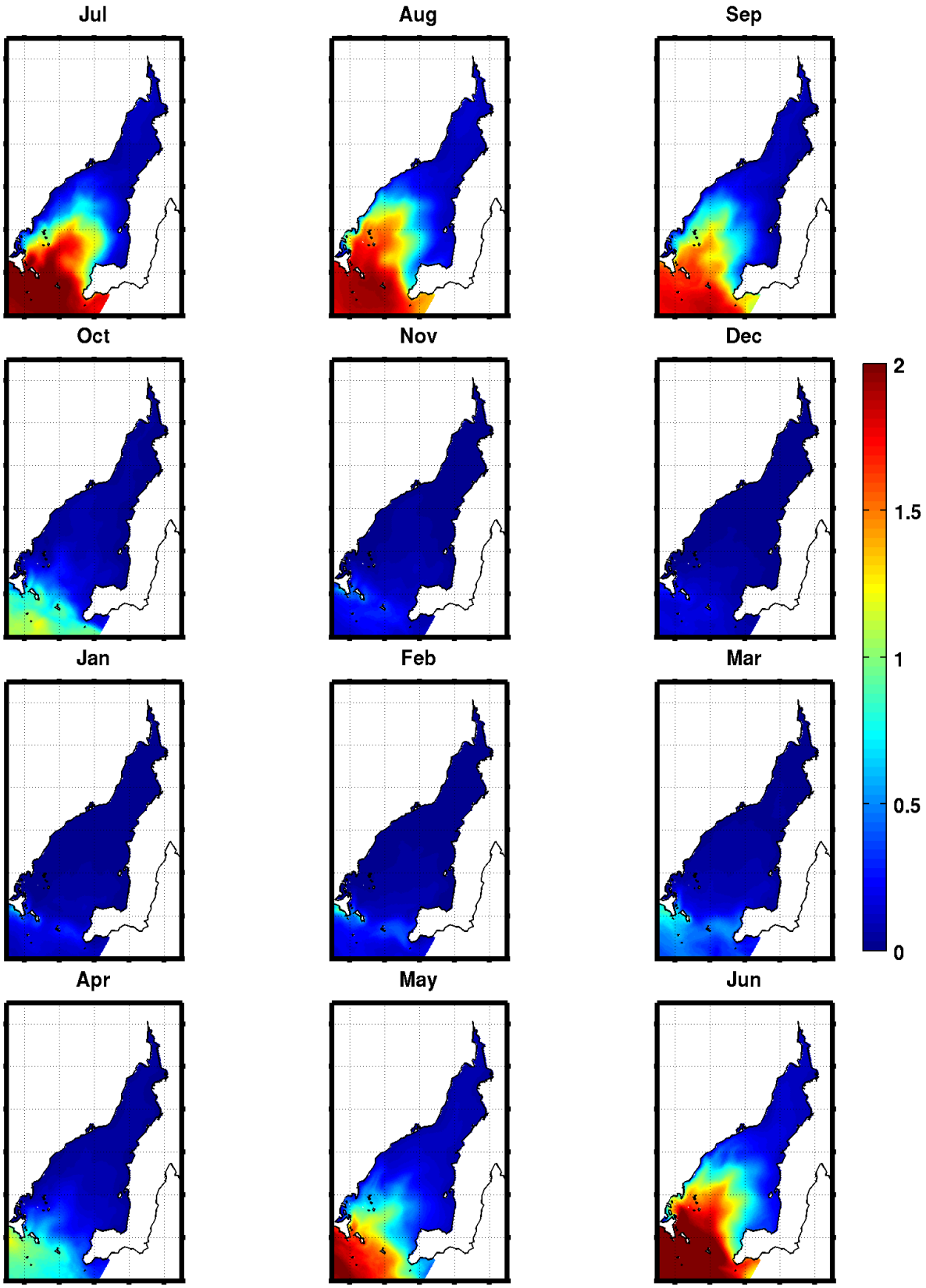

Figure 5.10 Monthly means of simulated surface nitrate (NO_3) concentrations in mmol N m^{-3} for July 2010 to June 2011.

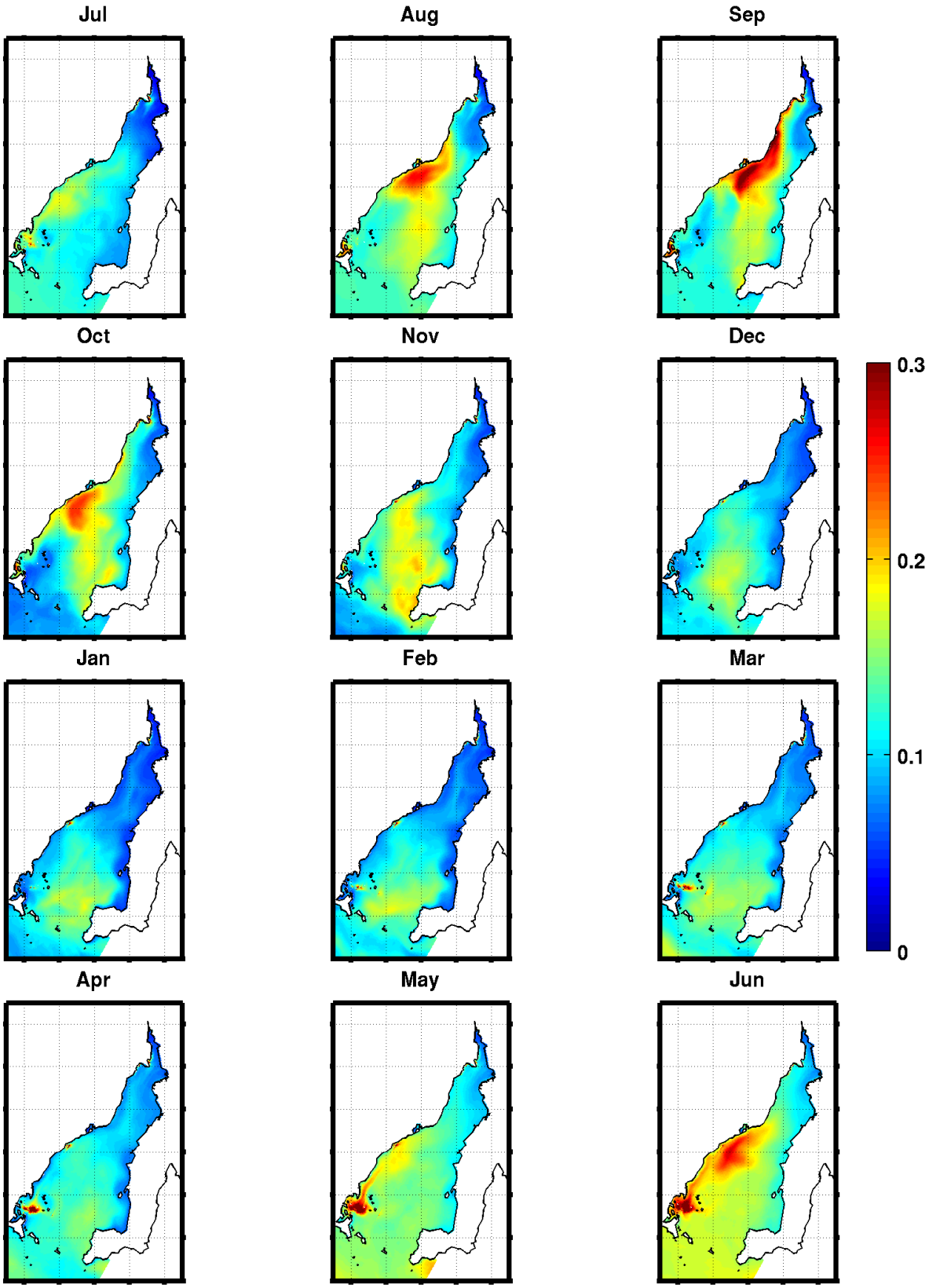

Figure 5.11 Monthly means of simulated surface ammonium (NH_4) concentrations in mmol N m^{-3} for July 2010 to June 2011. Elevated concentrations from aquaculture loads are clearly visible in aquaculture zones of Port Lincoln (Zone 1), Arno Bay (Zone 2) and Fitzgerald Bay (Zone 3) (see Fig. 1 for zone locations).

Mesoscale and Fine Scale Variability

The monthly averaged concentrations presented above smooth out the mesoscale (km) and fine scale (m) variability found at shorter temporal scales. Whilst simulated daily average concentrations for nutrients or phytoplankton never exceeded the ANZECCC/ARMCANZ (2000) water quality guidelines, significant variability in the concentration of chemical and biological components of the ecosystem was simulated across a range of spatial and temporal scales.

To demonstrate the mesoscale spatial patterns simulated over shorter temporal scales, Figure 5.12 shows a 6-day series of snapshots of daily averaged surface chlorophyll distributions. While day to day variations in the concentration of chlorophyll are relatively small, the differences between the first and last days are significant. Several eddy-like and filament-like structures can be observed. During this interval the daily mean wind values were dominated by northerly winds on 31st May and 1st June, before a south-westerly cold front crossed Spencer Gulf on 2nd and 3rd June. The front was followed by strong westerly winds on the 4th and 5th of June. Initially, northerly winds helped maintain elevated surface chlorophyll concentrations around the Port Lincoln aquaculture Zone 1, including adjacent bays and offshore islands. The high chlorophyll concentrations are then dispersed and transported northward along the western coastline and offshore with the passing of the cold front. Trailing westerly winds further disperse the phytoplankton from the inshore bays near Port Lincoln (i.e. Boston Bay). On the eastern side of the Gulf, slightly elevated concentrations initially observed in the central region of the Gulf are transported and accumulate along the south-eastern corner of the Gulf. This example demonstrates that phytoplankton show a high degree of mesoscale variability associated with changes in meteorological and oceanographic conditions over temporal scales of a few days.

As a second example, consider the year long time series of hourly averaged concentrations for several variables simulated at Station Z1 2 that lies in the south-west of the Gulf. Long-term seasonal changes for several variables have been discussed previously in the model validation (Chapter 5.3). During winter and spring, nitrate concentrations in the Gulf are relatively high due to the annual winter flushing (Chapter 1). Several small pulses of ammonium are transported through the station from the Port Lincoln aquaculture zone (Zone 1). Phytoplankton concentrations are high and typically show an inverse behaviour to nutrients, particularly nitrate. Summer concentrations of nutrients and phytoplankton are low due to the reduced flux of nutrients from the shelf (Fig. 5.10 and 5.11) and anthropogenic sources (Fig. 5.2). In early autumn (March, April 2011), multiple pulses (peaks) of ammonium, with temporal scales of about a week, are the result of increased feeding (Fig. 5.2). However, nitrate concentrations remain low as exchange between the shelf and Gulf is still largely blocked. Phytoplankton respond to the increased nutrients from aquaculture and, over temporal scales of several days, can double their concentration. The response of zooplankton typically lags phytoplankton by an additional few days. The simulation indicates that physical processes (e.g. transport) and biological processes (e.g. cycling within the ecosystem) can lead to high variability in nutrient, phytoplankton and zooplankton concentrations over time scales of days to weeks.

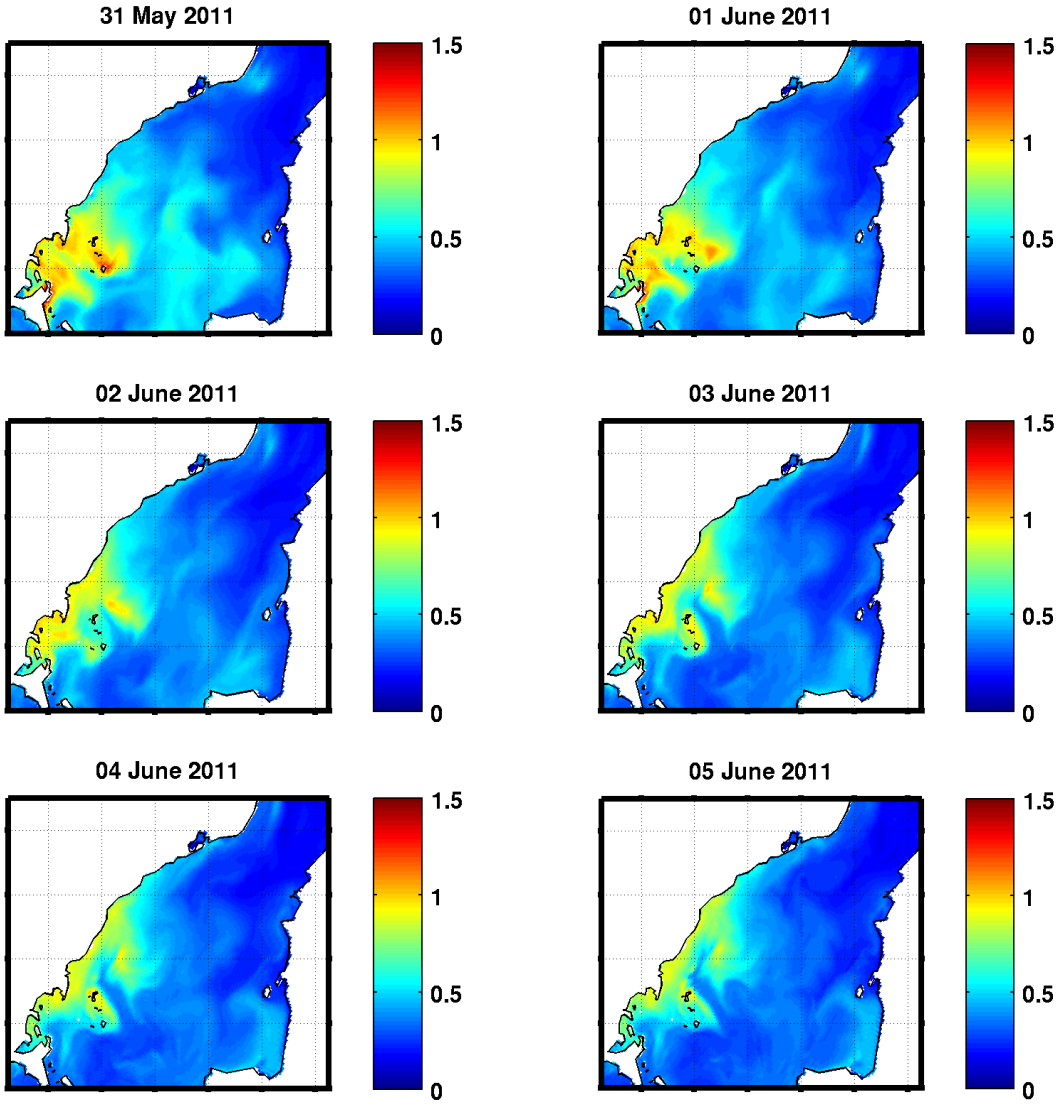

Figure 5.12 Daily snapshots of simulated daily averaged surface chlorophyll *a* concentrations in µg L^{-1}.

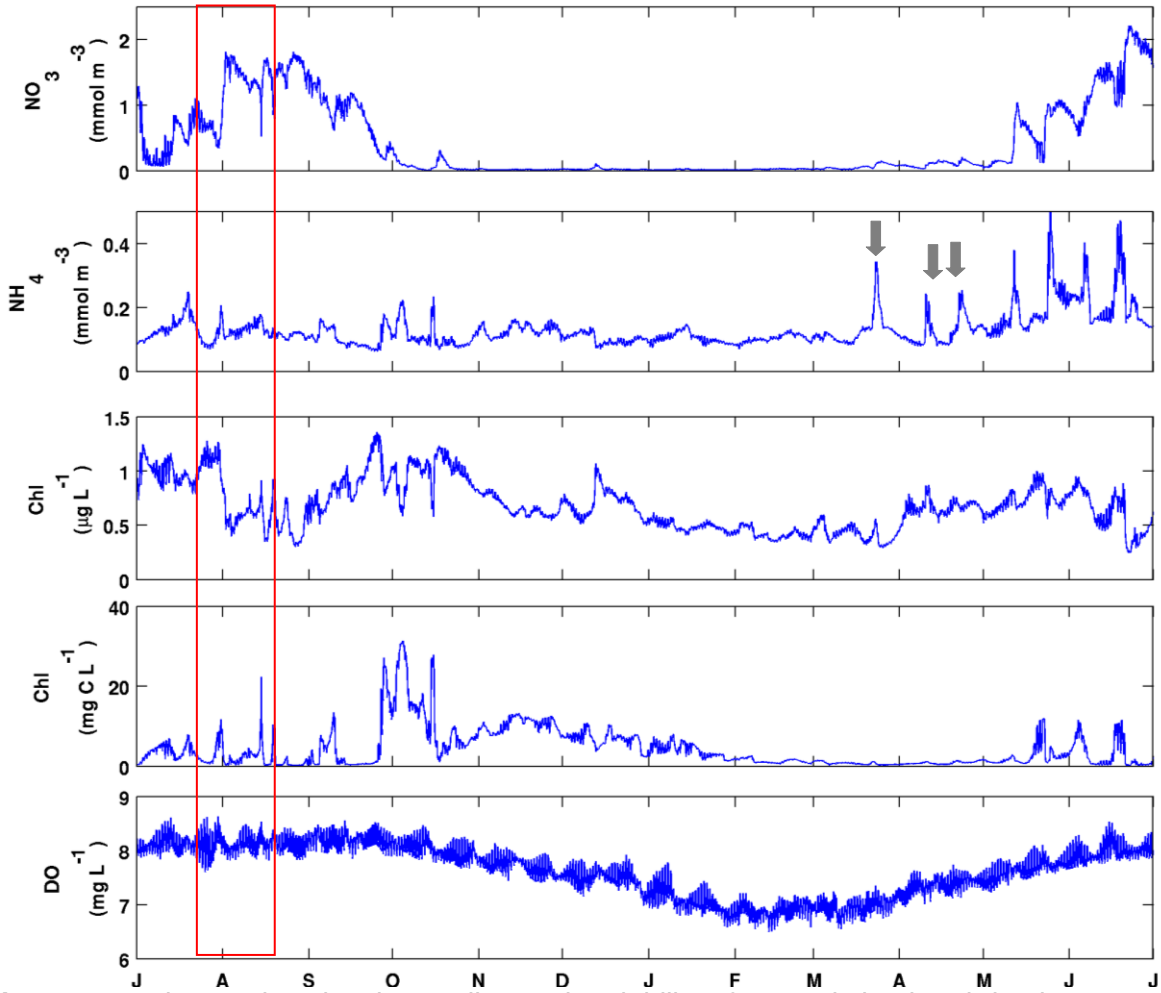

Figure 5.13 Time series showing cycling and variability of several simulated depth-averaged chemical and biological variables at station Z1 2 located on the western side of the gulf to the north of the Port Lincoln tuna aquaculture zone. From top to bottom: hourly and depth averaged concentrations are given for; nitrate, ammonium, phytoplankton (chlorophyll), zooplankton and oxygen. The red boxed region highlights cycling between the chemical and biological components of the model; phytoplankton show an inverse behaviour to nutrients and oxygen concentrations are decreased due to respiration. The zooplankton response lags behind the peak in phytoplankton concentrations. Grey arrows indicate pulses of ammonium transported from the Port Lincoln aquaculture zone in early autumn prior to the annual influx of nitrates from shelf. The figure corresponds to the validations presented for Z1 2 in Figs. 5.3-5.6.

Nitrogen Budget for Spencer Gulf

A nitrogen budget was derived by calculating model-simulated fluxes of organic matter and dissolved nutrients across a boundary at the Gulf's entrance, as well as inputs from anthropogenic sources (i.e. aquaculture, WWTP's and Onesteel) and losses due to sediment denitrification. Nutrients enter Spencer Gulf from the shelf with an estimated flux of 16.9 kilotons year^{-1}. This is more than 10-fold greater than that from anthropogenic sources within the Gulf. The largest sink for nitrogen is due to benthic denitrification. The simulation suggests denitrification removed 84% of nitrogen entering the Gulf. The mean annual denitrification flux for Spencer Gulf is estimated to be 0.12 mmol m^{-2} d^{-1} and is slightly less

than direct sediment denitrification measures of approximately 0.48 mmol m^{-2} d^{-1} taken at control sites within the Port Lincoln aquaculture zone (Lauer et al. 2007). The nitrogen budget is balanced by a net increase in nitrogen within the Gulf at the end of the simulation year. The budget indicates that the import of nitrogen from the shelf and nitrogen losses due to benthic (microbial) denitrification play a significant role in determining the carrying capacity of Spencer Gulf.

Alternative Scenario Studies: Effects of Finfish Aquaculture on Carrying Capacity

Using the model, multiple scenario studies (SS) were performed to estimate and understand the influence of anthropogenic nutrient inputs on water quality and carrying capacity. Table 5.2 summarises the various SS and their corresponding nutrient sources and annual loads. The physics of the system is not affected by the changing nutrient loads. For management purposes, the relative contribution of different sources and loads on predicted concentrations of chemical and biological variables for each SS can be easily explored using the 'CarCap 1.0' software presented in Chapter 6.

The following section provides a brief summary of nutrient sources and loads for each SS (Table 5.2). The control SS is a simulation of the 2010-11 period discussed above. SS1-SS4 are examples of load reduction experiments. SS1 includes imports of nutrients and organic matter from the shelf region as the sole source of nitrogen for Spencer Gulf. No anthropogenic sources are included, thereby allowing for an evaluation of the potential effect of current anthropogenic loads (control simulation) on carrying capacity. SS2-SS4 include only nitrogen discharges from finfish (SS2), tuna (SS3) and both finfish and tuna (SS4) aquaculture. SS5 is a repeat of the control simulation but includes the effect of waves on vertical mixing and bottom boundary layer fluxes through coupling with the SWAN model (Chapter 2). SS6 and SS7 are examples of increased aquaculture nutrient load experiments. SS6 investigates the case of maximum carrying capacity based on current PIRSA estimates of maximum stocking densities of 6 and 15 tonne ha^{-1} for tuna and finfish, respectively. Feed inputs for each lease and month were increased to reflect these production limits for a typical annual production cycle (Fig. 5.14). Following the scaling relations presented in Chapter 3, monthly feed inputs for each lease site in SS7 were increased by a factor proportional to the ratio of the ANZECC/ARMCANZ (2000) guideline concentration for ammonium divided by the monthly maximum ammonium value simulated at each lease site in the control study (Fig. 5.15). Consequently, monthly feed was increased by factors ranging from 1.6 to 53.5 across the leases. While both SS6 and SS7 both provide a similar (~ 4-fold) increase in the annual nutrient discharges from aquaculture, the distribution and timing of nutrient inputs from individual leases differ.

Table 5.2 Summary of the model scenario studies, associated sources and annual anthropogenic nutrient loads. Nutrient loads for dissolved inorganic nutrients are in units of kilotons year^{-1} (kT y^{-1}).

Scenario Study (SS)	Nutrient Sources	Anthropogenic nutrient load
Control	Shelf, SBT and YTK aquaculture, WWTP, Onesteel	1.5
1	Shelf	-
2	Shelf, YTK aquaculture	0.4
3	Shelf, SBT aquaculture	1.0
4	Shelf, SBT and YTK aquaculture	1.4
5	Shelf, SBT and YTK aquaculture, WWTP, Onesteel with SWAN waves	1.5
6	Shelf, SBT and YTK aquaculture at production max, WWTP, Onesteel	6.1
7	Shelf, SBT and YTK aquaculture at water quality max, WWTP, Onesteel	6.5

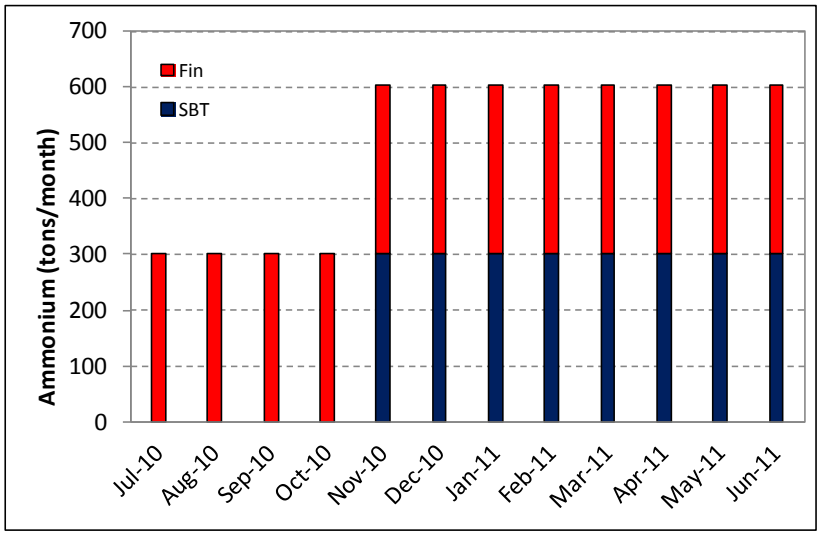

Figure 5.14 Total monthly ammonium loads (tons) discharged from southern bluefin tuna (SBT; blue) and yellowtail kingfish (YTK; red) aquaculture in Scenario Study 6.

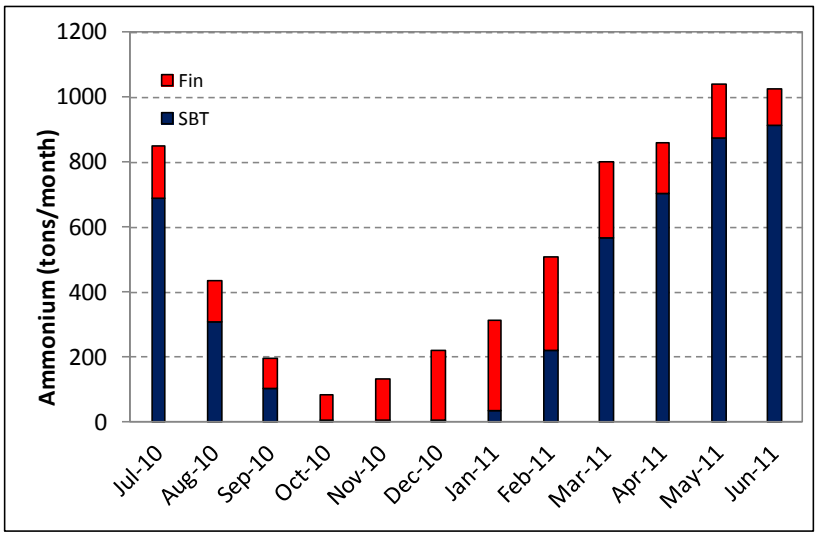

Figure 5.15 Total monthly ammonium loads (tons) discharged from southern bluefin tuna (SBT; blue) and yellowtail kingfish (YTK; red) aquaculture in Scenario Study 7.

At the Gulf scale, annual nitrogen budgets showed a decrease in the amount of nitrogen lost through sediment denitrification with increases in aquaculture nutrient loads. Nitrogen losses due to denitrification decreased from 87% for SS1 to 84% for the control simulation. Coupling with the SWAN wave model indicated waves may play a small role in increasing the annual denitrification flux with the annual denitrification loss estimated to be 85%. For SS6 and SS7, total nitrogen losses due to denitrification were reduced to 82% and 80% respectively, and were balanced by an increase in the inventory of total nitrogen (dissolved nutrients and organic matter) within Spencer Gulf. The results indicate the possibility of a reduction in the buffer capacity of sediment denitrification with subsequent increases in anthropogenic discharges.

The simulated increases in the concentration of nutrients and organic matter are not spread evenly across the Gulf, nor are they confined to their source regions (zones). To demonstrate the response of the ecosystem to increases (SS6 and SS7) and decreases (SS1) in anthropogenic nutrient loads, changes in the inventory of dissolved inorganic nutrients (DIN = ammonium + nitrate) and phytoplankton for each zone are presented in Figures 5.16 and 5.17 as a percentage of the control simulation.

The results for SS1 indicate that the aquaculture discharges significantly increased the levels of nutrients and phytoplankton within zones where supplementary feeding occurs (Fig. 5.16 and 5.17). For nutrients, increases in excess of 100%, 50% and 40% are estimated during periods of peak feeding in Zones 1, 2 and 3, respectively (Fig. 5.16). In response to the increased nutrient loads, the inventory of phytoplankton in these zones increases although the response is not linear. Phytoplankton levels are suggested to have increased by up to 25% in Zone 1 around the peak feeding period in May 2011 and by approximately 50% around peak feeding periods in Zones 2 and 3. For Zones 2 and 3, the response of nutrients and phytoplankton is faster and noisier than is observed in Zone 1. This increased variability is due to the more rapid cycling between chemical, biological and benthic components of the ecosystem in these regions of the Gulf. The comparison also suggests that discharges of anthropogenic nutrient loads have not impacted zones located on the eastern side of the Gulf (Zones 4, 5, 6). Since the Gulf is well mixed no effect was observed on oxygen levels.

SS6 and SS7 included significant increases in the monthly nutrient discharges from aquaculture compared to the control study (Table 5.2). Since the anthropogenic loads from WWTP's and Onesteel remained the same a direct comparison of the effect of increases in

aquaculture related discharges is inferred using these two scenario studies. Results indicate nutrient levels respond rapidly to increases, and changes, in nutrient discharges within the source zones (Zones 1, 2 and 3). Nutrient increases in excess of 50% are simulated across the year in Zones 1 and 2. The largest response to increased aquaculture discharges was observed in Zone 3, particularly in SS6 where discharges from finfish aquaculture are greatest. In response to the increased nutrient levels, phytoplankton increase by up to approximately 40% in Zones 1 and 2, and larger increases are predicted in Zone 3. Furthermore, the simulations suggest significant increases in nutrients and phytoplankton along the eastern side of the Gulf not seen in the previous comparison of the control study with SS1. This result suggests, for the simulated nutrient loads, the impact of increased aquaculture discharges may not be limited to the western side of the Gulf. In particular, Zones 4 and 6 show increases in nutrients and phytoplankton by up to 40% owing to the greater connectivity these zones have with the nutrient source zones and each other (Chapter 1). With the exception of poorly flushed inshore waters of Zones 1 and 3 (Chapter 2) the simulated concentrations of ammonium and phytoplankton remained within ANZECC/ARMCANZ (2000) water quality guidelines.

The management of aquaculture in Spencer Gulf is influenced by complex interactions between physical, chemical and biological processes, many of which cannot be controlled. This chapter demonstrates how the development and validation of an advanced three-dimensional ecosystem model can enhance our understanding of the interaction of natural ecosystem processes and human activities and their effect on water quality.

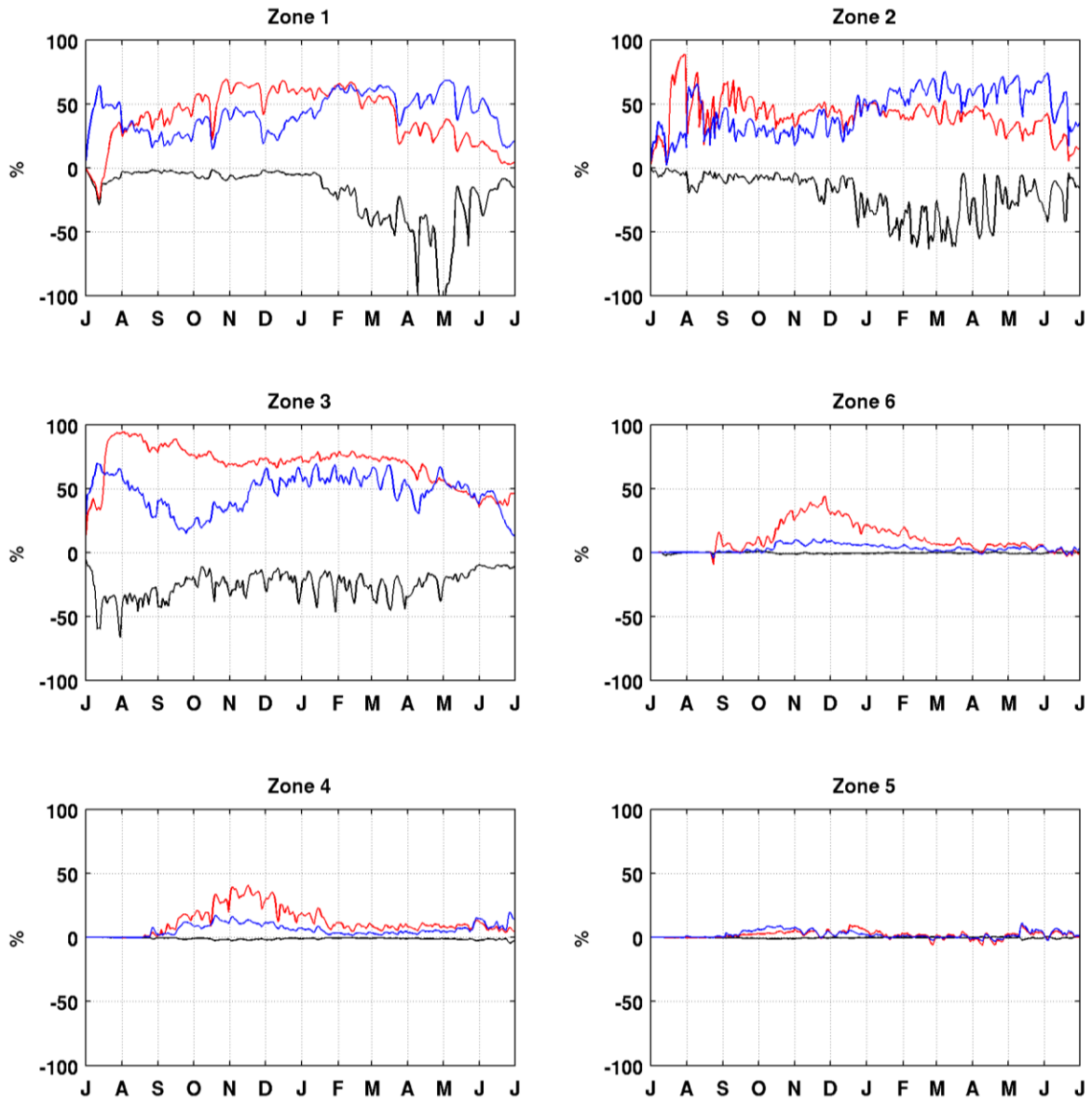

Figure 5.16 Scenario Study responses to anthropogenic load reduction (SS1; black line) and increases (SS6; red line, SS7; blue line) for nutrients (ammonium + nitrate) in each aquaculture lease zone in comparison to the control simulation. See Figure 1 for aquaculture zone locations.

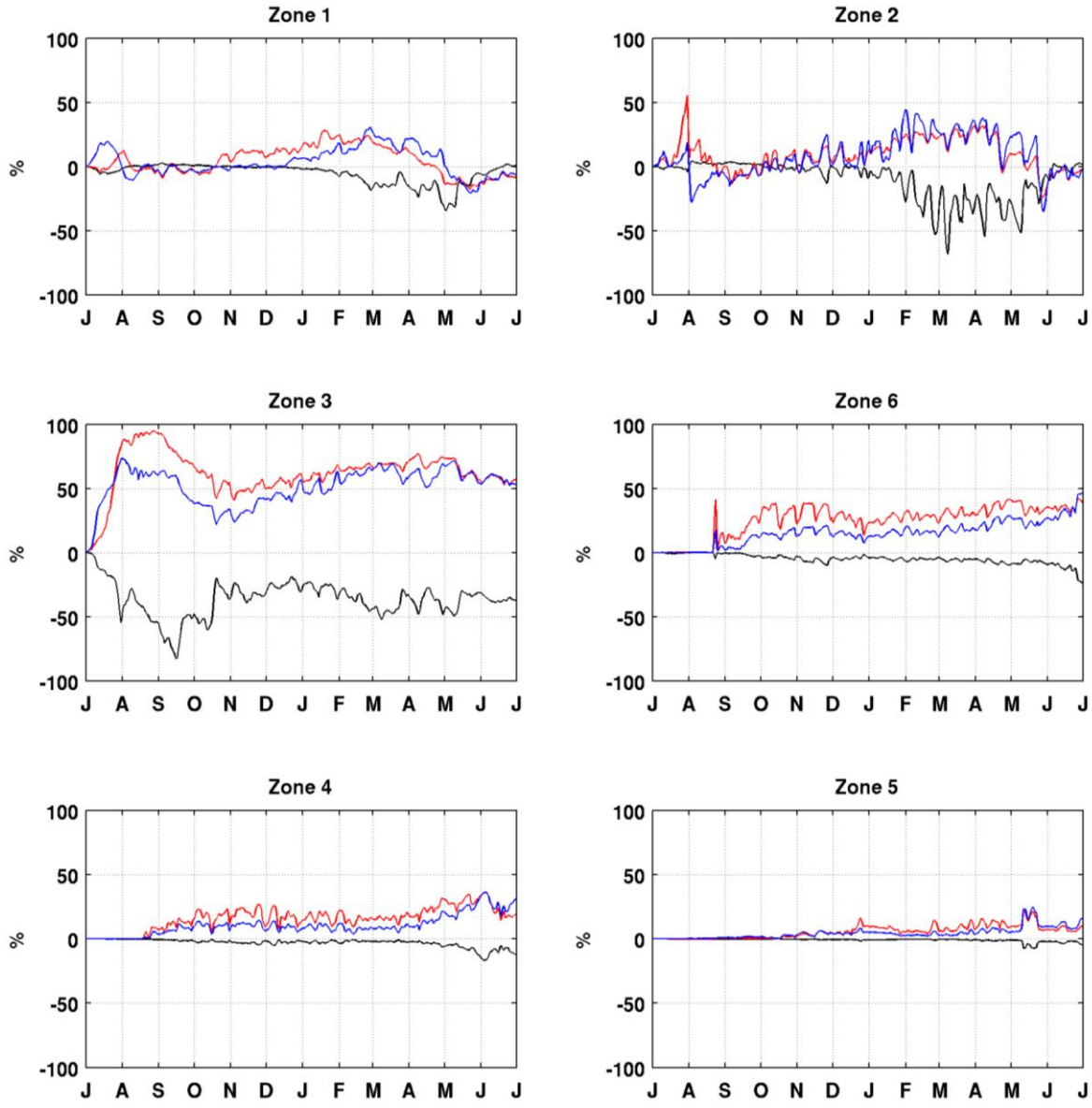

Figure 5.17 Scenario Study responses to anthropogenic load reduction (SS1; black line) and increases (SS6; red line, SS7; blue line) for phytoplankton in each aquaculture lease zone in comparison to the control simulation. See Figure 1 for aquaculture zone locations.

CHAPTER 6. A GRAPHICAL USER INTERFACE: A TOOL FOR MANAGEMENT OF CARRYING CAPACITY

CarCap1.0

Charles James, John Middleton, John Luick and Mark Doubell

6.1 Introduction and Summary

CarCap1.0 is a graphical user interface (GUI) package that has been developed to allow managers to rapidly identify regions at the scale of the gulf, lease and cage where finfish aquaculture might be introduced, or be increased/decreased in scale, based on nutrient and/or phytoplankton concentrations. This is done by comparing nutrient concentrations with maximum values c_P that have been determined elsewhere to ensure environmental health (e.g., ANZECC/ARMCANZ 2000).

The package enables management to select and evaluate carrying capacity from a list of several pre-run modelled scenarios which include nutrient inputs from finfish and/or anthropogenic sources including waste water and industrial outfalls (Objectives 4 and 7).

For new or existing lease sites, the package also enables management to estimate the maximum concentrations and associated feed rates under the ANZECC/ARMCANZ (2000) prescribed values or user defined values. This tool can therefore be used to choose sites that will maximise allowable feed rates and be of financial benefit to the lease holder.

6.2 Methods

The biogeochemical model output for 2010-2011 and for each of the scenario studies determined in Chapter 5 has been included in CarCap1.0: this output includes concentrations of nutrients (NO_3, NH_4), dissolved O_2 and phytoplankton. The spatial and temporal displays are made through the use of MATLAB software and installation of the GUI executable is described below.

For existing lease sites, CarCap1.0 takes the input feed rates, F_{in}, as used by the modelled scenario and estimates the time scale, T_M, of the flushing based on the ratio between the specified concentration level and the feed rate, $T_M = c_P/F_{in}$. The manager can use an existing prescribed maximum nutrient (or phytoplankton) concentration for c_P (e.g., ANZECC/ARMCANZ 2000) or a user defined value. If the relationship is linear, the resulting nutrient flux, $F = c_P/T_M$ should be an estimate of the maximum nutrient flux that will result in a local concentration that does not exceed c_P. This nutrient flux is converted to a feed rate and is referred to in CarCap1.0 as MFR1 or Maximum Feed Rate method 1. This estimate can only be made for existing lease sites.

For both new and existing lease sites, CarCap1.0 can estimate maximum feed rates using the methods outlined in Chapter 3. These are used to determine the time scale of flushing T* at a particular site using equation 2.5 from Chapter 3. Again, the user can use an existing prescribed maximum for c_P or specify a new value. CarCap1.0 then returns the maximum nutrient flux $F = c_P/T^*$ and associated monthly feed rate which is referred to in CarCap1.0 as MFR2 or Maximum Feed Rate, method 2. This is the recommended method.

Metadata (e.g., lease holder, feed rates with start and finish dates, species, other) on individual lease sites can be saved in the Excel.csv format which can be imported into most data processing and analysis packages.

6.3 Results and Discussion

Presented in Figure 6.1 is a screen shot of CarCap1.0. Options for presentation are shown on the right side of the screen. The concentrations of NH_4 shown are normalised by the value for NH_4 shown in the "Set Scale Limits" panel (in this case 1.0 which is equivalent to no scaling). Model values can be displayed in model units of mmol/m^3 or mass of nutrient per litre (i.e. μg N/L or mg O_2/L) by selecting the appropriate option from the drop down "Units" menu in the same panel.

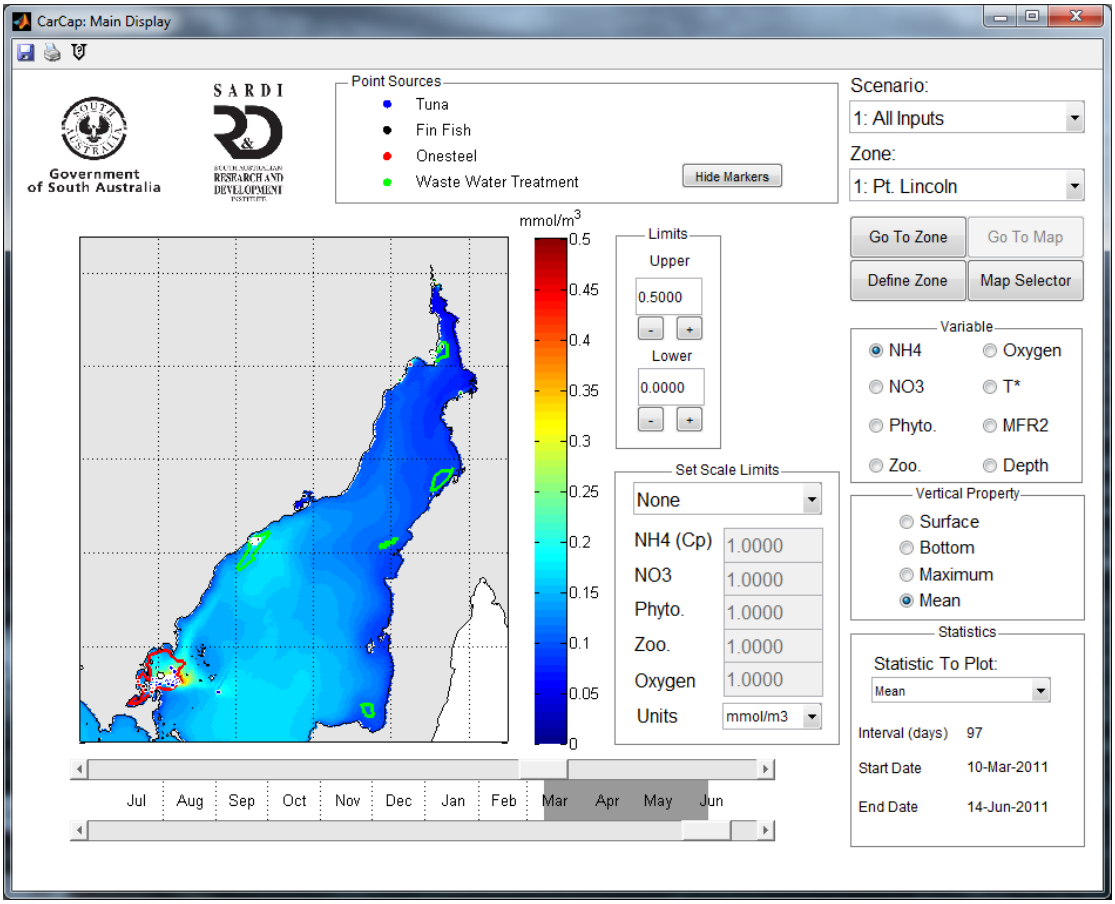

Figure 6.1 The main screen of CarCap1.0.

The user can go to a zone, or define a new one (to visualise), and then zoom in. The slide bars at the bottom allow the date and an averaging interval to be set if required; the user can also use the bars to scroll through the model in time.

The user can create a time series of concentrations at a point, or a transect of concentrations between two points, by choosing "Map Selector" from the cluster of 4 large buttons on the right. This will open a new window which presents the user with options to select a location. The site can be selected from a menu of existing lease site IDs, by entering a specific latitude and longitude, or by using the mouse to select a point or transect from the Main Display window.

Once a site has been selected the Time Series display window, shown in Figure 6.2, is presented showing the time series of selected biological variables and existing and potential feed rates at the site.

Figure 6.2 Time series of NH_4 (upper axis) and feed rates (lower axis) presented for an aquaculture site (redacted for purposes of commercial confidence). Also presented are statistics for the time interval set with the bottom slider bars in either this window or the Main Display. The bottom panel can display feed or the Maximum Feed Rate, method 1 (MFR1 and Maximum Feed Rate, method 2 (MFR2). The latter is recommended.

An example: estimating maximum feed rate at a new lease site

Having started CarCap1.0, the first step is to select a new location for a lease site. In this example the user has chosen to pick the site based on a low flushing time (T*~ 2 hrs) to the west of Port Lincoln. To do this the user first changes the variable selection to display the flushing time as determined by T* (Figure 6.3). This default flushing time is based on a lease size of 600 m but this can be modified in either the Main Display or the Time Series panel.

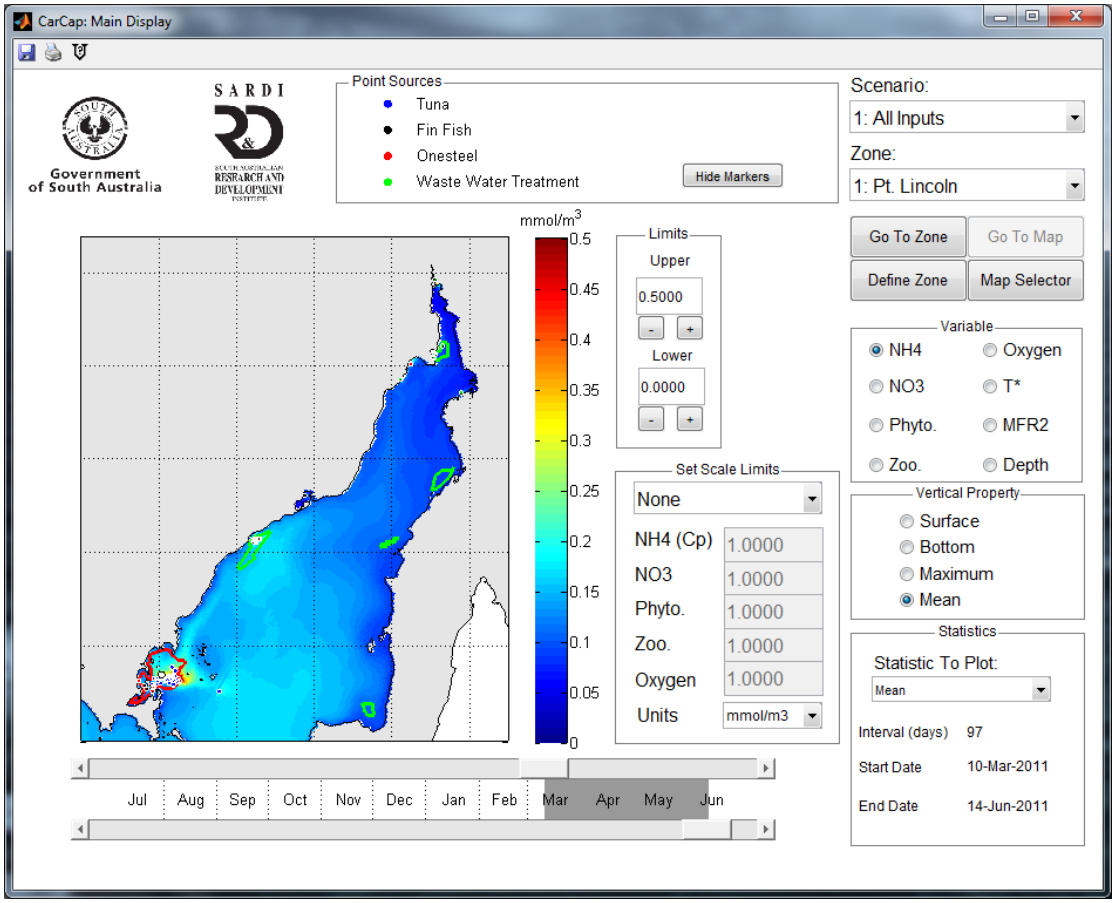

Figure 6.3 The user has selected the flushing time scale T* and displays this in hours. Regions where T* is small are rapidly flushed and will allow higher feed rates.

The user then uses the “Define Zone” button to select a region of interest (Figure 6.3). In this case the dark blue (low flushing time, high flushing rate) area just to the east of Port Lincoln has a small flushing time scale (T* ~ 2 hrs) and is chosen to investigate feed rates. The user drags a box over the region and this becomes the new active zone as indicated by the red square in Figure 6.4.

Now clicking on the “Go To Zone” button will zoom in on the region (Figure 6.5) allowing the user to see more detail. At this point the user can also change the colour limits using the Limits panel, if they change the settings from 0 to 10 hours to 0 to 2 hours (Figure 6.6) then they can find a region where the flushing time is typically less than 2 hours.

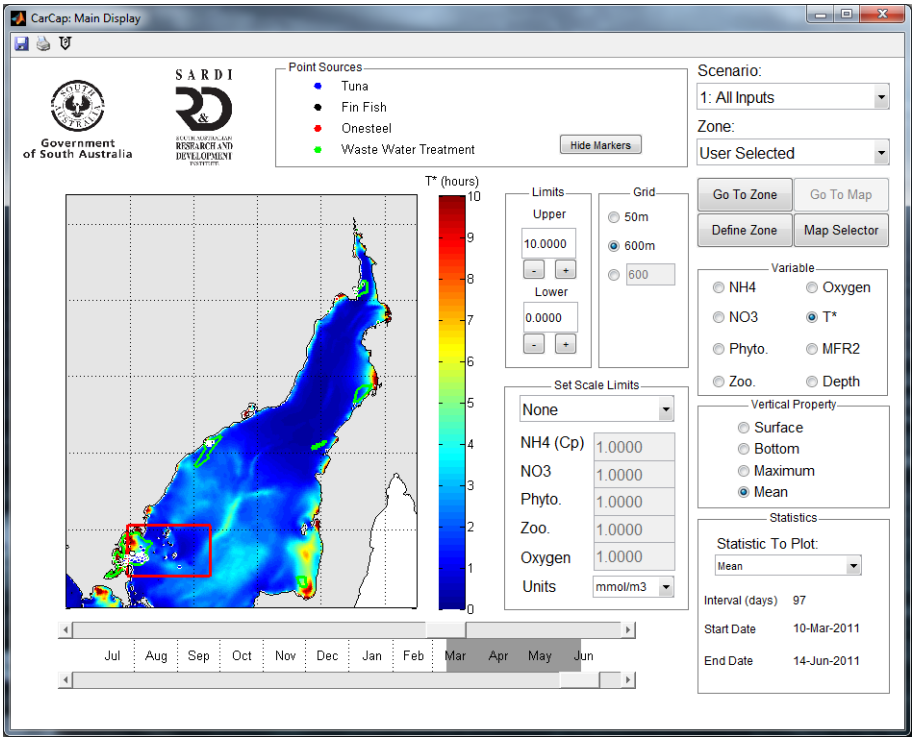

Figure 6.4 The user has chosen user selected zone and has created a box around the region of interest to the west of Port Lincoln (red square).

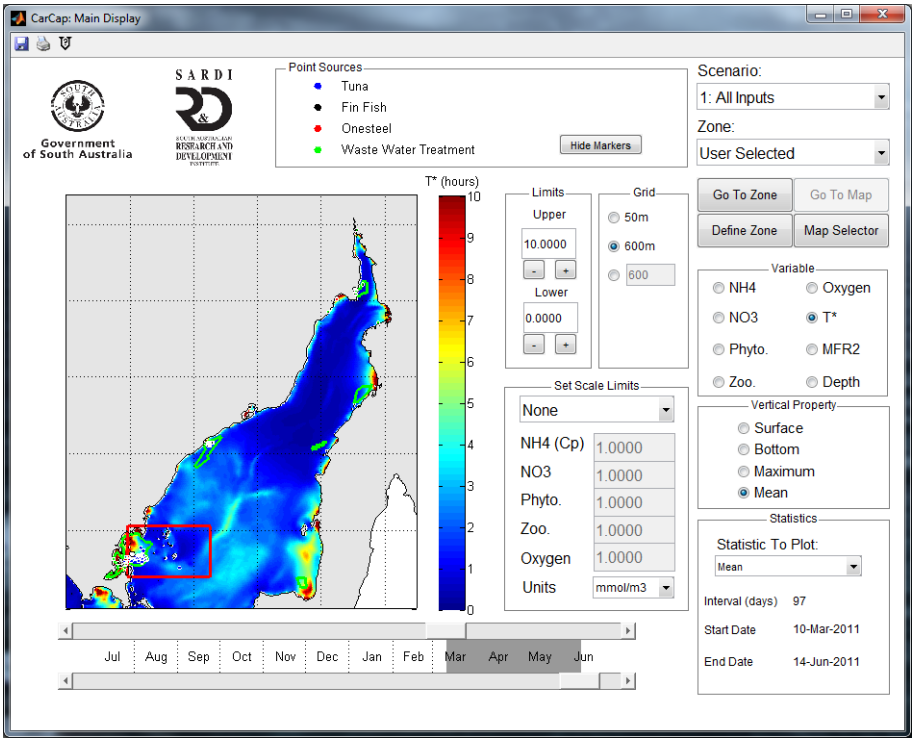

Figure 6.5 The user has zoomed in on the region of interest.

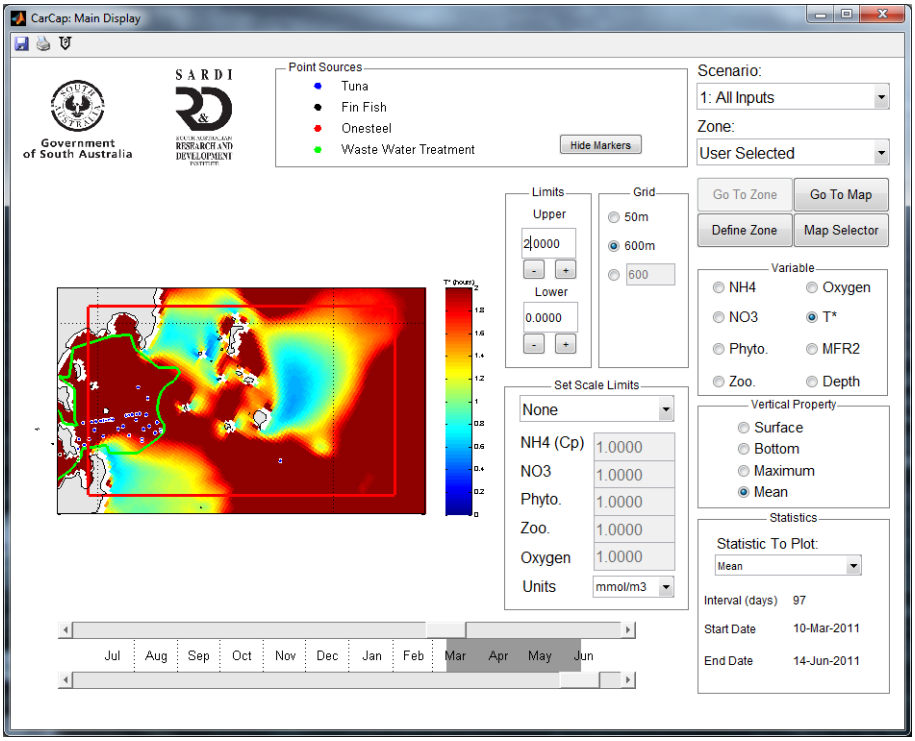

Figure 6.6 The user has changed the limits for the plot of T* to be 0 to 2 hrs for the region of interest.

The user may now select a point by using the “Select Point” button. In this case the user has selected a point in the middle of the darker blue region (Fig. 6.7). The point is shown as a white point and now the Time Series Display has appeared automatically.

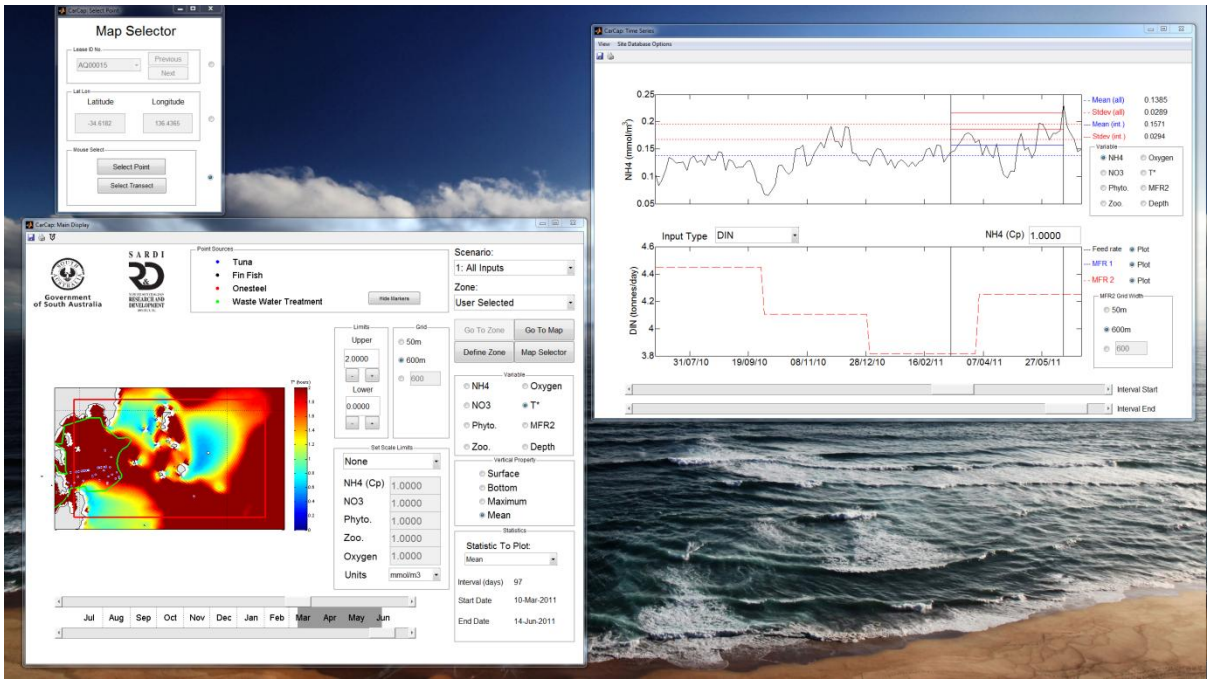

Figure 6.7 The user has selected a point (the white dot) in the domain where T* appears smallest. A time series display on a nutrient is then presented along with options for the maximum feed rate (MFR2).

Once the site location has been chosen the user can make an estimate of the maximum feed rate at the site. First returning to the "Main Display" window (Fig. 6.8) the user selects scale limits for the NH_4 based on the EPA standards.

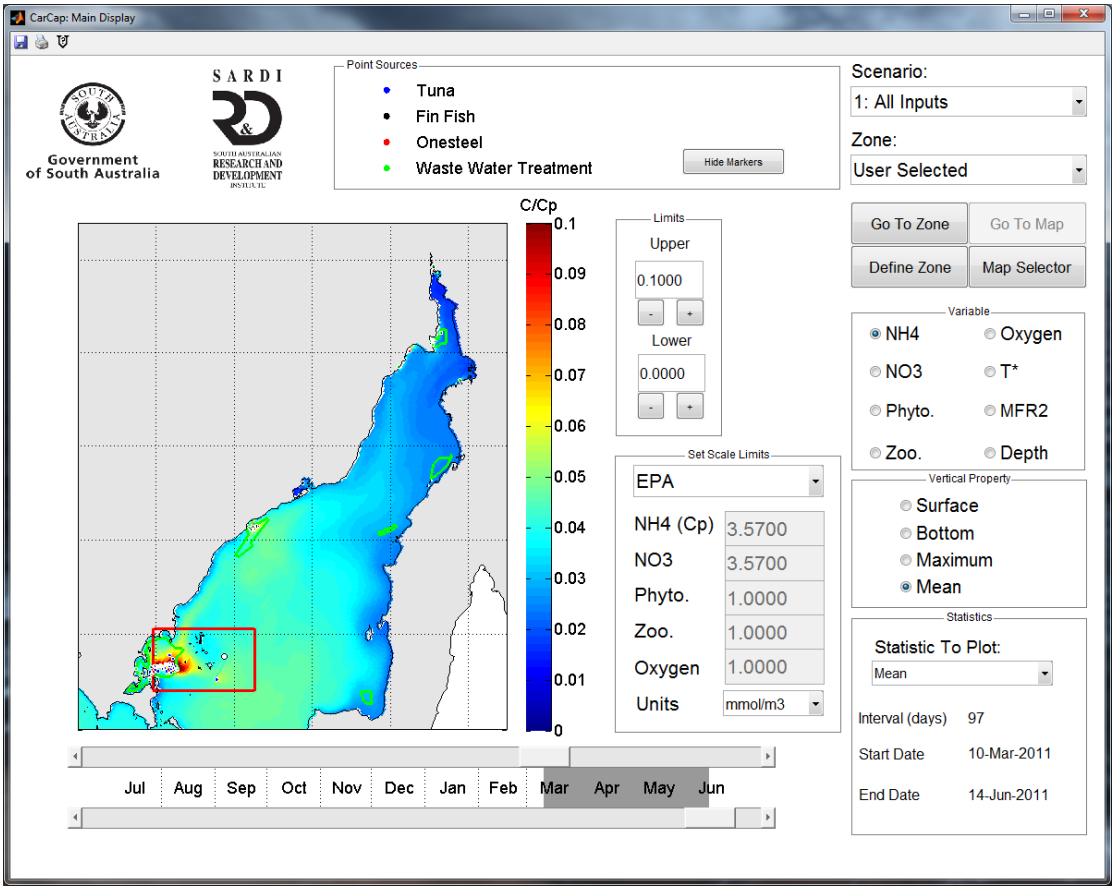

Figure 6.8 The user returns to the main window (zoomed out to full map) and selects the nutrient type (NH_4) and carrying capacity limit for c_P (the EPA standard) which will be used to determine the maximum feed rate.

This also changes the limits on the top axis of the model time series for NH_4 at this site which is automatically displayed in Figure 6.9 and sets the NH_4 scale used for the maximum feed rate MFR2 estimate which is plotted in the lower axis. Note that because this site doesn't have any existing feed rate information, only the MFR2 limit is plotted.

In this example the user has selected a site with a short flushing time; consequently the MRF2 limit is quite high suggesting that the site holder could use a relatively high feed rate without NH_4 concentrations exceeding the EPA guidelines. Also note that the feed rate is given in DIN units rather than fish or pellets. The conversion to units of Fish or Pellets can be made through the pop-up menu "Input Type" above the lower axis or in the Main Display if either T* or MFR2 has been selected as a variable.

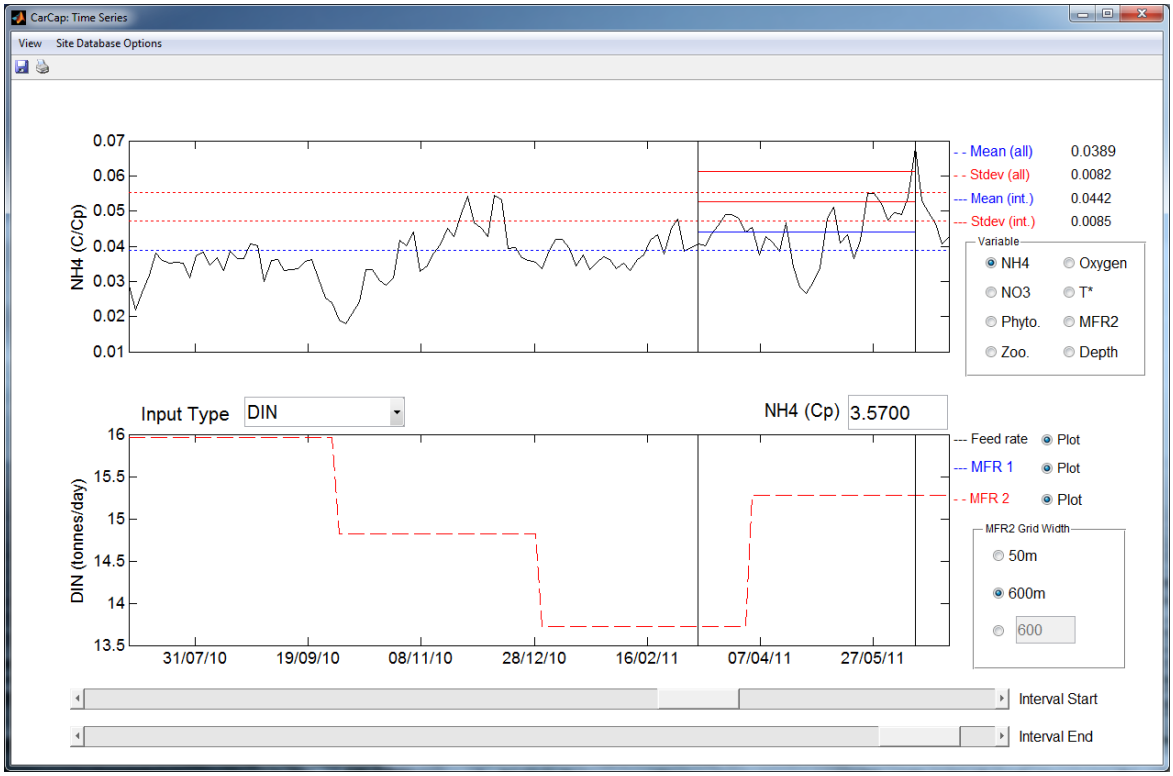

Figure 6.9 The time series of model NH4 scaled by the EPA maximum prescribed value (top axis) as well as the maximum feed rate MFR2 based on 3-month averaged model parameters providing four separate seasonal values (the red dashed line; bottom axis).

Finally the user might like to update an Excel compatible CSV file with the new information which they can do by selecting “Update Current Site” (Fig. 6.10) from the Site Database Options menu in Figure 6.9.

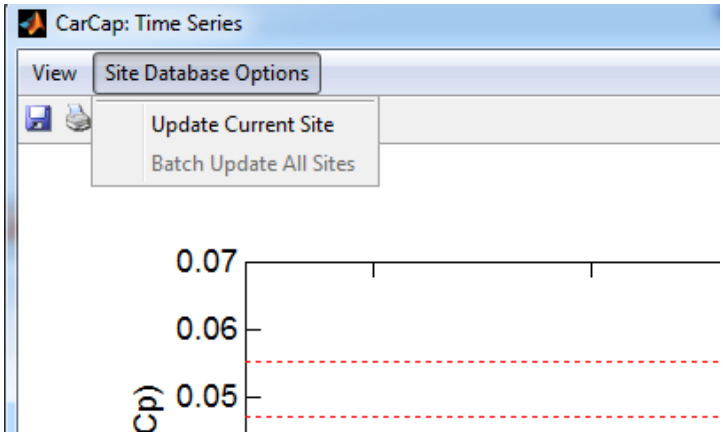

Figure 6.10 The Update Current Site menu is selected to save information to an Excel file. This will bring up a save file dialog (Fig. 6.11) where the user can choose a new or existing file to update. Unassigned lease sites such as this example are always added to the end of the file, but an existing lease site within the file will be updated so choose a new file if unsure if the new MFR1 and MFR2 estimates are what is required.

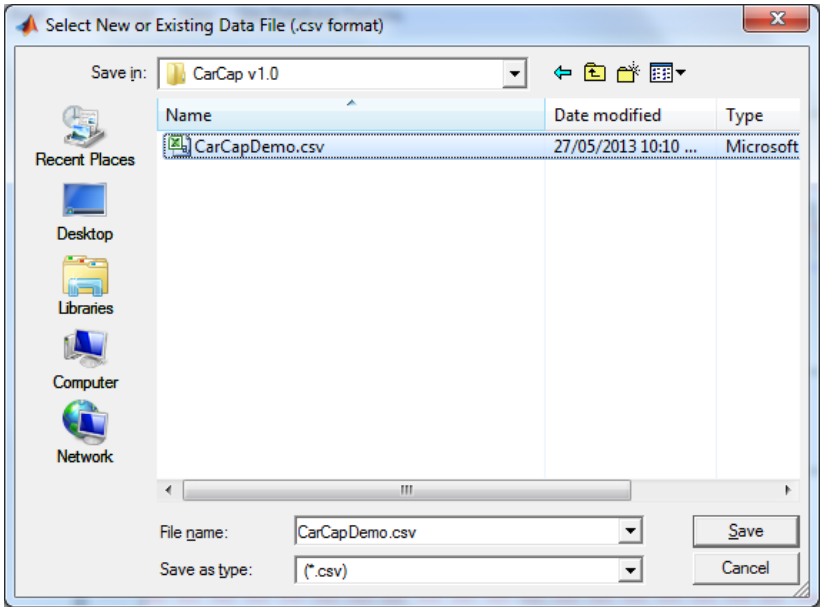

Figure 6.11 Choose filename and where to save the csv file.

The resulting csv file can be opened with Excel (Fig. 6.12) to show the contents which include site meta data. If this had been a lease site number, the MFR1 estimates would also have been included and an option to batch process all lease sites in the scenario with current grid and c_P settings would be available under the Site Database Options menu.

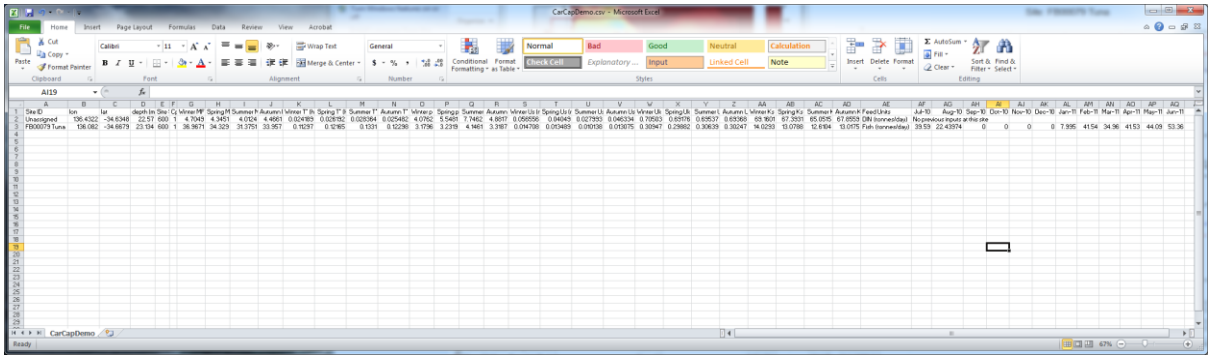

Figure 6.12 The csv Excel file showing the meta data stored in the example CarCapDemo.csv file. Also included is information on oceanographic parameters used to calculate T* and the feed rate for each season (see Chapter 3).

CHAPTER 7. STRATEGIES FOR LONG-TERM PERFORMANCE MONITORING, MANAGEMENT AND MITIGATION

John Middleton, Mark Doubell, Paul van Ruth

7.1 Monitoring Strategies

The models developed in this project have been demonstrated to provide PIRSA Fisheries and Aquaculture with improved estimates in relation to nutrient fluxes, feed rates and their consequences for the marine environment. In this context, a marine monitoring program (Objective 7) is outlined below with three objectives.

The first is to further refine and validate the developed models for future application to the sustainable development of finfish and shellfish aquaculture in Spencer Gulf. The monitoring program is designed to capture variability of the key physical, chemical and biological components of the Spencer Gulf marine ecosystem relative to the continued development of the models. The collected data will provide required information across scales from hours to days that are most relevant to local scale aquaculture operations, and longer term intra- (seasonal) and inter-annual changes required to assess long term, whole of Gulf ecosystem functioning. The use of these data and its incorporation into models developed for assessing carrying capacity is then detailed with a focus on aquaculture management and mitigation strategies.

The second objective of the monitoring program is to assess the impacts of aquaculture and other anthropogenic sources on ecosystem health. In this case, the model could also be used to indicate site locations where impacts resulting directly from aquaculture are likely to be greatest (e.g. areas where nutrient or phytoplankton concentrations are highest). Monitoring of these locations should be done at a minimum on a monthly basis (or better automatically) so as to provide for the early detection of declines, or shifts, in ecosystem status or functioning.

A third objective of the monitoring program is to assess possible changes to the winter flushing and summer blocking of the Gulf that might arise from climate change. As shown in this study, the lower trophic ecosystem of the Gulf has adapted to this seasonal variability. However, a reduction in upwelling or an increase in atmospheric heating could both reduce summer blocking. Thus, a long term (decadal) monitoring system would be needed to monitor this exchange and the associated drivers of salinity, temperature and ecosystem productivity.

In light of the above, eight ecosystem monitoring sites are proposed. The first is already in place at the eastern side of the Gulf mouth and forms part of the Southern Australian Integrated Marine Observing System. At this site, (labelled SAM8SG in Figure 1), currents, temperature, salinity, fluorescence, turbidity and dissolved oxygen (DO) are continuously recorded through a subsurface mooring. In addition, samples are taken 4-8 times per year for nutrients and phytoplankton abundance and community composition. This provides data related to the Gulf outflow.

A second and new monitoring site is suggested to be to the south of the aquaculture zones and seaward of Boston Island. Current, temperature and salinity data should be obtained continuously, as well as seasonal (2 x per season, 4 seasons per annum) triplicate water sampling of surface nutrients, phytoplankton and zooplankton, and seasonal studies of primary and secondary productivity. The purpose of these data would be to monitor long term mass and nutrient inflows and their variability into the Gulf that might arise from climate change.

The third and fourth monitoring sites ideally would be located in the Boston Island and Arno Bay regions where finfish aquaculture is most intense. The weekly, or automated sampling, here would enable the monitoring of nutrient and phytoplankton levels so as to provide for the early detection of elevated concentrations which may affect ecosystem status and the development of localised water quality guideline levels. Additionally, intensive sampling would be done seasonally over a four day period each year spanning the dodge tide when mixing is weakest. The purpose will be to determine the temporal and spatial variability of the water quality parameters in relation to tidal mixing across scales of hours and kilometres.

The fifth and sixth monitoring sites would be located between the Port Lincoln and Arno Bay and the Arno Bay and Fitzgerald Bay aquaculture zones. It is recommended that water quality parameters and rates of primary and secondary productivity should be sampled on a seasonal basis. The purpose of the data collected from these two sites will be to monitor the connectivity of nutrient discharges between aquaculture zones in relation to seasonal circulation patterns and ecosystem processes.

The seventh monitoring site should be in the ecologically distinct and significant upper Gulf region (Z3). BHP has run a measurement program for currents, salinity and temperature in this region and these data might be supplemented by a long term mooring to measure temperature and salinity fluorescence, photosynthetically available radiation (PAR), turbidity and DO and seasonal examinations of water quality parameters and rates of primary and secondary productivity. This mooring, and the seasonal sampling might be done off the end of the long jetty at Point Lowly.

The eighth monitoring site should be at Wallaroo (Z4 in Fig. 1), with water quality parameters and rates of primary and secondary productivity measured on a monthly basis. Data collected at this site, located on the eastern side of the Gulf, is essential to the regional validation of the models in relation to the Gulf's circulation patterns and overall ecosystem functioning.

7.2 Management and Mitigation Strategies

Based on the validated models and analysis presented, the graphical user interface tool (CarCap1.0) has been developed to assist in the management of existing and future aquaculture activities (Objectives 4 and 7). There are two components of CarCap1.0. The first allows managers to rapidly estimate the optimal location of new lease sites. This is done by determining the optimal nutrient fluxes F and associated feed rates that will lead to maximum concentrations that are no larger than prescribed environmental guideline values (c_P). These prescribed values have been estimated elsewhere as an upper bound for concentrations that ensure ecosystem health. Estimates of the fluxes can be obtained at any point in Spencer Gulf and allow management to choose new lease sites that are relatively well flushed and for which F and feed rates can be greater. In general, flushing offshore is larger than at the coast so that feed rates, and thus farmed fish biomass, can be larger offshore. CarCap1.0 can also be used to evaluate the likely maximum concentrations that arise from new industrial, waste water or desalination outfalls.

There are restrictions to this "single lease" approach since concentrations are not cumulative with that from other leases. Moreover, nutrients are not taken up by phytoplankton. To allow for these restrictions, a coupled hydrodynamic – biogeochemical model was developed and validated against data collected. For the most realistic scenario, where all anthropogenic nutrient sources are included, CarCap1.0 can be used to display concentrations of nutrients, oxygen and phytoplankton at the scale of the Gulf, zone and lease and also in time. Through

comparison with the prescribed maximum environmental concentrations (c_P), decisions can be made as to whether lease sites might need to be relocated to mitigate against harm to the ecosystem. A variety of scenarios were also run to enable managers to easily determine the relative contributions made by natural nutrient sources (the adjacent shelf) and anthropogenic sources: these include farmed southern bluefin tuna and yellowtail kingfish, as well as industrial and waste water outfalls. These scenarios allow managers to determine the significance of individual sources.

The coupled hydrodynamic – biogeochemical model has been run for the 2010 - 2011 period and using the nutrient inputs for that year. In the future, new nutrient sources in the Gulf are expected including new aquaculture lease sites, as well as additional industrial and waste water sites and changing boundary conditions. These can be readily included in the models, which could then be validated against the data from the monitoring program outlined above. The CarCap1.0 package can then be updated to include changes to the nutrient sources and additional scenario studies.

BENEFITS AND ADOPTION:

As noted below (Planned Outcomes), several workshops and presentations have been given to PIRSA Fisheries and Aquaculture and relevant industry associations. PIRSA is now using the results of this study (particularly CarCap 1.0) to further refine and develop policy for the future regulation of the carrying capacity of aquaculture production within Spencer Gulf. In support of this, long-term performance monitoring, management and mitigation strategies have been developed and are outlined above. These outcomes will further justify the South Australian Government's approach to sustainable aquaculture development as directed by the *Aquaculture Act 2001*. Through application of the model and methods developed, the carrying capacity methodology can be applied to deliver the above outcomes for other areas (e.g., shelf waters off Ceduna). This will help PIRSA Fisheries and Aquaculture to determine future resource requirements for other areas of South Australia.

The methods and approach for this study can form the basis for future studies elsewhere within South Australia, Australia and internationally. Although Spencer Gulf specific data collected in this project cannot be transferred to other areas, the methods and approach to better define environmental carrying capacity are applicable to other geographical areas.

In addition, the rapid assessment methods developed in Chapter 3 can be used to estimate carrying capacity for ocean outfalls such as waste water and desalination outfalls. Indeed, the results of this study and CarCap 1.0 software should be of direct benefit to industry stakeholders in Spencer Gulf through the capacity developed to a) optimise the location of proposed outfall and aquaculture sites and b) evaluate the cumulative expected response of Spencer Gulf.

The primary beneficiaries of this project include PIRSA and the South Australian southern bluefin tuna, yellowtail kingfish and oyster aquaculture industries. All will be provided with a copy of the final report.

The results of the project have been communicated through several workshops and presentations. These include:
PIRSA Fisheries and Aquaculture, 7th June 2013 and 9th July 2013
The Australian Southern Bluefin Tuna Association and Clean Seas Tuna 19th August 2013
S.A. Sardine Industry Association, 22nd August 2013
S.A. Oyster Growers Association, 10th September 2013

A final workshop for other interested groups (e.g., S.A. EPA) will be held in early 2014. Results will also be presented at the World Adelaide Aquaculture Conference in June 2014. Four papers will be submitted to peer reviewed journals on the material in Chapters 3, 4 and 5.

Currently, the models have also been adopted in the FRDC projects 2008/011 (Optimising the Prawn Harvest) and 2011/205 (Spencer Gulf Research Initiative). The former uses the hydrodynamic model to predict prawn larval dispersal. The latter project uses the biogeochemical model to provide estimates of primary productivity to feed into a trophodynamic model.

FURTHER DEVELOPMENT:

The analytic solutions for carrying capacity (Chapter 3) assume a constant nutrient flux and can be extended to examine the effects of time dependent fluxes; in reality farmed fish are fed on a daily basis.

The CarCap 1.0 software package will need routine updating to take into account new lease sites and other sources of nutrients. To do this, the coupled models will need to be re-run to determine the cumulative impacts of the different nutrient sources**.**

The models themselves should be compared and validated against additional data collected using the strategy proposed for monitoring in Chapter 7. At present the data and models pertain to the 2010/2011 period and the extension to other years will build further confidence in the results. Additional scenario studies can also be conducted by SARDI in a cost effective manner. In addition, key results from the model studies regarding fluxes related to the dominant source (i.e. nutrient import from the shelf) and sink (i.e. sediment denitrification) require comparison with data to validate their respective roles in determining the carrying capacity of Spencer Gulf.

The biogeochemical model may be improved by the inclusion of additional processes relevant to ecosystem functioning in Spencer Gulf. These include:

- Inclusion of particulate waste from supplementary feeds to determine the near field impact of carbon deposition to the sediments.
- Inclusion of a macrophyte component (macro algae/seagrass) in the biogeochemical model
- Inclusion of nutrient co-limitation (phosphorus) and competition between different groups of phytoplankton (i.e. large cells representative of diatoms and small cells representative of flagellates and cyanobacteria) is likely to allow for a better prediction of both the total biomass and the potential for harmful algal blooms.
- Suspension of filter feeders.
- Detritus uptake by the benthos (e.g. sea cucumbers)

The models could be rapidly implemented for Gulf St Vincent, as the physical and biological systems are likely to be quite similar (van Ruth 2010, 2012). Extension to the shelves is also possible and would take advantage of the data streams that are collected as part of the Southern Australian Integrated Marine Observing System.

The models developed might also find application in biosecurity issues for the dispersal, transport and development of an epidemic of viral or bacterial pathogens.

The coupled hydrodynamic and biogeochemical models and proposed monitoring system could also be applied to examine possible causes of fish mortalities in South Australia.

PIRSA has also asked how the models and analysis would help in improving models of carbon deposition beneath finfish aquaculture pens. Excessive levels of carbon deposition can be harmful to benthic ecosystem health. The carbon deposition estimates obtained by PIRSA are obtained from a simple model (Gowen et al. 1994) based on limited data, highly simplified hydrodynamics and an assumed Gaussian distribution of organic matter underneath sea-cages. Such models, while simple, provide only a first order approximation since they do not allow for temporal variation in vertical current shear and re-suspension of organic matter by tides and waves. These effects can be incorporated through an extension of the hydrodynamic, wave and biogeochemical models developed in this project. In particular, a very high resolution model (5 m grid size) needs to be embedded in each of the three (1200 m scale) models developed to date. The 1200 m grid models developed here would provide boundary information for the 5 m grid scale models. The region of study would

be an aquaculture lease region, where data on sediments and settling velocities can be obtained. Finally, the organic matter sediment transport model of Warner et al. (2010) would need to be coupled to the models we have already developed.

All objectives of the project have been met and/or exceeded. An exception here is that the modelling and impact of non-supplementary fed species (e.g. oysters and mussels) was not undertaken (with agreement by PIRSA). The reason for this is that a) the feeding ecology, including information on food preferences, feeding rates and growth of South Australian non-supplementary fed species are very poorly understood, b) there are no data to validate these models, and c) oyster food uptake is strongly dependent on the details of ocean circulation at the scale of the individual oyster baskets (Dr Craig Stevens, NIWA, personal comm.). The numerical models developed here only resolve scales down to 600 m. Future projects currently being developed by PIRSA and SARDI regarding the feeding ecology of South Australian shellfish should provide key data for the future parameterisation and integration of shellfish into the models developed in this project.

The recommended limits for maximum carrying capacity concentration c_P provided by ANZECC/ARMCANZ (2000) or the S.A. EPA also need to be further developed. Information on how long concentrations can exceed some prescribed value c_P requires definition, since depending on feed rates, concentrations may exceed c_P for only a few hours or days or not at all. Moreover, the relationship between the guideline limits and measures of ecosystem health are poorly established.

The data collected for this project is stored through SARDI Aquatic's StateNet server (25 Grenfell St, Adelaide, S.A. 5000).

PLANNED OUTCOMES:

PIRSA is already using the results of this study to further refine and develop policy for the future regulation of the carrying capacity of aquaculture production within Spencer Gulf. The area specific differences within Spencer Gulf have been defined at the scales of the cage, lease and zone, and will allow for the development of long-term performance monitoring, management and mitigation strategies for aquaculture zones within Spencer Gulf that take into account the variability among the areas and the need for area specific requirements. These outcomes will further justify the South Australian Government's approach to sustainable aquaculture development as directed by the *Aquaculture Act 2001.*

The ability to deliver the above for other areas has been determined (e.g., shelf waters off Ceduna) and will help PIRSA to determine future resource requirements for other areas of South Australia. The "whole of gulf" approach taken here allows PIRSA Fisheries and Aquaculture and other Government agencies to evaluate the relative importance of both natural and anthropogenic nutrient sources (aquaculture, waste water and industrial ocean outfalls).

The methods and approach for this study can form the basis for future studies elsewhere. Although Spencer Gulf specific data collected in this project cannot be transferred to other areas, the methods and approach to better define environmental carrying capacity of a given body of water with various sources of nutrient inputs are applicable to other geographical areas, as well as to other aquaculture, fisheries and marine-based commercial activities that involve nutrient inputs.

CONCLUSIONS:

Objective 1 *To provide PIRSA Fisheries and Aquaculture with estimates of sustainable carrying capacity by region, season and species for Spencer Gulf, and to investigate the impact of non-supplementary fed species (e.g., oysters) on these estimates.*

This overarching objective has been achieved through the development of several models of hydrodynamics, waves, nutrient dispersal and biogeochemistry, and through the development of a graphical user interface (CarCap1.0) for rapid assessment by PIRSA of proposed aquaculture sites. Details are outlined below.

Objective 2 *To achieve this overall objective, we will collect data from five areas so as to build, calibrate and validate hydrodynamic, biogeochemical and wave models that describe the biophysical properties of the Gulf.*

Physical and biogeochemical data were collected at 5 zones around the Gulf and during 10 separate field trips in 2010/2011. This, and other historical data, are described in Chapter 1 (hydrodynamic), Chapter 2 (waves) and Chapters 4 and 5 (biogeochemical).

These data were then used to calibrate and validate hydrodynamic, wave and biogeochemical models. The high resolution hydrodynamic model was able to accurately reproduce a) the tidal currents (Chapter 1) which were shown to be very important to nutrient dispersal (Chapter 3) and b) the clockwise circulation, summer blocking and winter flushing of the Gulf that is important for the flux of nutrients from the shelf. The wave model was also reasonably accurate (Chapter 2) but had no significant impact on the mixing or dispersal of the nutrients. It was therefore not used further.

The biogeochemical model was found to reproduce the concentrations of nutrients (NO_2 and NH_4) and phytoplankton to within a factor of 2. This is comparable to other biogeochemical modelling that has been published in the international literature.

Objective 2 *(continued) The models and data will then be used to determine the following:*

Objective 3 *Provide measures of connectivity of nutrients for the Gulf, including aquaculture (supplementary fed species) and non-aquaculture (natural and industry) derived nutrient inputs.*

The issues of connectivity were addressed in Chapters 1 and 5 using a particle tracking scheme and the coupled hydrodynamic/biogeochemical model. The former simulation results showed the connectivity between aquaculture zones was greatest between northern and eastern zones during spring and summer. Connectivity between the western zones was greatest during autumn and winter. The biogeochemical model also showed that the nutrients from the Boston Island region are swept to the north along the western coast during the late autumn and winter and as far as Arno Bay (Fig. 1). Scenario studies showed (Chapter 5) that the primary sources of nutrient (averaged over the Gulf) were in the following order; the continental shelf, finfish aquaculture and waste water/industry, with ratios of about 100:10:1.

Objective 4 *Provide management with solutions to questions of carrying capacity, sustainability and impact for existing and proposed sites of aquaculture (supplementary fed species).*

This objective was achieved in two ways that have been well received by PIRSA. The first involves the development of a rapid assessment tool for evaluating finfish carrying capacity at the scale of the cage, lease or zone. Carrying Capacity here is taken to be defined as the maximum nutrient flux F and associated feed rates that lead to nutrient concentrations (c_P) that do not exceed those recommended by ANZECC/ARMCANZ (2000). It was shown (Chapter 3), that these quantities are approximately related through the expression $F = c_P / T^*$ where T^* is a time scale of flushing T^* based on both advection by mean currents and diffusion due to the tides. The scale T^* is estimated at every 600 m grid cell of the gulf using the hydrodynamic model results. For a given maximum concentration c_P, the maximum flux F and associated feed rates for any new lease region can be rapidly determined.

These results have been incorporated into the interactive software package CarCap1.0 that will, for a given choice of c_P, allow managers to immediately estimate the optimal nutrient fluxes and feed rates at any point in the Gulf and at the scale of the cage or lease. Moreover, since T^* and F vary strongly with location, CarCap1.0 will also enable new aquaculture sites to be chosen to ensure maximal flushing and larger nutrient fluxes and feed rates: the latter may ensure a greater biomass of caged fish. The tool can also be used to determine carrying capacity and impacts for ocean outfalls, as well as maximum concentrations that might arise from proposed desalination plant discharges.

The second approach taken for this objective was to couple the hydrodynamic model to a biogeochemical model that more realistically allows nutrient concentrations from different sources to be cumulative and recycled between phytoplankton, zooplankton, detritus and sediments. A variety of model scenarios were run to determine the relative importance of various sources of nutrients, including natural (adjacent shelf waters) and anthropogenic (aquaculture, Onesteel steel works and waste water). Natural sources were found to be the largest source of nutrients to the Gulf, and loss to the atmosphere the largest sink. The additional anthropogenic nutrients input to the Boston Bay region lead to the largest concentrations of phytoplankton in the south-west corner and along the west coast of the Gulf.

All scenario studies have been incorporated into the CarCap1.0 software. The software allows managers to assess the relative importance of existing sources of nutrients at the scale of the Gulf, as well as providing the ability to “zoom in” at the scale of the zone and lease. Nutrient, oxygen and phytoplankton concentrations can be examined, and their evolution in time and space readily explored and compared to user prescribed concentrations, or those determined elsewhere (e.g. ANZECC/ARMCANZ 2000). Again, CarCap1.0 will allow environmental managers to make better informed decisions regarding existing and proposed lease sites, including (re)location and monthly feed rates.

Objective 5 *Use the carrying capacity estimates to validate or otherwise, earlier estimates that were obtained from simplified flushing models.*

The lease/zone flushing model used by SARDI to date has only included advection by mean currents (Collings et al 2007). In Chapter 4, this model was extended more realistically, to include diffusive flushing. Results show that the Collings model applied at the scale of the lease may predict concentration values that may be misleading and small compared to that found at the scale of the cage or lease.

Objective 6 *Develop and incorporate models for non-supplementary fed species (oysters and mussels) with parameters identified that are critical to model sensitivity.*

With the agreement of PIRSA, this objective was not attempted or met. The reason for this is that a) the feeding ecology, including information on food preferences, feeding rates and growth of South Australian non-supplementary fed species are very poorly understood b) there are no data to validate these models, and c) oyster fed uptake is strongly dependent on the details of ocean circulation at the scale of the individual oyster baskets (Dr Craig Stevens, NIWA, personal comm.). The numerical models developed here only resolve scales down to 600 m. Future projects currently being developed regarding the feeding ecology of South Australian shellfish should provide key data for the future parameterisation and integration of shellfish into the models developed in this project.

Objective 7 *Develop strategies for long-term performance monitoring, management and mitigation strategies.*

The proposed long-term monitoring program (Chapter 8), is based on three objectives:

- To further refine and validate the models.
- To assess the impacts of aquaculture and other anthropogenic sources on ecosystem health.
- To assess possible long-term changes to the critical summer blocking and winter flushing of the gulf which largely control the dispersal of nutrients.

The management and mitigation tool has been provided through the CarCap1.0 user interface (Chapter 7). This tool allows managers to assess new and existing lease sites and determine optimal spatial siting of finfish aquaculture effort.

Objective 8 *Determine limitations in the ability to deliver the above for other areas (e.g. shelf waters off Ceduna) or species.*

The approach taken for Spencer Gulf may in a general sense be adopted for other finfish sites such as the shelf waters of Ceduna. Differences will relate to the oceanographic circulation where for shelf waters, the tides are smaller than in the Gulf but advection by weather-band forced currents is much larger. Differences might also be expected in ecosystem behaviour that underpins the biogeochemical model developed here. The shelf waters in the eastern Great Australian Bight are subject to large nutrient sources that arise from summer upwelling. This nutrient rich water is blocked from entering the Gulf during summer. As noted above (Objective 6), there is insufficient information to discuss other (non-finfish) species.

REFERENCES:

Alves, J. H. G. M., Y. Y. Chao and H. L. Tolman, 2005: *The Operational North Atlantic Hurricane Wind-Wave Forecasting System at NOAA/NCEP.* NOAA / NWS / NCEP / MMAB Technical Note Nr. 244, 59 pp

ANZECC/ARMCANZ (2000) Australian and New Zealand guidelines for fresh and marine water ecology. Canberra, ACT.

APHA-AWWA-WPCF (1998a) Method 4500-NH3-I. Standard methods for the examination of water and wastewater. L. S. Clesceri, A. E. Greenberg and A. D. Eaton. Washington, American Public Health Association**:** pp. 4-111.

APHA-AWWA-WPCF (1998b) Method 4500-NO3-I. Standard methods for the examination of water and wastewater. L. S. Clesceri, A. E. Greenberg and A. D. Eaton. Washington, American Public Health Association**:** pp. 4-121.

APHA-AWWA-WPCF (1998c) Method 4500-PG. Standard methods for the examination of water and wastewater. L. S. Clesceri, A. E. Greenberg and A. D. Eaton. Washington, American Public Health Association**:** pp. 4-149.

APHA-AWWA-WPCF (1998d) Method 4500-SiO2-F. Standard methods for the examination of water and wastewater. L. S. Clesceri, A. E. Greenberg and A. D. Eaton. Washington, American Public Health Association**:** pp. 4-169.

Avnimelech Y. (1999) Carbon nitrogen ratio as a control element in aquaculture systems. *Aquaculture*, 176: 227-235.

Bianucci L., Fennel K. and Denman K.L. (2012) Role of sediment denitrification in water column oxygen dynamics: comparison of the North American East and West Coasts. Biogeoscience 9: 2673-2682.

Bierman P., Lewis M., Tanner J. and Ostendorf B. (2009) Chapter 6: Remote Sensing – Validation, spatial and temporal patterns in seas surface temperature and chlorophyll –*a*. In Tanner J., & Volkman J. (Eds.) *AquaFin CRC – Southern Bluefin Tuna Aquaculture Subprogram: Risk & Response – Understanding the Tuna Farming Environment*. Technical report, Aquafin CRC Project 4.6, FRDC Project 2005/059. Aquafin CRC, Fisheries Research & Development Corporation and South Australian Research & Development Institute (Aquatic Sciences), Adelaide. SARDI Publication No F2008/0000646-1, SARDI Research Report Series No 344, 287pp.

Bode A., Alvarez-Ossorio M.T. and Gonzalez N. (1998) Estimations of meso-zooplankton biomass in a coastal upwelling area off NW Spain. *Journal of Plankton Research* 20(5): 1005-1014.

Booij N, Ris R.C. and Holthuijsen L.H. (1999) A third-generation wave model for coastal regions, Part I, Model description and validation. *J. Geophys. Res.*, 104, (C4): 7649-7666.

Bullock D.A. (1975) The general water circulation of Spencer Gulf, South Australia, in the period February to May. *Trans. Roy. Soc. South Aust*., 99, 43-53.

Collings G,, Cheshire A, and Tanner J. (2007) Carrying Capacity modeling, p238-260. In, Southern Bluefin Tuna Aquaculture, Sub-Program: Tuna environment subproject – Development of regional environmental sustainability assessments for tuna sea-cage aquaculture. Tech. Rep., Ed. Tanner J, Aquafin CRC Project 4.3.3, FRDC Project 2001/104.

Aquafin CRC, Fisheries and Research Development Corporation and South Australia Research & Development Institute, Adelaide, SARDI Publication No F2007/000803-1 SARDI Research report Series No. 235, 286pp.

Conover R.J. (1978) Transformations of organic matter. *In* Kinne O. (Ed.), *Marine Ecology V. 4. Dynamics*. John Wiley, Chichester, 221-456.

De Silva Samarasinghe J.R., Bode L. and Mason L.B. (2003) Modelled response of Gulf St Vincent (South Australia) to evaporation, heating and winds. *Cont. Shelf Res*., 23, 1285-1313.

Doubell M.J., Yamazaki H., Li H. and Kokubu Y. (2009) A new laser based fluorescence microstructure profiler (TurboMAP-L) for measuring bio-physical coupling in aquatic systems. *Journal of Plankton Research* 31(12): 1441-1452.

Doubell M.J., James C.E., Luick J., van Ruth P. and Middleton J.F. (2013) Nitrogen cycling in Spencer gulf and exchange with the southern shelf: A model study with implications for Aquaculture *(in preparation).*

Easton, A.K. (1978) A Reappraisal of the Tides in Spencer Gulf, South Australia. *Aust. J. Mar. Freshwater Res.,* 29, 467-477.

Econsearch (2012) The economic impact of aquaculture on the South Australian state and regional economies, 2010/11. Report prepared for PIRSA Aquaculture by Econsearch, Marryatville, SA, 73pp.

Eppley R.W., Rogers J.N. and McCarthy J.J. (1969) Half-saturation constant for uptake of nitrate and ammonium by marine phytoplankton. *Limnology and Oceanography* 14: 912-920.

Fennel K., Wilkin J., Levin J., Moisan M. O'Reilly J. and Haidvogel D. (2006) Nitrogen cycling in the Middle Atlantic Bight: Results from a three-dimensional model and implications for the North Atlantic nitrogen budget. *Global Biogeochemical Cycles,* Vol 20: GB03007, doi:10.1029/2005GB002456.

Fernandes M., Cheshire A. and Doonan A. (2006) Sediment geochemistry in lower Spencer Gulf, South Australia: implications for southern bluefin tuna farming. *Aust. J. Earth Sci.,* 53, 421-432.

Fernandes M. and Tanner J.E. (2008) Modelling of nitrogen loads from the farming of yellowtail kingfish *Seriola lalandi* (Valenciennes, 1833). *Aquaculture Research* 39, 1328–1338.

Fernandes M., Angove M., Sedawie T., and Cheshire A. (2007) Dissolved nutrient release from solid wastes of southern bluefin tuna (*Thunnus Maccoyii*, Castelnau) aquaculture.

Fischer H.B., List E.J., Koh R.C.Y., Imberger J., and Brooks N.H., (1979) *Mixing in Inland and Coastal Waters.* New York: Academic Press, pp 483.

Gaylard S. (2012) Marine Pollution in Chapter 27, Industrial and Urban Development in *Natural History of Spencer Gulf* Madigan S., Shepherd S.A., Gillanders B., Murray-Jones S. and Wiltshire D. (in preparation) *Roy. Soc. Sth. Aust.,* Adelaide

Gecek, S and Legovic, T., (2010) Towards carrying capacity assessment for aquaculture in the Bolinao Bay, Philippines: a numerical study of tidal circulation, *Ecological Modelling,* 221, 1394–1412.

Gibbs C.F., Tomczak M., Longmore A.R. (1986) The Nutrient Regime of Bass Strait. *Australian Journal of Marine and Freshwater Research* 37: 451-466.

Gowen R.J., Smyth D. and Silvert W. (1994) Modelling the spatial distribution and loading of organic fish farm waste to the seabed. In *Modelling Benthic Impacts of Organic Enrichment from Marine Aquaculture* (Hargrave, BT Ed.). Canadian Technical Report of Fisheries and Aquatic Sciences, Canada, pp. 19–30.

Haidvogel D.B., Arango H.G., Hedstrom K., Beckmann A., Malanotte-Rizzoli P. and Shchepetkin A.F. (2000) Model Evaluation Experiments in the North Atlantic Basin: Simulations in Nonlinear Terrain-Following Coordinates. *Dynamics of Atmospheres and Oceans.* 32: 239-281.

Hallegraeff G.M., (1993). A review of harmful algal blooms and their apparent global increase. *Phycologia,* 32: 79-99.

Hanson C.E., Pattiaratchi C.B. and Waite A.M. (2005). Sporadic upwelling on a downwelling coast: Phytoplankton responses to spatially variable nutrient dynamics off the Gascoyne region of Western Australia. *Continental Shelf Research* 25: 1561-1582.

Hemer M.A. and Bye J.A.T. (1999) The swell climate of the South Australian Sea. *Trans. R. Soc. S. Aust.,* 123, 107-113.

Hertzfeld M., Middleton J.F., Andrewartha J.R., Luick J., and Wu L., (2009). Chapter 1: Hydrodynamic modeling and observations of the tuna farming zone, Spencer Gulf. In Tanner J. and Volkman J. (Eds.) *AquaFin CRC – Southern Bluefin Tuna Aquaculture Subprogram: Risk & Response – Understanding the Tuna Farming Environment*. Technical report, Aquafin CRC Project 4.6, FRDC Project 2005/059. Aquafin CRC, Fisheries Research & Development Corporation and South Australian Research 7 Development Institute (Aquatic Sciences), Adelaide. SARDI Publication No F2008/0000646-1, SARDI Research Report Series No 344, 287pp.

Howarth R.W. (1988) Nutrient limitation of net primary production in marine ecosystems. *Ann. Rev. Ecol.Syst*. 19: 89–11.

Howarth R.W. and Marinao R. (2006) Nitrogen as the limiting nutrient for eutrophication in coastal marine systems: Evolving views over three decades. *Limnol. Oceanogr.,* 51(1,part2): 364-376.

Jassby A.D., and Platt T. (1976) Mathematical formulation of the relationship between photosynthesis and light for phytoplankton. *Limnol. and Oceanogr.,* 21(4): 540-547.

Jones E.M., Kaempf J. and Fernandes M. (2012) Characterisation of the wave field and associated risk of sediment re-suspension in a coastal aquaculture zone. *Ocean and Coastal Management*, Volume 69: 16-26.

Lauer P., Fernandes M., Fairweather P., Cheshire A. and Tanner J. (2007) Chapter 5: Effects of SBT farming on benthic metabolism. In Fernandes M., Lauer P., Cheshire A., Svane I., Putro S., Mount G., Angove M., Sedawie T., Tanner J., Fairweather P., Barnett J., and Doonan A. (Eds.) *AquaFin CRC – Southern Bluefin Tuna Aquaculture Subprogram:*

Tuna Aquaculture Subproject :Evaluation of Waste Composition and Waste Mitigation. Technical Report, Aquafin CRC Project 4.3.2, FRDC Project 2001/103. Aquafin CRC, Fisheries Research & Development Corporation and South Australian Research & Development Institute (Aquatic Sciences), Adelaide. SARDI Publication No RD03/0037-9, SARDI Research Report Series No 207, 289pp.

Lennon G.W., Bowers D.G., Nunes R.A., Scott B.D., Ali M., Boyle J., Wenju C., Herzfeld M., Johansson G., Nield S., Petrusevics P., Stephenson P., Suskin A.A. and Wijffels S.E.A. (1987) Gravity currents and the release of salt from an inverse estuary. *Nature,* 327, 695-697.

Lohrenz S.E., Wiesenberg D.A., Rein C.R., Arnone R.A., Taylor C.D., Knauer G.A. and Knap A.H. (1992) A comparison of *in-situ* and simulated *in-situ* methods for estimating oceanic primary production. Journal of Plankton Research 14(2): 201-221.

Longhurst A., Sathyendranath S., Platt T., Caverhill C., (1995) An estimate of global primary production in the ocean from satellite radiometer data. *Journal of Plankton Research* 17: 1245-1271.

Mackas D.L., Denman K.L. and Abbott M.R. (1985) Plankton patchiness: biology in the physical vernacular. *Bulletin of Marine Science*, 37: 652-674.

Mackey D.J., Parslow J., Higgins H.W., Griffiths F.B., O'Sullivan J.E. (1995) Plankton productivity and biomass in the western equatorial pacific: Biological and physical controls. *Deep Sea Research* Part 2 42(2-3): 499-533.

Mann K.H. and Lazier J.R.N. (1996) *'Dynamics of marine ecosystems'*. (Blackwell Science, London).

Martin A. (2003) Phytoplankton patchiness: the role of lateral stirring and mixing. *Prog. Oceanogr.,* 57: 12-174.

Maranon E., Behrenfeld M.J., Gonzalez N., Mourino B. and Zubkov, M.V., 2003. High variability of primary production in oligotrophic waters of the Atlantic ocean: uncoupling from phytoplankton biomass and size structure. *Marine Ecology Progress*, Series 257: 1-11.

Middleton J.F. and Doubell M.J. (2013) Carrying Capacity for Aquaculture. Part I – near-field semi-analytic solutions. *Submitted to Aquaculture Engineering*.

Middleton J.F. J. Luick and James, C. (2013) Carrying Capacity for Aquaculture. Part II – rapid assessment using hydrodynamic and near-field semi-analytic solutions. *Submitted to Aquaculture Engineering*.

Naylor R. and Burke M. (2005) Aquaculture and ocean resources: raising tigers of the sea. *Annual Rev Environ Resour,,* 30:185–218.

Nixon J.B. and Noye B.J. (1999) Prawn Larvae Advection-Diffusion Modelling in Spencer Gulf, In Noye, BJ, ed., *Modelling Coastal Sea Processes,* p189-218.

Nixon S. W. 1995. Coastal Marine Eutrophication - a Definition, Social Causes, and Future Concerns. *Ophelia,* 41: 199-219.

Nixon S.W. and Pilson M.E.Q. (1983) *Nitrogen in estuarine and coastal marine ecosystems,* in Nitrogen in the Marine Environment, edited by E.J. Carpenter and D.G. Capone, pp. 565-648, Elsevier, New York.

North, E. W., Z. Schlag, R. R. Hood, M. Li, L. Zhong, T. Gross and Kennedy, V. S. (2008) Vertical swimming behavior influences the dispersal of simulated oyster larvae in a coupled particle-tracking and hydrodynamic model of Chesapeake Bay. *Marine Ecology Progress Series* 359: 99-115.

Nunes R.A. and Lennon G.W. (1987) Episodic Stratification and Gravity Currents in a Marine Environment of Modulated Turbulence. *J. Geophys. Res.,* 92, 5465-5480.

Parsons T.R., Maita Y. and Lalli C.M. (1984) *A Manual of Chemical and Biological Methods for Seawater Analysis,* Pergamon Press Ltd., Oxford.

Pätsch J. and Kühn W. (2008) Nitrogen and carbon cycling in the North Sea and exchange with the North Atlantic-A model study.Part I. Nitrogen budget and fluxes. *Cont. Shelf Res.,* 28:767-787.

Petrusevics P.M. (1993) SST fronts in inverse estuaries, South Australia – indicators of reduced gulf-shelf exchange *Aust. J. Mar. Freshwater Res.,* 305-323.

Sathyendranath S., Stuart V., Nair A., Oka K., et al. (2009) Carbon-to-chlorophyll ratio and growth rate of phytoplankton in the sea. *Marine Ecology Progress* Series 383: 73-84.

Schendel E.K., Nordstrom S.E., Lavkulich L. M. (2004) Floc and sediment properties and their environmental distribution from a marine fish farm. *Aquaculture Research,* 35: 483-493.
Stolte W. and Riegman R. (1995) Effect of phytoplankton cell size on transient-state nitrate and ammonium uptake kinetics. *Microbiology,* 141: 1221:1229.

Seuront L., Schmitt F. and Lagadeuc Y. (2001) Turbulence intermittency, small-scale phytoplankton patchiness and encounter rates in plankton: where do we go from here? *Deep-Sea Res.,* I 48: 1199-1215.

Seuront L., Gentilhomme V. and LagadeucY. (2002) Small-scale nutrient patches in tidally mixed coastal waters. *Mar. Ecol. Prog.,* Series 232: 29-44.

Talling J.F. (1957) The phytoplankton population as a compound photosynthetic system. *The New Phytologist* 56: 133-149.

Tanner, J.E., Clark, T.D., Fernandes, M. and Fitzgibbon, Q. (2007) Innovative Solutions for Aquaculture: Spatial Impacts and Carrying Capacity – Further Developing, Refining and Validating Existing Models of Environmental Effects of Finfish Farming. South Australian Research and Development Institute (Aquatic Sciences), Adelaide, 126pp. SARDI Aquatic Sciences Publication Number F2007/000537.

Tanner J. and Volkman J. (2009) *AquaFin CRC – Southern Bluefin Tuna Aquaculture Subprogram: Risk & Response – Understanding the Tuna Farming Environment*. Technical report, Aquafin CRC Project 4.6, FRDC Project 2005/059. Aquafin CRC, Fisheries Research & Development Corporation and South Australian Research 7 Development Institute (Aquatic Sciences), Adelaide. SARDI Publication No F2008/0000646-1, SARDI Research Report Series No 344, 287pp.

Thompson P., Fernandes M., Tanner J., Volkman J., Wild-Allen K., Jones E. and van Ruth P. (2009) Chapter 5: Nutrients. In Tanner J. and Volkman J. (Eds.) *AquaFin CRC – Southern Bluefin Tuna Aquaculture Subprogram: Risk & Response – Understanding the Tuna Farming*

Environment. Technical report, Aquafin CRC Project 4.6, FRDC Project 2005/059. Aquafin CRC, Fisheries Research & Development Corporation and South Australian Research & Development Institute (Aquatic Sciences), Adelaide. SARDI Publication No F2008/0000646-1, SARDI Research Report Series No 344, 287pp.

van Heukelem L. and Thomas C.S. (2001) Computer-assisted high-performance liquid chromatography method development with applications to the isolation and analysis of phytoplankton pigments. *Journal of Chromatography* A, 910: 31 – 49.

van Ruth P.D. (2010) Adelaide desalination project plankton characterisation study, prepared for Adelaide Aqua. SARDI Publication. South Australian Research and Development Institute (Aquatic Sciences), Adelaide. SARDI Publication No. F2010/000378-1. SARDI Research Report Series No. 487. 39 pp.

van Ruth P.D. (2012) Adelaide Desalination Project Plankton Characterisation Study – Phase 2. Prepared for Adelaide Aqua. South Australian Research and Development Institute (Aquatic Sciences), Adelaide. SARDI Publication No. F2010/000378-2. SARDI Research Report Series No. 606. 40pp.

van Ruth P.D., and Doubell M.J. (2013) Spatial and temporal variation in phytoplankton abundance and community composition in Spencer Gulf, South Australia. In preparation.

van Ruth P. D., Ganf G.G. and Ward T.M. (2010a) Hot-spots of primary productivity: An alternative interpretation to conventional upwelling models. Estuarine, Coastal and Shelf Science 90: 142-158.

van Ruth P.D., Ganf G.G. and Ward T.M. (2010b) The influence of mixing on primary productivity: A unique application of classical critical depth theory. Progress in Oceanography 85: 224-235.

van Ruth P., Thompson P., Blackburn S. and Bonham P. (2009a) Temporal and spatial variability in phytoplankton abundance and community composition, and pelagic biogeochemistry in the tuna farming zone. *In* Tanner J.E. and Volkman J. (Eds.) 2009. Aquafin CRC - Southern Bluefin Tuna Aquaculture Subprogram: Risk and Response – Understanding the Tuna Farming Environment. Technical report, Aquafin CRC Project 4.6, FRDC Project 2005/059. Aquafin CRC, Fisheries Research & Development Corporation and South Australian Research & Development Institute (Aquatic Sciences), Adelaide. SARDI Publication No F2008/000646-1, SARDI Research Report Series No 344, 287 pp.

van Ruth P., Bonham P., Jones E. and Thompson P. (2009) Plankton ecology: Primary productivity, zooplankton community composition and grazing. . *In* Tanner, J.E. and J. Volkman (Eds.) 2008. Aquafin CRC - Southern Bluefin Tuna Aquaculture Subprogram: Risk and Response – Understanding the Tuna Farming Environment. Technical report, Aquafin CRC Project 4.6, FRDC Project 2005/059. Aquafin CRC, Fisheries Research & Development Corporation and South Australian Research & Development Institute (Aquatic Sciences), Adelaide. SARDI Publication No F2008/000646-1, SARDI Research Report Series No 344, 287 pp.

van Ruth P., Thompson P., Bonham P. and Jones E. (2009c) Primary productivity and zooplankton ecology in the Port Lincoln Tuna Farming Zone. Technical report, Aquafin CRC Project 4.6, FRDC Project 2005/059. Aquafin CRC, Fisheries Research & Development Corporation and South Australian Research & Development Institute (Aquatic Sciences), Adelaide. SARDI Publication No F2008/000789-1, SARDI Research Report Series No 343, 58 pp.

Warner JC, Armstrong B., He R. and Zambon J.B., (2010) Development of a Coupled Ocean-Atmosphere-Wave-Sediment Transport (COAWST) modeling system: *Ocean Modeling,* 35, no. 3, p. 230-244.

Wiebe P.H. (1988) Functional regression equations for zooplankton displacement volume, wet weight, dry weight, and carbon. A correction. Fisheries Bulletin 86: 833-835.

Wiebe P.H., Boyd S. and Cox J.L. (1975) Relationship between zooplankton displacement volume, wet weight, dry weight and carbon. Fisheries Bulletin 73: 777-786.

Xu J. and Hood R.R. (2006) Modeling biogeochemical cycles in Chesapeake Bay with a coupled physical-biological model. *Estuarine, Coastal and Shelf Science,* 69: 19-46.

APPENDIX 1: Intellectual Property.

This report will be made freely available to the public. The CarCap1.0 software designed to assist environmental managers in the assessment of carrying capacity was developed utilising funds unrelated to this project and will remain the IP of SARDI. The software has been licenced to PIRSA Aquaculture under condition and specific direction that it not be disseminated without prior SARDI approval.

APPENDIX 2: Staff

John Middleton, Mark Doubell, Charles James, Paul van Ruth, John Luick, Paul Malthouse, Peter Lauer, Sonja Hoare, Kelly Newton, James Patterson, Jason Nichols